MIAMI UNIVERSITY
The Graduate School

Certificate for Approving the Dissertation

We hereby approve the Dissertation

of

Fengfeng Ren

Candidate for the Degree

DOCTOR OF PHILOSOPHY

C. Scott Hartley, Director

Richard Taylor, Reader

Dominik Konkolewicz, Reader

David Tierney, Reader

Justin Saul, Graduate School Representative

ABSTRACT

DYNAMIC COVALENT SELF-ASSEMBLY OF 2- AND 3-TIERED STACKS

by

Fengfeng Ren

Dynamic covalent chemistry is a powerful synthetic tool for the construction of complex molecules. Imine formation is a well-characterized dynamic covalent reaction that has been extensively applied to the synthesis of various two-dimensional and three-dimensional covalent organic materials.

In chapter two, simple discotic cores functionalized with rigid reactive arms have been assembled into two- and three-tiered covalent stacks through imine formation. The targets are obtained in good yields, but competing formation of misassembled byproducts highlights some of the challenges inherent to the thermodynamically controlled assembly of rigid, compact, three-dimensional architectures. The structures comprise a central stack of arenes surrounded by a triple helix of interconnected arms. The racemization rate is strongly dependent on the number of tiers, suggesting that cooperative conformational coupling rigidifies these multi-tiered structures.

In chapter three, some alternate strategies were examined to address some problems encountered during the assembly of the 3-tiered stacks in Chapter 2: there was competing formation of misassembled byproducts and a halting of assembly at the 2-tiered stack. In an effort to overcome these challenges, different monomers were synthesized and studied. Two monomers were successfully prepared; however, no desired 2- and 3-tiered stacks were obtained.

In chapter four, benzene cores functionalized with flexible amino and aldehyde-arms were assembled into 2- and 3-tiered covalent stacks through imine formation. The benzene core and

the reactive arms were connected with ethylene groups. This introduced more flexibility to the monomers compared to our previously used monomers, which were connected through acetylene moieties. The new stacks were obtained in good yield despite the increased flexibility of the systems. Further, the previous problems in assembling rigid three-tiered stacks, which showed competing byproduct formation, were solved. Structural flexibility affords a faster conformational racemization rate.

Dynamic Covalent Self-Assembly of 2- and 3-Tiered Stacks

A DISSERTATION

Presented to the Faculty of

Miami University in partial

fulfillment of the requirements

for the degree of

Doctor of Philosophy

Department of Chemistry and Biochemistry

by

Fengfeng, Ren

The Graduate School
Miami University
Oxford, Ohio

2018

Dissertation Director: C. Scott Hartley

TABLE OF CONTENTS

LIST OF TABLES

LIST OF FIGURES

LIST Of ABBREVIATIONS

ACKNOWLEDGEMENTS

First I want to thank my advisor Dr. C. Scott Hartley, for his guidance, support, patience and encouragement throughout my graduate study. I have been amazingly fortunate to have Dr. Hartley as my advisor. Besides all the research techniques, abilities, he taught me to be positive when encountered with difficulties in research, to be patience on the road to the results, and to slow down and think about all kinds of possible failure reasons before start any new experiments. All these great qualities support me and help me throughout my graduate studies. Dr. Hartley is also an outstanding role model not only as an excellent chemist, but also as a person with great personality. His generous support helped me overcome lots of difficulties in my research and life. All I have learned from him will benefit me throughout my whole career and life.

Many thanks go to my committee professors: Dr. Wang, Dr. Taylor, Dr. Tierney, and Dr. Konkolewicz and Dr. Saul for their time, patience, wonderful suggestions and contributions to this dissertation.

I am grateful to all the past and current Hartley group members, Dr. Sanyo Mathew, Dr. Meng Chu, Zach Kinney, Gopi Vemuri. Special thanks go to Dr. Wang and Dr. Konkolewicz and again Dr. Hartley for providing the great opportunity to have a joint group meeting, in which I learned a lot more than only covalent self-assembly materials in the past five years.

I would also like to thank Miami University and Department of Chemistry and Biochemistry for providing great opportunities to study and meet all the good people. Thanks to NSF for providing financial support for my research.

Many many thanks go to all my friends in Oxford, Dr. Yang Zhang, Dr. Chen Ling, Dr. Min Li, Dr. Jie Wang, Dr. Yongan Tang, Dr. Lin Dai, Yi Hu, et al. Their accompany and friendship give me so much comfort while living so far away from China.

My deepest gratitude goes to my parents, Mr. Huanliang Ren and Ms. Linmei Qiu, my little sister, Ms Yanhong Ren. Their unconditional love gives me strength and courage to face all kinds of challenge in my life.

Most importantly, I want to thank my husband, Yongming Deng. He is the most important reason for me to attend Miami University, to meet everyone in Oxford and to attain my Doctoral degree. Without his support and love, I would never have accomplished what I have.

Chapter 1 Introduction

1.1 Dynamic Covalent Chemistry

Dynamic covalent chemistry (DCC) relates to chemical reactions based on reversible covalent bond formation under equilibrium control.[1] For systems at equilibrium, the relative free energies of products determine their proportions. The reversible nature of dynamic covalent reactions introduces error-checking and proof-reading into the synthesis process. The composition of equilibria can be adjusted by changing the reaction conditions (for example, temperature, concentration, solvents, presence of a template). DCC has become a powerful synthetic tool to construct complex assemblies such as covalent organic frameworks, molecular knots, polymers, and novel macrocycles and molecular cages.[2-7]

Traditionally, kinetically controlled reactions play an important role in the synthesis of organic compounds. To obtain the kinetic product in cases where the kinetic and thermodynamic products are different (purple route in **Figure 1.1**), reagents and conditions are chosen very carefully for irreversible bond formation. Lower activation energies ($\Delta G^{\neq}$) lead to faster formation of kinetic products resulting in their preferential formation initially. Thus, in kinetically controlled reactions the relative magnitudes of the activation energies determine the distribution of products. In contrast, reactions under thermodynamic control produce thermodynamically stable products. In such transformations (red route in **Figure 1.1**), covalent bonds are broken and formed repeatedly until the system reaches equilibrium. Thus, Gibbs' free energies (ΔG°) determine the distribution of products. In this manner, relatively high yields can be obtained if the starting materials are carefully designed so that the target structure is favored at equilibrium.

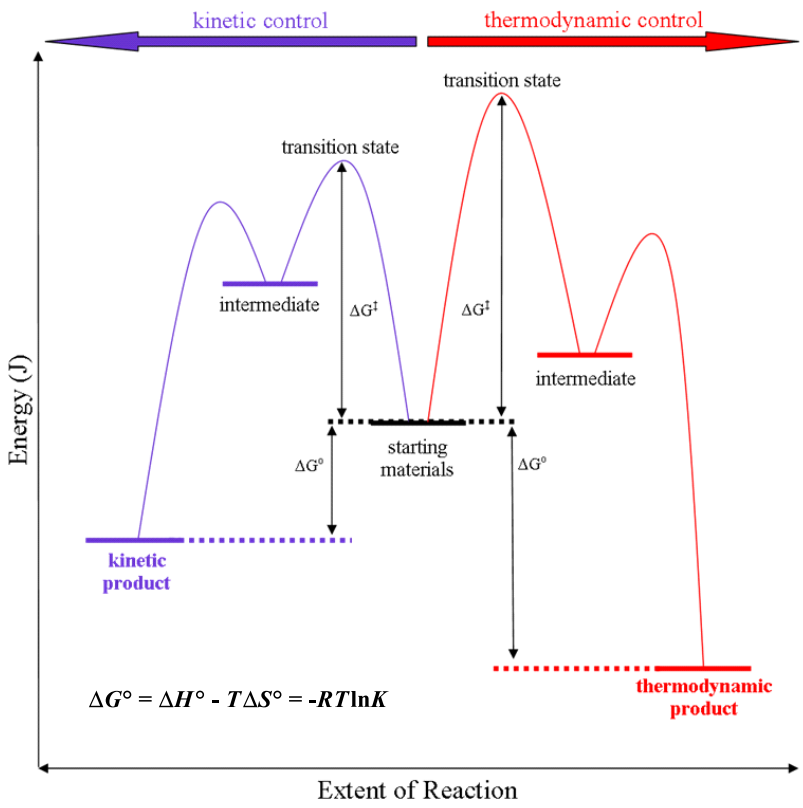

Figure 1.1 Thermodynamic control and kinetic control.

For a dynamic reaction to favor the products ($K > 1$), the free energy of products must be lower than that of starting materials. For example, consider the system in **Figure 1.1**. If the temperature is set very low at first, slowly increasing it until there is just enough energy to pass over the barrier toward the kinetic product and then isolating the products will give the products under kinetic control. If the temperature is raised further, such that there is sufficient energy to overcome all of the barriers, the kinetic product will, eventually, be converted to the (more stable) thermodynamic product.

1.2 Imine Formation, Exchange, and Metathesis

There is a wide range of reversible covalent reactions that have been utilized in constructing organic molecules under thermodynamic control. Generally, these reversible reactions can be categorized into two different types. a) The formation of new reversible covalent bonds: like the example shown in **Scheme 1.1a**, an aldehyde and an amine can be reacted to form an imine accompanied by the removal of one molecule of water. b) Exchange of

the same type of covalent bond: like the examples of **Scheme 1.1b**, an imine bond can be broken and reformed during the transimination process or exchange in imine metathesis. Examples of common dynamic covalent reactions include imine formation,[8-11] boronic acid condensation,[12,13] disulfide exchange reactions,[14,15] and alkyne metathesis[16-20] and olefin metathesis[21,22]. Usually, efficient catalysts are required to achieve thermodynamically stable product efficiently.

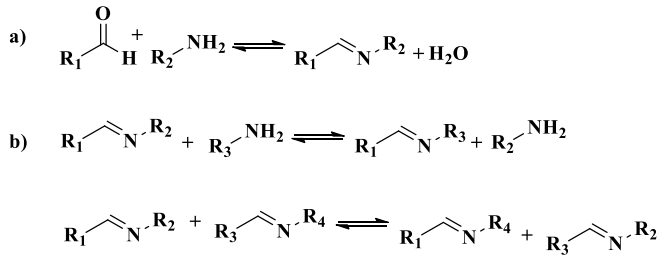

Scheme 1.1 Two types of DCC reactions: a) formation or scission of a new bond (for example, imine bond formation from aldehyde and amine condensation); b) exchange reaction (for example, imine exchange between imine and amine reactants (transamination) or imine exchange between two imines (imine metathesis)).

Imine formation is a well-characterized dynamic covalent reaction that has been extensively applied to the synthesis of covalent organic materials.[23] Moreover, Lewis acids have been found to efficiently catalyze imine metathesis to realize equilibria on appropriate time scales.[24] Imine metathesis was applied to the assembly of hemicarcerands[25] by the Stoddart group.[26] More recently, the assembly of a number of covalent cages through imine formation have been extensively explored by the Warmuth group.[27,28] Similarly, Cooper reported a number of imine-based cage compounds that exhibit structure-dependent gas adsorption selectivity and uptake of inorganic guests,[29-31] and Zhang has demonstrated some example of covalent organic frameworks and porous cages that exhibit significant gas adsorption and gas selectivity.[32,33]

1.3 Construction of Complex Architectures through Imine Formation

1.3.1 Shape-Persistent Macrocycles

Shape-persistent macrocycles are cyclic oligomeric analogues of rigid polymers, which have a non-collapsible backbone and an inside cavity ranging from one to several nanometers. Shape-persistent macrocycles have been extensively studied, partly because of their propensity to aggregate into stacked three-dimensional structures.

For flexible macrocycles, angle strain tends to be small regardless of their size, and the distribution of products is mainly entropically driven. Small macrocycles (cyclic monomers, cyclic dimers) are therefore preferred at equilibrium. However, for shape-persistent macrocycles (with rigid monomers), high angle stain will typically be present in small-sized macrocycles. In this way, larger macrocycles with more monomer subunits are enthalpically favored; the thermodynamic stability of shape-persistent macrocycles of a given size depends on both macrocyclic strain and entropy. As a result, moderate size is expected for many shape-persistent macrocycles prepared by reversible processes.

Dynamic covalent self-assembly offers tremendous potential to use monomer design to spontaneously generate macrocycles; however, structures prepared through self-assembly tend to be uniformly functionalized. For example, several C_3-symmetric imine macrocycles were prepared from a single fragment by the Hughes group in a one-pot procedure.[34] Such symmetrical rigid macrocycles are ideal candidates for aggregating to larger nanomaterials; however, the uniform functionality limits their utility of imine macrocycles. Recently the Olson group reported the synthesis of C_3 symmetric trianglimine macrocycles through [3+3] cyclocondensation of disubstituted biphenyl dialdehydes with (1R,2R)-1,2-diaminocyclohexane.[7] With the strategy presented by the Olson group, more functionality was introduced in imine macrocycles; however, different macrocycles were formed simultaneously in low yields. The Moore group has reported the construction of an unsymmetrical macrocycle with a controlled sequence.[35] The directionality of the imine bond was utilized to program the self-assembly process. In other words, the imine has distinct N-donor and C-donor components (akin to donors and acceptors in hydrogen bonding). Thus, three distinct monomers could be assembled into unsymmetrical macrocycles, as shown in **Scheme 1.2**. The arrangement of the building blocks in the final products is dictated by the binary N-/C-donor sequence in the diphenylacetylene precursors (CN, NN, CC for **1**, **2**, and **3**, respectively).

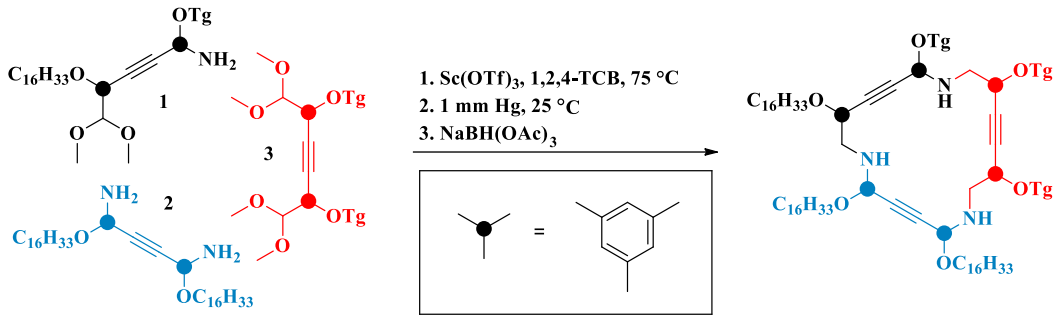

Scheme 1.2 Programmed assembly of unsymmetrically functionalized macrocycles dictated by N-/C-donor sequence. **OTg = $O(CH_2CH_2O)_3CH_3$.**[35] (Redrawn with permission from (*J. Am. Chem. Soc.* **2007**, *129*, 11682.). Copyright (2007) American Chemical Society.)

1.3.2 Covalent Organic Frameworks

Covalent organic frameworks (COFs) are porous, crystalline polymers comprising secondary building units which assemble to form a periodic framework.[36] The first reported COFs were linked by boronate esters and boroxines, but these linkages are easily hydrolyzed or oxidized. Imine-linked COFs, which are more chemically stable than boron-linked ones, are more promising for a broad range of applications, including energy storage,[37] catalysts,[38] and drug delivery.[39]

The Zhang group reported the synthesis of COFs through imine condensation of different amines and aldehydes.[10,40] A uniform-pore imine-linked covalent organic framework was first synthesized from terephthalaldehyde **4** and D_{3h} symmetric 1,3,5-trihexyl-2,4,6-tris(4-aminophenyl)benzene (**5**) at the air/water interface (**Scheme 1.3-a**,**c**).[10] A desymmetrized vertex design strategy was introduced in their work, which led to the successful preparation of two novel COFs with heterogeneous pore structures. The monomers were changed from D_{3h}-symmetric to C_{2v}-symmetric (**Scheme 1.3-c**[10] **and 1.3-d**[40]). As shown in **Scheme 1.3-b**, imine condensation of 5-(4-formyl-phenyl)isophthalaldehyde (**7**) or 5-((4-formyl-phenyl)ethylene)isophthalaldehyde (**8**) with linear hydrazine linker (**6**) yields **HP-COF-1** and **HP-COF-2**.[40] The desymmetrized vertex design strategy is generally applicable and opens new possibilities for developing COFs with heterogeneous pore structures targeting specified material properties.

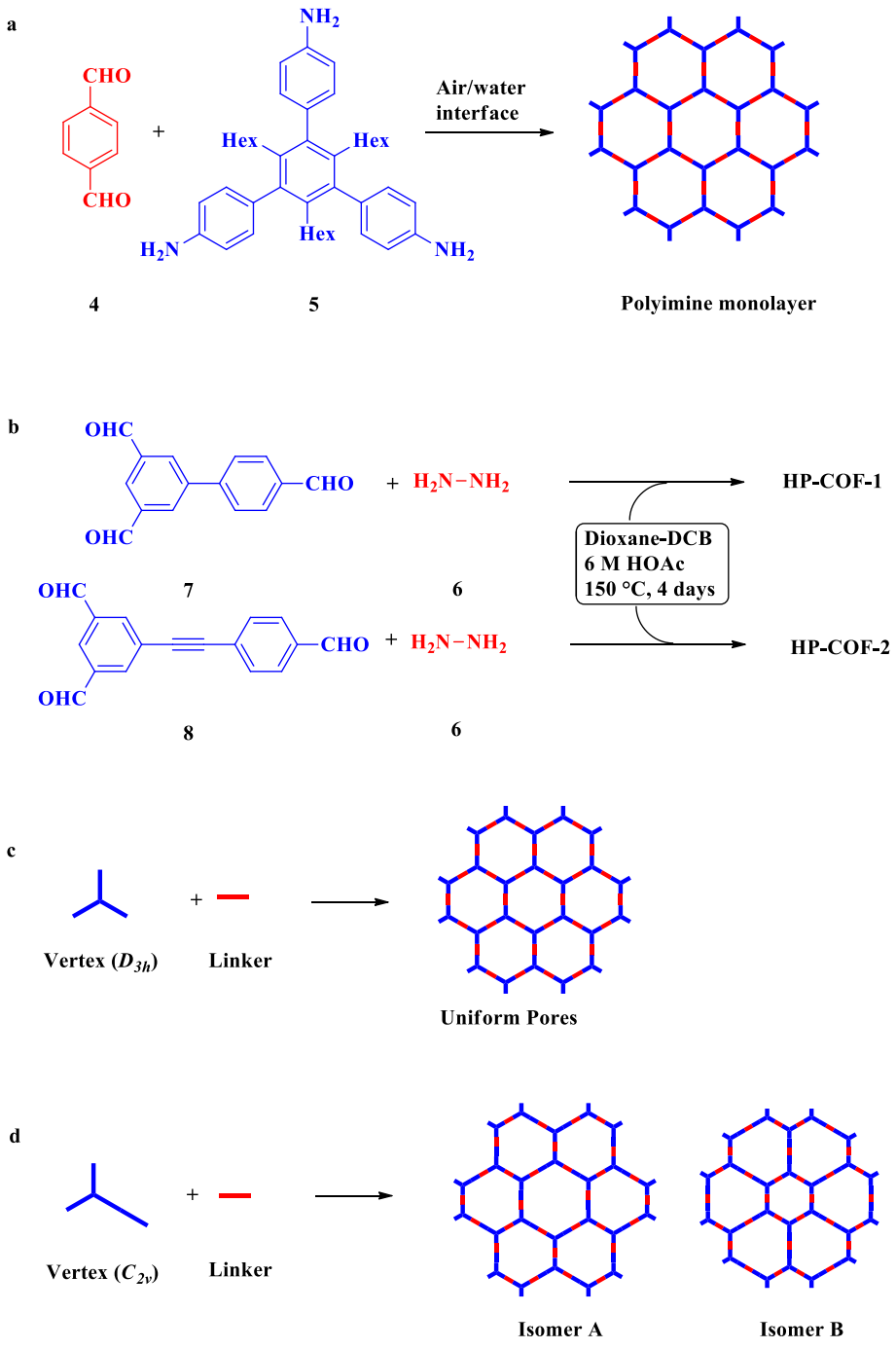

Scheme 1.3 a) Synthesis of an imine COF from dialdehyde **4** and triamine **5**; b) Synthesis of HP-COFs with desymmetrized trialdehyde **7**,**8** and hydrazine **6**; c) Model of uniform pore COF synthesis; d) Model of heterogeneous pore COFs synthesis strategy.[10,40] (Redrawn with permission from (*J. Am. Chem. Soc.* **2015**, *137*, 13772.). Copyright (2015) American Chemical Society.)

1.3.3 Molecular Ladders

A molecular ladder is a molecular fragment with a double-stranded structure that connected through chemical bonds. DCC has drawn lots of interest in the self-assembly of molecular ladders because of 1) the error-checking mechanisms, which are critical for the selective fabrication of intricate nanostructures; and 2) the robustness of covalent bonding. Intermediates in the assembly of molecular ladders undergo dynamic exchange and reorganization processes through the reversible formation and breakage of covalent bonds to achieve the desired products under thermodynamic control.

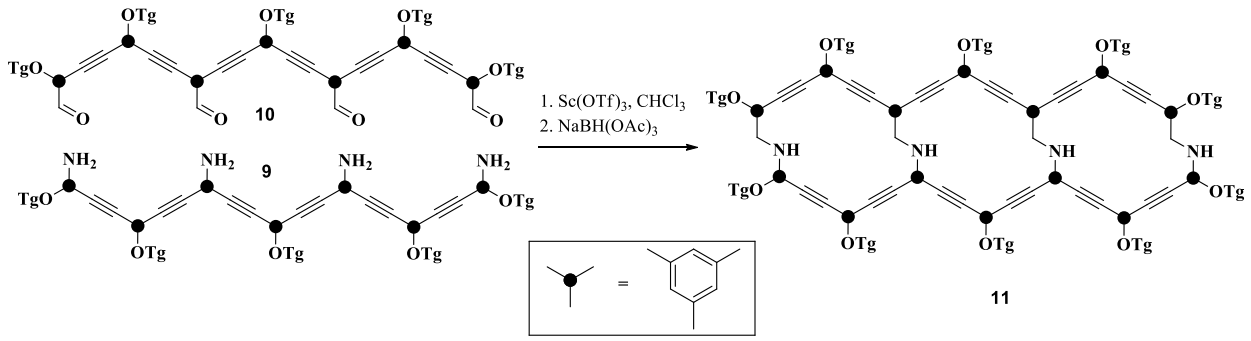

Scheme 1.4 DCC assembly of a molecular ladder from phenylene ethynylene oligomers. OTg = $O(CH_2CH_2O)_3CH_3$.[41] (Redrawn with permission from (*J. Am. Chem. Soc.* **2007**, *129*, 4512.). Copyright (2015) American Chemical Society.)

Moore et al. reported the first example of molecular ladders assembled with a DCC-based strategy.[41] As shown in **Scheme 1.4**, imine condensation of complementary m-phenylene ethynylene oligomers functionalized with amines (**9**) and aldehydes (**10**) led to the formation of [n]-rung molecular ladders ($\mathbf{11}^n$, n = 3-6). The largest ladder $\mathbf{11}^6$ was approximately 6.2×1.6 nm. The successful synthesis of these ladders demonstrates that it is viable to construct multi-topic large covalent architectures through dynamic covalent assembly. However, this approach does have practical limits: the system becomes kinetically trapped if there are four or more crosslinks between monomer units.[42] In other words, when n≥4, once the misaligned byproduct is formed, it does not dissociate to form the desired ladder under the conditions used. While this limitation will obviously depend on the architecture being examined, the specific coupling reaction being used, and the conditions (e.g., solvent, temperature), it is a significant design consideration for self-assembly using DCC. That said, strategies for overcoming this problem have recently been reported by Sanders.[43]

In contrast to the previous ladders assembled from m-phenylene ethynylene oligomers, Scott and others successfully constructed molecular ladders with up to twelve rungs from peptoid-based oligomers utilizing Vernier templating.[44] Vernier templating is a self-assembly strategy that employs oligomeric precursors with mismatched coordination numbers to construct assembled structures where each component precursor only participates in as many interactions as its number of reactive functional groups allows; the total number of interaction sites on the Vernier complex is equal to the lowest common multiple of the functionality on the respective precursors. For example in **Scheme 1.5**, a three-amine pendant oligomer (**12)** reacts with a four-aldehyde pendant oligomer (**13)**; after assembly, all misaligned intermediates were dissociated to form the 12-rung molecular ladder (**14**). The major peak in the MALDI mass spectrum was assigned to this product. This result demonstrates that Vernier-templated dynamic covalent self-assembly can be successfully utilized to curtail the kinetic trapping of thermodynamically disfavored products.

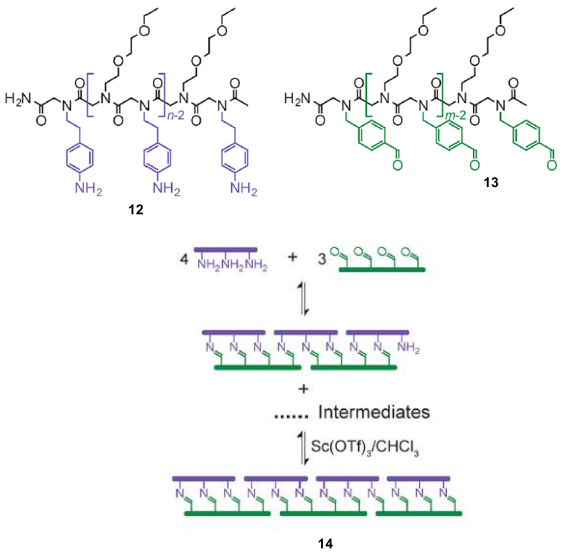

Scheme 1.5 Vernier-templated assembly of complementary oligopeptoids with non-commensurate functionalities into molecular ladders with 12 rungs. (Reprinted with permission from (*J. Am. Chem. Soc.* **2015**, *137*, 16196.). Copyright (2015) American Chemical Society.))

1.3.4 Molecular Cages

Molecular cages offer an important research target for the development of host-guest chemistry. The design and synthesis of molecular cages have attracted intense attention recently

owing to their broad applications in gas storage and adsorption, catalysts, and electronic devices. DCC offers an efficient strategy for the construction of molecular cages.

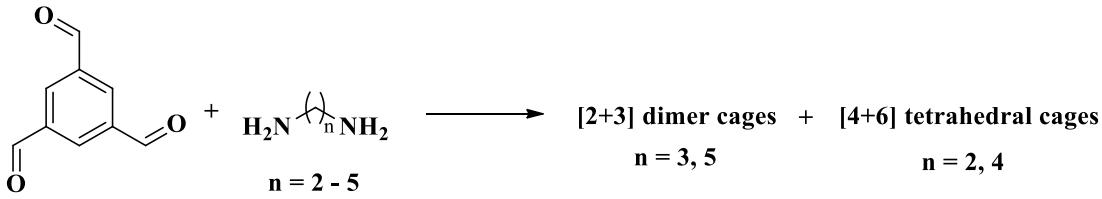

Scheme 1.6 Alternation of dimer cages and tetrahedral cages with odd or even alkyl chain length.

Seminal work about the synthesis of three-dimensional (3D) imine cages has been accomplished by the Cooper group.[45,46] Although molecular cages synthesized with DCC have been studied a lot, the design of precursors and the prediction of major products are still challenging. For example, the Cooper group discovered an odd-even rule with the synthesis of [2+3] and [4+6] imine cages. When 1,2-ethane diamine was used in the synthesis, a [4+6] tetrahedral imine cage was obtained. In contrast, 1,3-propane diamine led to the formation of a [2+3] imine cage (**Scheme 1.6**).[47] Computational studies could be used to predict the experimental results. Thus, in theory, this rule could be applied to prediction of major molecular cages with similar precursors.

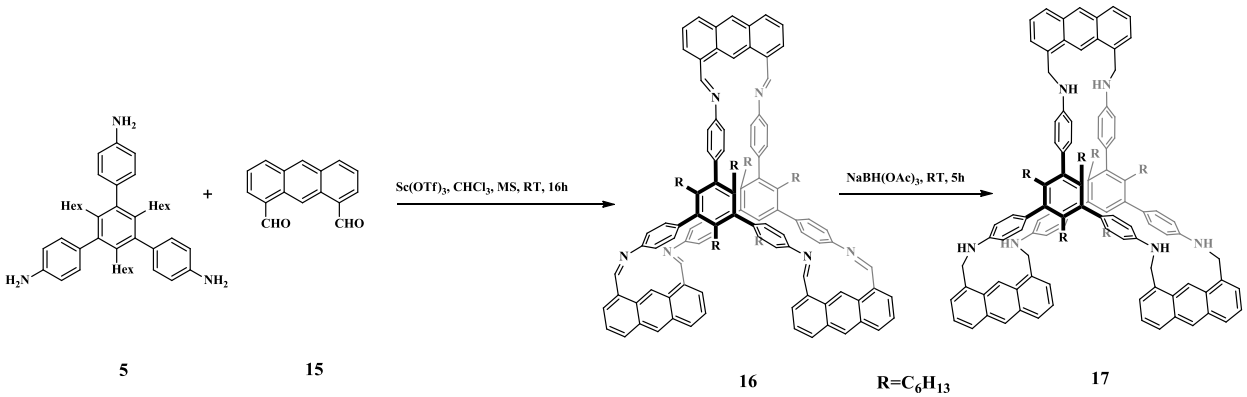

Scheme 1.7 Self-assembly of the cage molecule **17** from triamine **5** and dialdehyde **15**. MS = molecular sieves, Tf = trifluoro-methane-sulfonyl.[32] (Redrawn with permission from (*Angew. Chem. Int. Ed.* **2010**, *49*, 6348.). Copyright (2010) John Wiley and Sons.)

Although imines are broadly used in DCC, their chemical instability can limit their broader applications. The reduction of imines (to amines) improves stability toward hydrolysis. For example, the Zhang group demonstrated three-dimensional porous cages through imine metathesis.[32] Under thermodynamic control, two equivalents of 1,3,5-trihexyl-2,4,6-tris(4-aminophenyl)benzene **5** were reacted with three equivalents of anthracene-1,8-dicarbaldehyde **15** to yield an imine trigonal-prismatic cage **16** as the major product at equilibrium. The imine cage was then reduced to amine cage **17** (**Scheme 1.7**). Although these molecular trigonal-prismatic cages are the simplest architectures among three-dimensional constructs, the material exhibited significant CO_2 adsorption selectivity over N_2. Materials of this type have great potential for gas separation.

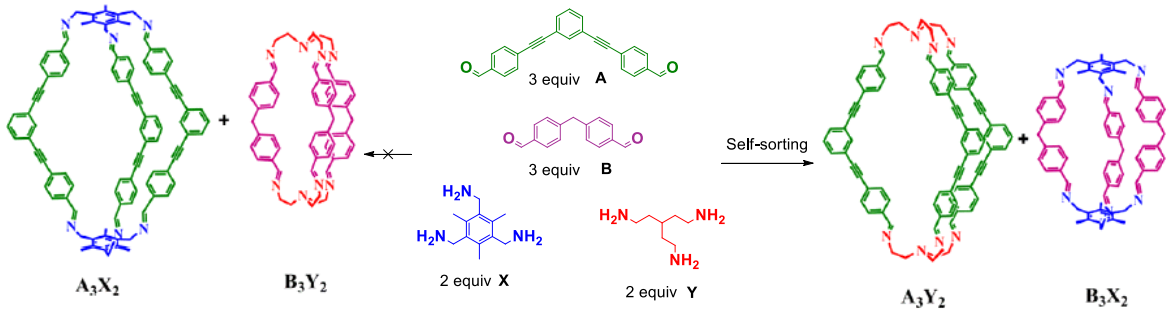

Scheme 1.8 Self-sorting of two dialdehyde **A**, **B** and two triamine **X**, **Y**. (Adapted with permission from (*J. Am. Chem. Soc.***2013**, *135*, 554). Copyright (2013) American Chemical Society.)

Imine exchange can be utilized in adaptive systems. Mukherjee et al. reported the self-sorting of 3D imine cages under thermodynamic control (**Scheme 1.8**).[48] First, imine condensation between triamines (**X**, **Y**) and dialdehydes (**A**, **B**) led to four different cages $\mathbf{A_3X_2}$, $\mathbf{A_3Y_2}$, $\mathbf{B_3X_2}$ and $\mathbf{B_3Y_2}$. As shown in **Scheme 1.8**, two preferred cages $\mathbf{A_3Y_2}$ and $\mathbf{B_3X_2}$ were formed as result of self-sorting between **A**, **B,** and **X**, **Y**. In addition, $\mathbf{B_3Y_2}$ could be transformed to $\mathbf{B_3X_2}$, and $\mathbf{A_3Y_2}$ when **X** or **A** was added to $\mathbf{B_3Y_2}$, respectively. The Mukherjee group first demonstrated the self-sorting behavior of two triamines and two dialdehydes. Two specific imine cages were produced out of several possibilities. Their pioneering research sheds some light on the self-sorting behavior of DCC.

1.4 Applications

Porous organic materials constructed through DCC have shown great potential in applications such as gas storage and separation, catalysis, molecular recognition and chemical sensing. Among these, gas storage and separation are the most studied by researchers.

Gas adsorption has been studied systematically by Cooper's group. Molecular cages are good candidates for porous liquids, which are liquids containing permanent intrinsic cavities or pores, first proposed by James et al. in 2007.[49] Cooper's study demonstrated that large quantities of gases could be absorbed by the porous liquids.[50] Furthermore, by using non-chemical triggers loaded gases could be reversibly released.

The Zhang group discovered a porous organic cage which gave high CO_2/N_2 adsorption selectivity at ambient temperature and pressure.[32] In addition, they also investigated the relationship between the structures of organic cages and gas selectivity.[33] Structure-property relationships revealed that a high CO_2 selectivity was related to a high amino group density and that bigger cage pore size resulted in higher N_2 adsorption capacity.

Shape-based separation is another important application of porous organic cages. The pore size of organic cages is on the order of small molecules (< 2 nm). The Cooper group performed a systematic study of molecular separation with covalent organic cages. They investigated shape-sorting of aromatic compounds, separation of krypton/xenon mixtures and separation of chiral alcohols.[51] They also utilized porous organic cages as a chromatographic stationary phase for GC separation of a range of mixtures including aromatic compounds, racemic mixtures, and branched alkanes.[52]

1.5 Introduction to Dynamic Covalent Assembly of Two- and Three-Tiered Stacks

As demonstrated by the many remarkable achievements discussed above, dynamic covalent self-assembly allows chemists to construct various two-dimensional (2D) and three dimensional (3D) organic materials. The overall goal of the project in this dissertation was to examine the tradeoff between the complexity of compounds that could be assembled and their size. A multitopic DCC strategy was used to assemble multiple distinct building blocks (monomers) into larger structures. The ultimate targets of this project were monodisperse stacks constructed through the axial self-assembly of discotic monomers as shown in **Figure 1.2**. This heterosequenced stack motif would provide a simple platform for the investigation of synthetic techniques.

The general principles developed in this project should be broadly applicable to the synthesis of nanoscale molecules with non-uniform structures (e.g., Janus capsules). These kind of monodisperse, short stacks of discs[53] are an attractive class of compounds for the study and exploitation of through-space interactions between chromophores. The potential utility of these compounds is illustrated in part by DNA, which exhibits remarkable charge-transport phenomena.[54] More generally, interactions between stacked aromatics are of key importance to energy- and charge-transport in organic semiconductors[55] and dye aggregates,[56] and may be useful in the creation of single-molecule devices.[57,58] Classic examples of these structures are multi-layered cyclophanes and related compounds which exhibit through-space delocalization.[59,60] Stacked architectures inspired by the cartoon in **Figure 1.2** complemented existing uses of covalent self-assembly in the synthesis of 2D macrocycles and 3D capsules and cages.

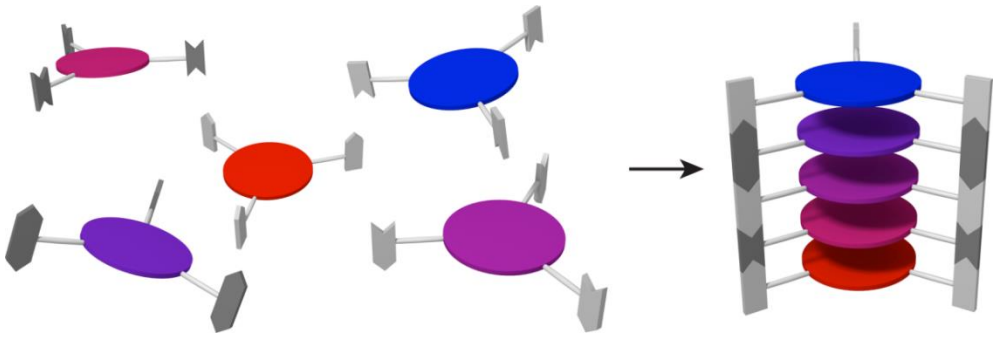

Figure 1.2 Axial self-assembly of a heterosequenced stack from discotic components.

The project presented here focuses on the synthesis of stacks with the controlled sequence. The discotic "cores" in this project were simple benzene rings, but could be changed to other extended or functionalized chromophores or macrocycles. With these changes, the materials synthesized with the strategies developed from this dissertation could be customized for specific applications in molecular recognition and catalysis.

Imine formation was selected as the main DCC reaction for covalent assembly. The directionality of the imine bond was utilized to control the self-assembly process. Different amine and aldehyde monomers were connected by covalent bonds to give helical stacks. We were trying to construct the four-tiered stacks with four different monomers, as shown in **Scheme 1.10**.

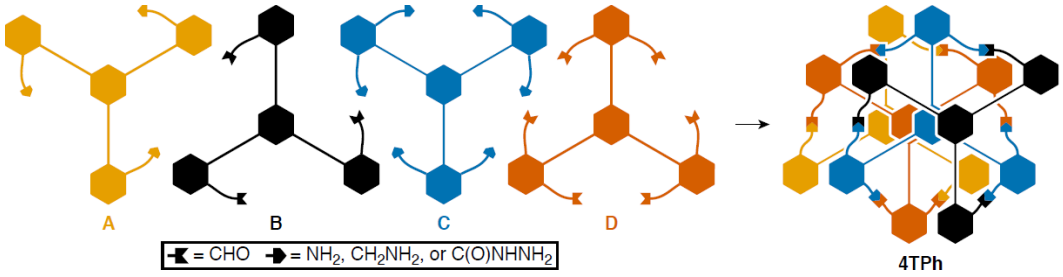

Scheme 1.10 Four component synthesis of four-tiered **4TPh**.

The first goal of this project was to develop a simple platform for the axial self-assembly of discotic monomers. Simple discotic cores functionalized with aniline and benzaldehyde arms were assembled into two- and three-tiered covalent stacks through imine formation as shown in Scheme 1.11. The structures comprise a central stack of arenes surrounded by a triple helix of interconnected arms. Two- and three-tiered stacks were obtained in good yields, but unexpected misaligned isomer was formed during the self-assembly process to three-tiered stack. The alternate route was also examined; however, only the partially assembled two-tiered stack was obtained. The formation of misaligned isomer and incompletely assembled two-tiered stack highlights some challenges of designing systems for thermodynamically controlled assembly.

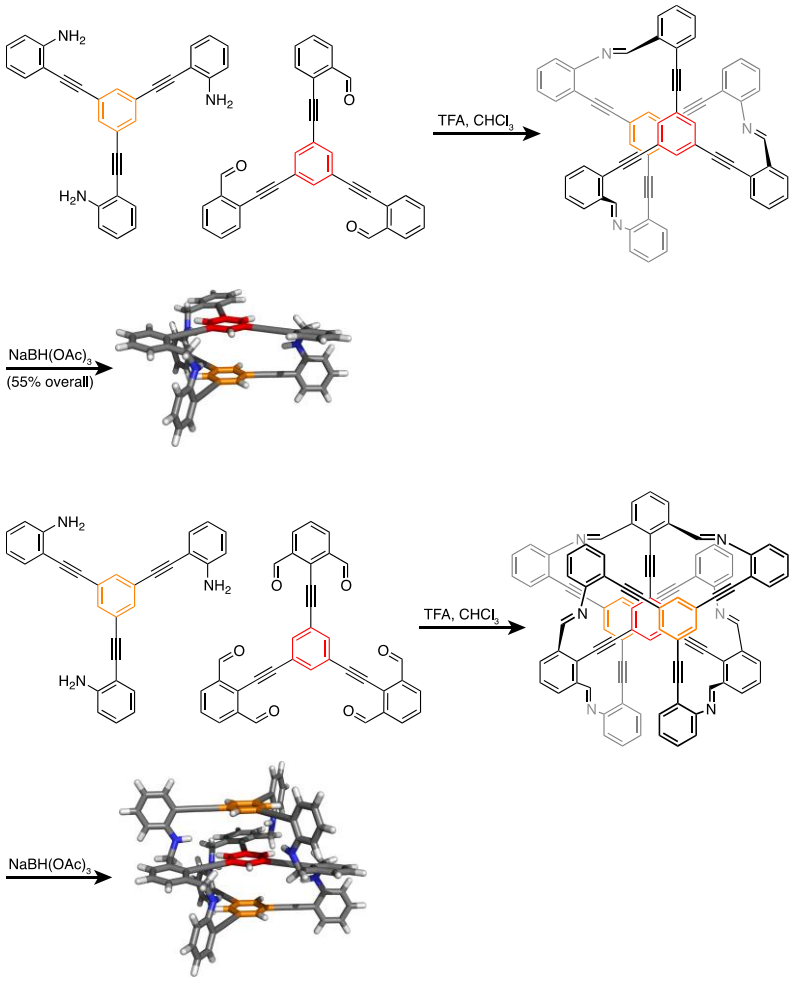

Scheme 1.11 Dynamic covalent assembly of 2-tiered stack and 3- tiered stack. The red and orange circles represent discotic moieties (e.g., arenes).

Several approaches were tried to suppress the formation of the misaligned three-tiered stack. First, various solubilizing and stabilizing groups have been introduced to monomers. This strategy was intended to increase the solubility of dialdehyde monomers. However, the new monomers synthesized with this strategy did not yield any three-tiered stacks. Longer linkers were also examined to introduce more space between the monomers during self-assembly. This strategy was intended to alleviate the strain presented in the previous stacks. Unfortunately, no efficient solutions were developed.

Another strategy we explored was to use ethylene groups to connect the benzene cores and reactive arms as shown in **Scheme 1.12**. In this way, more flexibility was introduced to the monomers compared with the acetylene linkers used before. The flexible stacks were obtained in

good yield by the covalent assembly of the flexible monomers. Further, the previous problems in assembling rigid three-tiered stacks, which showed competing misaligned isomer formation and incomplete assembly, were solved.

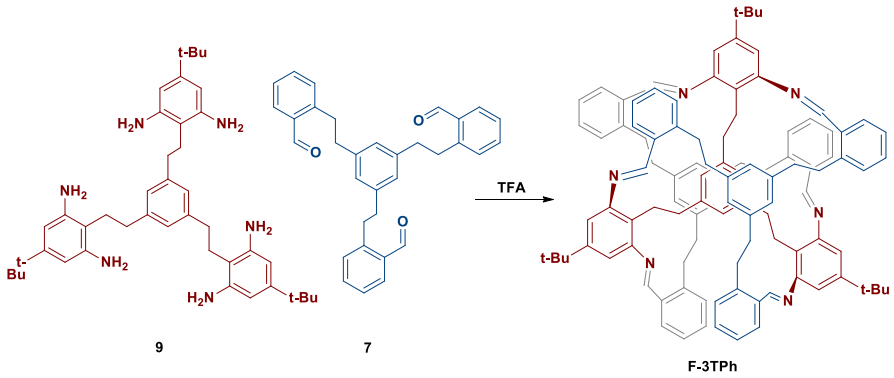

Scheme 1.12 Covalent assembly of flexible three-tiered stack.

Reference

(1) Rowan, S. J.; Cantrill, S. J.; Cousins, G. R. L.; Sanders, J. K. M.; Stoddart, J. F. *Angew. Chem. Int. Ed.* **2002**, *41*, 898.

(2) Corbett, P. T.; Leclaire, J.; Vial, L.; West, K. R.; Wietor, J.-L.; Sanders, J. K. M.; Otto, S. *Chem. Rev.* **2006**, *106*, 3652.

(3) Vitaku, E.; Dichtel, W. R. *J. Am. Chem. Soc.* **2017**, *139*, 12911.

(4) Tominaga, M.; Takahashi, E.; Ukai, H.; Ohara, K.; Itoh, T.; Yamaguchi, K. *Org. Lett.* **2017**, *19*, 1508.

(5) Šolomek, T.; Powers-Riggs, N. E.; Wu, Y.-L.; Young, R. M.; Krzyaniak, M. D.; Horwitz, N. E.; Wasielewski, M. R. *J. Am. Chem. Soc.***2017**, *139*, 3348.

(6) Cao, P.-F.; Rong, L.-H.; Mangadlao, J. D.; Advincula, R. C. *Macromolecules* **2017**, *50*, 1473.

(7) Wang, Z.; Nour, H. F.; Roch, L. M.; Guo, M.; Li, W.; Baldridge, K. K.; Sue, A. C. H.; Olson, M. A. *JOC* **2017**, *82*, 2472.

(8) Briggs, M. E.; Cooper, A. I. *Chem. Mater.* **2017**, *29*, 149.

(9) Briggs, M. E.; Jelfs, K. E.; Chong, S. Y.; Lester, C.; Schmidtmann, M.; Adams, D. J.; Cooper, A. I. *Cryst. Growth Des.* **2013**, *13*, 4993.

(10) Dai, W.; Shao, F.; Szczerbiński, J.; McCaffrey, R.; Zenobi, R.; Jin, Y.; Schlüter, A. D.; Zhang, W. *Angew. Chem. Int. Ed.***2016**, *55*, 213.

(11) Slater, A. G.; Little, M. A.; PulidoA; Chong, S. Y.; HoldenD; ChenL; MorganC; WuX; ChengG; ClowesR; Briggs, M. E.; HasellT; Jelfs, K. E.; Day, G. M.; Cooper, A. I. *Nat. Chem.* **2017**, *9*, 17.

(12) Nishiyabu, R.; Kubo, Y.; James, T. D.; Fossey, J. S. *Chem. Comm.* **2011**, *47*, 1124.

(13) Severin, K. *Dalton Trans.* **2009**, 5254.

(14) P Black, S.; Sanders, J.; Stefankiewicz, A. *Chem. Soc. Rev.*, **2014**,*43*, 1861.

(15) Hunt, R. A. R.; Otto, S. *Chem. Comm.* **2011**, *47*, 847.

(16) Wang, Q.; Yu, C.; Zhang, C.; Long, H.; Azarnoush, S.; Jin, Y.; Zhang, W. *Chem. Sci.* **2016**, *7*, 3370.

(17) Yang, H.; Zhu, Y.; Du, Y.; Tan, D.; Jin, Y.; Zhang, W. *Mater. Chem. Front.* **2017**,*1*, 1369.

(18) Yu, C.; Long, H.; Jin, Y.; Zhang, W. *Org. Lett.* **2016**, *18*, 2946.

(19) Lee, S.; Yang, A.; Moneypenny, T. P.; Moore, J. S. *J. Am. Chem. Soc.* **2016**, *138*, 2182.

(20) Ge, P.-H.; Fu, W.; Herrmann, W. A.; Herdtweck, E.; Campana, C.; Adams, R. D.; Bunz, U. H. F. *Angew. Chem. Int. Ed.* **2000**, *39*, 3607.

(21) Moneypenny, T. P.; Liu, H.; Yang, A.; Robertson, I. D.; Moore, J. S. *J. Polym. Sci. Part A: Polym. Chem.* **2017**,*55*, 2935.

(22) Ayme, J.-F.; Gil-Ramírez, G.; Leigh, D. A.; Lemonnier, J.-F.; Markevicius, A.; Muryn, C. A.; Zhang, G. *J. Am. Chem. Soc.* **2014**, *136*, 13142.

(23) Belowich, M. E.; Stoddart, J. F. *Chem. Soc. Rev.* **2012**, *41*, 2003.

(24) Giuseppone, N.; Schmitt, J.-L.; Schwartz, E.; Lehn, J.-M. *J. Am. Chem. Soc.* **2005**, *127*, 5528.

(25) Dutasta, J.-P. *Angew. Chem. Int. Ed.* **1995**, *107*, 2771.

(26) Ro, S.; Rowan, S. J.; Pease, A. R.; Cram, D. J.; Stoddart, J. F. *Org. Lett.* **2000**, *2*, 2411.

(27) Xu, D.; Warmuth, R. *J. Am. Chem. Soc.* **2008**, *130*, 7520.

(28) Sun, J.; Warmuth, R. *Chem. Comm.* **2011**, *47*, 9351.

(29) Jones, J. T. A.; Hasell, T.; Wu, X.; Bacsa, J.; Jelfs, K. E.; Schmidtmann, M.; Chong, S. Y.; Adams, D. J.; Trewin, A.; Schiffman, F.; Cora, F.; Slater, B.; Steiner, A.; Day, G. M.; Cooper, A. I. *Nature* **2011**, *474*, 367.

(30) Hasell, T.; Schmidtmann, M.; Cooper, A. I. *J. Am. Chem. Soc.* **2011**, *133*, 14920.

(31) Tozawa, T.; Jones, J. T. A.; Swamy, S. I.; Jiang, S.; Adams, D. J.; Shakespeare, S.; Clowes, R.; Bradshaw, D.; Hasell, T.; Chong, S. Y.; Tang, C.; Thompson, S.; Parker, J.; Trewin, A.; Bacsa, J.; Slawin, A. M. Z.; Steiner, A.; Cooper, A. I. *Nat. Mater.* **2009**, *8*, 973.

(32) Jin, Y.; Voss, B. A.; Noble, R. D.; Zhang, W. *Angew. Chem. Int. Ed.***2010**, *49*, 6348.

(33) Jin, Y.; Voss, B. A.; Jin, A.; Long, H.; Noble, R. D.; Zhang, W *J. Am. Chem. Soc.* **2011**, *133*, 6650.

(34) Korich, A. L.; Hughes, T. S. *Org. Lett.* **2008**, *10*, 5405.

(35) Hartley, C. S.; Moore, J. S. *J. Am. Chem. Soc.* **2007**, *129*, 11682.

(36) Diercks, C. S.; Yaghi, O. M. *Science* **2017**, *355*.

(37) Mulzer, C. R.; Shen, L.; Bisbey, R. P.; McKone, J. R.; Zhang, N.; Abruña, H. D.; Dichtel, W. R. *ACS Cent. Sci.* **2016**, *2*, 667.

(38) Lin, S.; Diercks, C. S.; Zhang, Y.-B.; Kornienko, N.; Nichols, E. M.; Zhao, Y.; Paris, A. R.; Kim, D.; Yang, P.; Yaghi, O. M.; Chang, C. J. *Science* **2015**, *349*, 1208.

(39) Mitra, S.; Sasmal, H. S.; Kundu, T.; Kandambeth, S.; Illath, K.; Díaz Díaz, D.; Banerjee, R. *J. Am. Chem. Soc.* **2017**, *139*, 4513.

(40) Zhu, Y.; Wan, S.; Jin, Y.; Zhang, W. *J. Am. Chem. Soc.* **2015**, *137*, 13772.

(41) Hartley, C. S.; Elliott, E. L.; Moore, J. S. *J. Am. Chem. Soc.***2007**, *129*, 4512.

(42) Elliott, E. L.; Hartley, C. S.; Moore, J. S. *Chem. Comm.* **2011**, *47*, 5028.

(43) Beeren, S. R.; Pittelkow, M.; Sanders, J. K. M. *Chem. Comm.* **2011**, *47*, 7359.

(44) Wei, T.; Jung, J. H.; Scott, T. F. *J. Am. Chem. Soc.* **2015**, *137*, 16196.

(45) Slater, A. G.; Cooper, A. I. *Science* **2015**, *348*.

(46) Liu, M.; Little, M. A.; Jelfs, K. E.; Jones, J. T. A.; Schmidtmann, M.; Chong, S. Y.; Hasell, T.; Cooper, A. I. *J. Am. Chem. Soc.* **2014**, *136*, 7583.

(47) Jelfs, K. E.; Eden, E. G. B.; Culshaw, J. L.; Shakespeare, S.; Pyzer-Knapp, E. O.; Thompson, H. P. G.; Bacsa, J.; Day, G. M.; Adams, D. J.; Cooper, A. I. *J. Am. Chem. Soc.* **2013**, *135*, 9307.

(48) Acharyya, K.; Mukherjee, S.; Mukherjee, P. S. *J. Am. Chem. Soc.* **2013**, *135*, 554.

(49) O'Reilly, N.; Giri, N.; James, S. L. *Chem. Eur. J.* **2007**, *13*, 3020.

(50) Greenaway, R. L.; Holden, D.; Eden, E. G. B.; Stephenson, A.; Yong, C. W.; Bennison, M. J.; Hasell, T.; Briggs, M. E.; James, S. L.; Cooper, A. I. *Chem. Sci.* **2017**, *8*, 2640.

(51) Mitra, T.; Jelfs, K. E.; Schmidtmann, M.; Ahmed, A.; Chong, S. Y.; Adams, D. J.; Cooper, A. I. *Nat. Chem.* **2013**, *5*, 276.

(52) Kewley, A.; Stephenson, A.; Chen, L.; Briggs, M. E.; Hasell, T.; Cooper, A. I. *Chem. Mater.* **2015**, *27*, 3207.

(53) Klosterman, J. K.; Yamauchi, Y.; Fujita, M. *Chem. Soc. Rev.* **2009**, *38*, 1714.

(54) Joy, A.; Schuster, G. B. *Chem. Comm.* **2005**, 2778.

(55) Wu, W.; Liu, Y.; Zhu, D. *Chem. Soc. Rev.* **2010**, *39*, 1489.

(56) Chen, Z.; Lohr, A.; Saha-Moller, C. R.; Wurthner, F. *Chem. Soc. Rev.* **2009**, *38*, 564.

(57) Schneebeli, S. T.; Kamenetska, M.; Cheng, Z.; Skouta, R.; Friesner, R. A.; Venkataraman, L.; Breslow, R. *J. Am. Chem. Soc.* **2011**, *133*, 2136.

(58) Solomon, G. C.; Herrmann, C.; Vura-Weis, J.; Wasielewski, M. R.; Ratner, M. A. *J. Am. Chem. Soc.* **2010**, *132*, 7887.

(59) Bartholomew, G. P.; Bazan, G. C. *Acc. Chem. Res.* **2001**, *34*, 30.

(60) Boydston, A. J.; Bondarenko, L.; Dix, I.; Weakley, T. J. R.; Hopf, H.; Haley, M. M. *Angew. Chem. Int. Ed.***2001**, *40*, 2986.

Chapter 2 . Rigid Two- and Three-tiered Stacked Architectures by Covalent Assembly

Paper published from the work in this chapter: F. Ren, K. Day, C. S. Hartley, *Angew. Chem. Int. Ed.* 2016, *55*, 8620-8623.

All computational calculations and figures in this chapter were performed by Dr. C. Scott Hartley.

2.1 Introduction

Dynamic covalent chemistry (DCC) is a powerful approach to the synthesis of large organic molecules. Because its reversibility allows for error-checking as the system approaches equilibrium, many bonds can be formed in a single assembly step.[1] Thus, remarkable examples of macrocycles, cages, ladders, and more-complex architectures have been prepared using DCC.[2–10] We are interested in the general problem of using DCC to assemble discotic monomers into multi-tiered stacks; formally, this corresponds to the creation of fused cages (albeit with little free volume). General strategies toward such structures, essentially multitiered cyclophanes,[11–13] would enable the efficient synthesis of finite stacks of chromophores for through-space energy and charge transport[14] and tubular structures through the stacking of macrocycles.[15] Discrete discotic stacks have been prepared, for example, by using coordination chemistry[16,17] or in the solid state.[18] However, fully organic, solution-phase multi-tiered architectures, while already known to have interesting electronic properties,[19–21] are typically prepared using stepwise, often low-yielding syntheses.[11–13,22,23] Here, we show that imine formation can be used to assemble two- and three-tiered stacked architectures. The strategy is effective considering the complexity of the products, although unexpected side-products are formed, underscoring the challenges of assembling rigid, three-dimensional molecules at equilibrium. The target stacks are chiral triple helices, with conformational dynamics that depend strongly on the number of tiers.

2.2 Results and Discussion

2.2.1 Synthesis

Our synthetic strategy is to functionalize a core structure—benzene for these proof-of-principle studies—with arms bearing aldehyde and amino coupling partners. As a first step, we tested the assembly of two-tiered stack **2T**, as shown in **Scheme 2.1**. In the presence of trifluoroacetic acid (12 mol%) in chloroform-d, monomers **1** (10 mM) and **2** (1.1 eq) assemble to give **2T**, as judged by ^{1}H NMR (see **Figure 2.1**). Only signals corresponding to **1**, **2T**, and a partially assembled diimine (i.e., **2T** but with one uncoupled aldehyde/amino pair) are observed. The reaction proceeds quickly, with high conversion after only 15 min, and approximately 90% **2T** after 24 h (**Figure 2.1**). When carried out preparatively, the imines were reduced with $NaBH(OAc)_3$ to facilitate isolation; compound **2T′** was obtained in 78% overall yield.

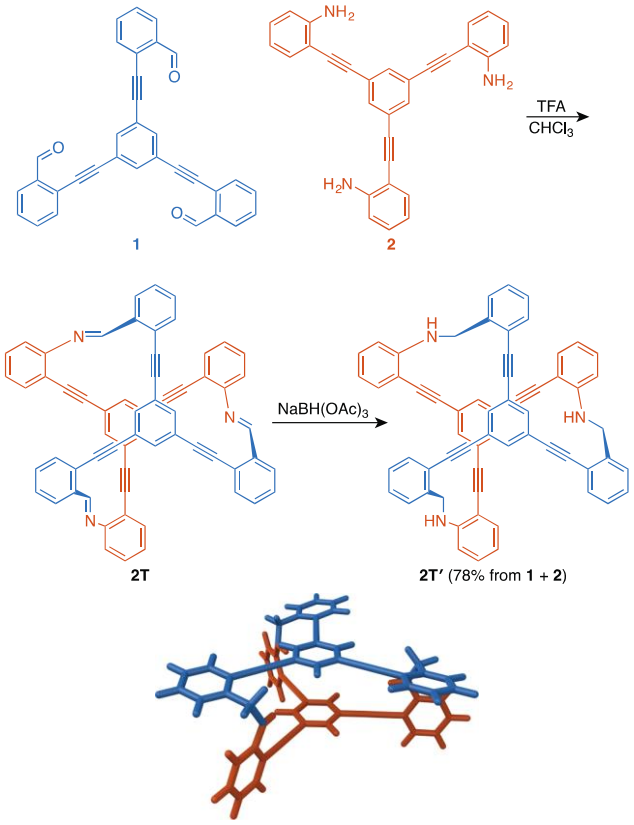

Scheme 2.1 Assembly of two-tiered stacks **2T**/**2T′**. The molecular model is of **2T′** (B3LYP/6-31G(d)).

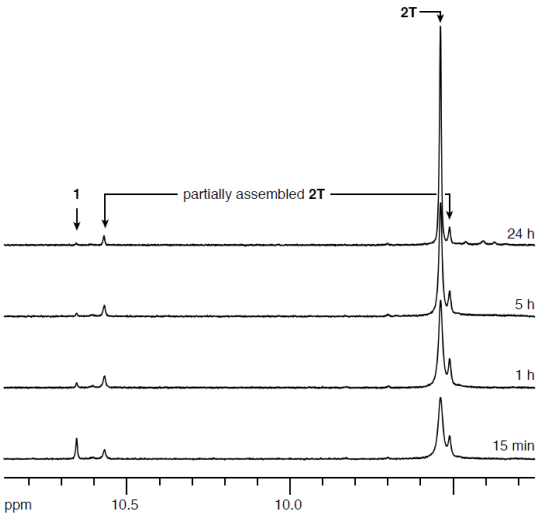

Figure 2.1 ^{1}H NMR monitoring of 2T.

We then attempted to prepare the three-tiered structure **3T** and its reduced form **3T′**, as shown in **Scheme 2.2**. Monomer **3**, with six pendant aldehydes, was combined with **2**. Using the same conditions as for the two-tiered system, the target (reduced) stack **3T′** was indeed isolated in 39% yield. However, unlike for the synthesis of **2T′**, a different, major product was isolated in 51% yield. This compound is isomeric with **3T′** and twofold symmetric (on the NMR timescale). NMR assignments, based on a rich ROESY spectrum, suggest that this product is $\mathbf{3T_{iso}'}$, a three-tiered structure with the "wrong" connectivity. ^{1}H NMR monitoring (**Scheme 2**.2) indicates that the reaction mixture at equilibrium consists of a mixture of primarily $\mathbf{3T_{iso}}$ and a unsymmetrical species with six distinct imine/aldehyde peaks that likely represents a direct precursor to **3T** with a free aldehyde/amine pair.

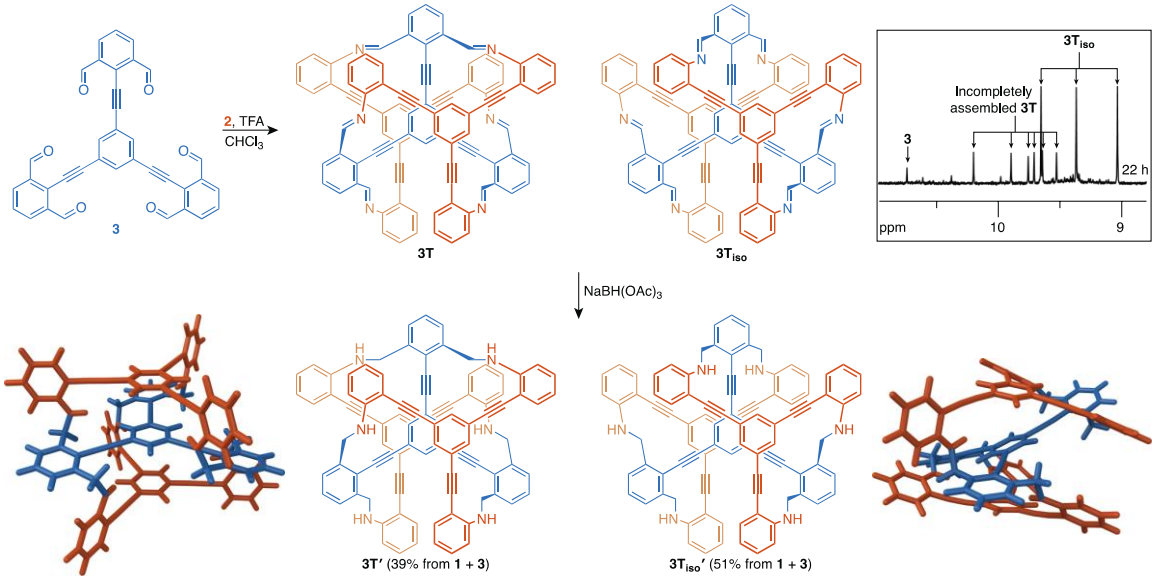

Scheme 2.2 Assembly of three-tiered stacks **3T**/**3T′** and misaligned isomers $\mathbf{3T_{iso}}$/$\mathbf{3T_{iso}'}$. The molecular models are of **3T′** and $\mathbf{3T_{iso}'}$ (B3LYP/6-31G(d)). Top right: ^{1}H NMR spectrum (22 h) of the mixture of **3**, $\mathbf{3T_{iso}}$, and an incompletely assembled stack.

We also examined the alternate route to three-tiered stacks with the same ABA stacking pattern. Thus, we prepared diamino monomer **4** (the tert-butyl groups were included for synthetic convenience, but radiate outward from the structure and should not influence assembly). Surprisingly, as shown in **Scheme 2.3**, when combined with two equivalents of monomer **1**, ^{1}H NMR monitoring indicates that assembly stops at the two-tiered stack $\mathbf{2T_B}$, leaving one equivalent of **1** unreacted. After reduction, we obtained the partially assembled $\mathbf{2T_B'}$ in 52% yield as the only isolable product. Attempts to construct $\mathbf{3T_B'}$ by a subsequent reductive amination of $\mathbf{2T_B'}$ with additional **1** were unsuccessful.

The isolation of $\mathbf{3T_{iso}}$ and $\mathbf{2T_B}$ highlights some of the challenges of designing systems for thermodynamically controlled assembly. The formation of $\mathbf{2T_B}$ was especially surprising since we had assumed that addition of the first tier would, by freezing out the rotational freedom available to diamino monomer **4**, preorganize the amino groups for addition of the next equivalent of **1**. Taken together, the byproducts suggest that there is a small amount of strain inherent to the basic **2T**/**3T**/$\mathbf{3T_B}$ architecture, likely because of the twisting of the arms out of conjugation with the central arene unit and subtle angle strain in the final assemblies. The target architectures are fairly rigid and compact (see below), which allows only limited flexibility to

relieve such strain. Nevertheless, the strategy described here is an efficient route to multi-tiered, multi-component covalent structures: despite their complexity, compounds **2T′** and **3T′** are each available in only three total steps from commercially available starting materials.

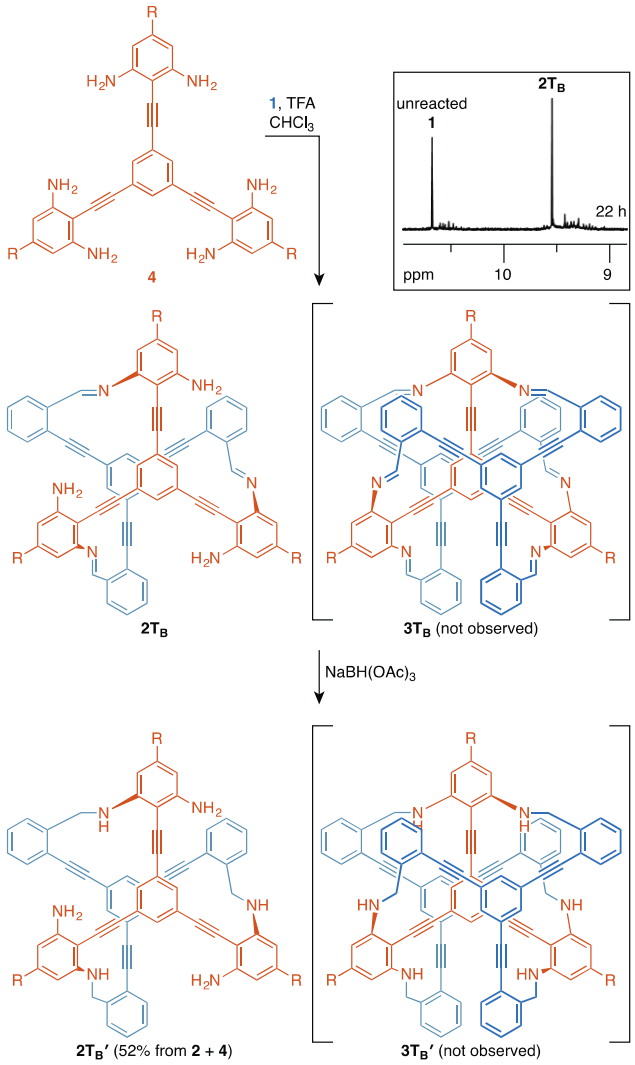

Scheme 2.3 Attempted assembly of three-tiered stack $\mathbf{3T_B}$. Top right: ^{1}H NMR monitoring of the assembly of **1** (2 eq) and **4**.

2.2.2 Conformational Analysis

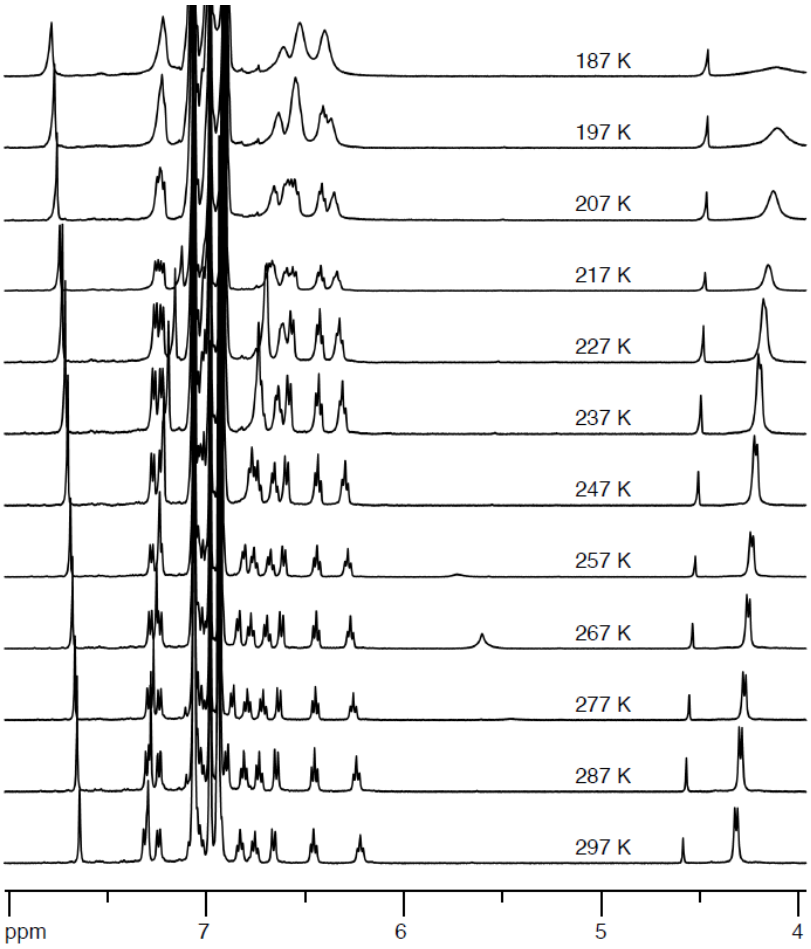

Figure 2.2 Variable temperature ^{1}H NMR of 2T′. (toluene-d_8, 500 MHz).

To better understand the structures of **2T′** and **3T′**, their geometries were optimized by DFT. At the B3LYP/6-31G(d) level, the optimized structures, shown in **Schemes 2.1** and **2.2**, are highly symmetrical, in the C_3 and D_3 point groups, respectively. The structure of **2T′** is reminiscent of recent (two-tiered) cages from Zhang[24] and Katoono.[25] For both **2T′** and **3T′**, the stacked central arenes are twisted by 28 °and separated by 4.15 Å.

For these stacked, helical architectures, racemization should occur via a twisting of the overall structure (e.g., **Figure 2.3**, top). The conformational dynamics of **2T′** and **3T′** are surprisingly different, however. For **2T′** at room temperature (toluene-*d*8), only one ^{1}H NMR signal is observed for the diastereotopic methylene protons (**C<u>H</u>$_2$NH**). Cooling the solution causes little change until shortly before all of the signals broaden around −50 °C (see **Figure 2.2**). In contrast, as shown in **Figure 2.3**, the two methylene protons of **3T′** are clearly distinguishable

by ^{1}H NMR at room temperature; thus, interconversion between the (*M*)- and (*P*)-enantiomers of **3T′** is slow on the NMR time scale. On heating, the signals broaden, nearly reaching coalescence at 370 K (the upper limit for the experiment), giving a free energy of activation of $\Delta G^{\neq}_{370} \approx 17$ kcal/mol.

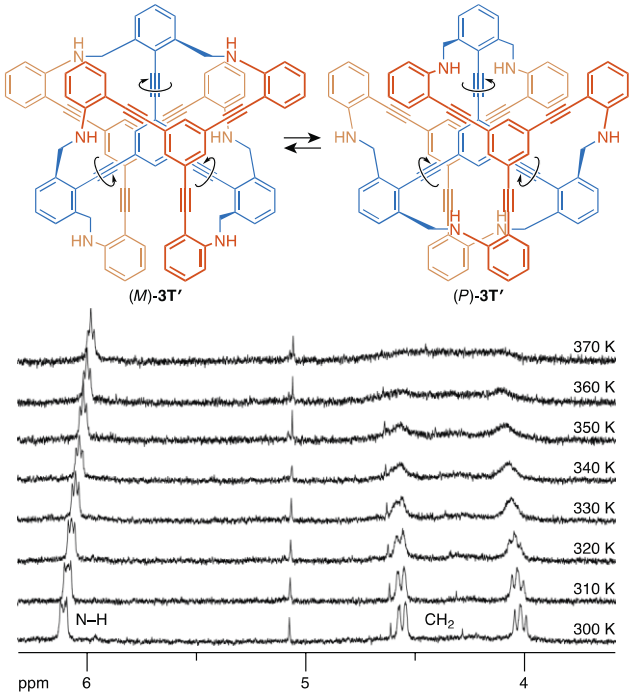

Figure 2.3 Variable temperature 1H NMR of **3T′** (toluene-d_8, 500 MHz).

This contrast between the two- and three-tiered structures is remarkable. For **2T′**, either the behavior parallels that of **3T′**, but (1) the methylene NMR signals are coincidentally isochronous or (2) (*M*)- and (*P*)-**2T′** interconvert quickly; or (3) the conformational behavior is distinct from **3T′** in that many conformational states are sampled. DFT calculations (B3LYP/6-31G(d)) suggest that the diastereotopic protons in both **2T′** and **3T′** should have nearly identical chemical shifts; option 1 is therefore unlikely. To better understand the conformational behavior, we calculated the conformational potential energy surface (PES) of **2T′** and **3T′** using the semi-empirical PM6 method,[26] which allowed a large number of conformational states to be explicitly optimized. We focused on simultaneous rotation about two of the three aldehyde-derived arms, as defined by the dihedral angles φ_1 and φ_2 in **Figure 2.4**, near the global energy minimum ($\varphi_1 \approx \varphi_2 \approx 0°$). The calculations do not identify any additional conformers for **2T′**; thus,

option 3 is unlikely. The two-tiered stack therefore adopts well-defined enantiomeric conformers that simply interconvert much more rapidly than for **3T′**. The VT NMR results indicate that the barrier to racemization for **2T′** must be at least ~10 kcal/mol below that of **3T′**, assuming a negligible $\Delta S^{\neq}$. One contribution to the smaller barrier is that the three-tiered structure adds an additional stacking interaction between the central arenes. However, this alone can only account for only a fraction of the difference. The third tier must also add an element of coupling that is not present in **2T′**; that is, conformational changes in **3T′** are slower because one part of the molecule cannot move without perturbing another in these rigid, interconnected structures.

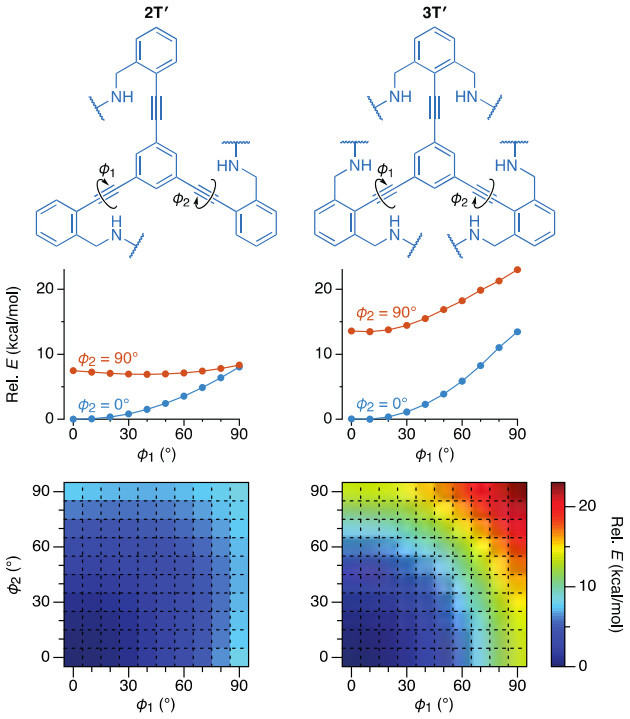

Figure 2.4 PM6 conformational energy surfaces for rotation about φ1 and φ2 in 2T′ and 3T′. Middle: relative energy vs φ_1 for limiting values of φ_2. Bottom: Heat map of the conformational energy as a function of both φ_1 and φ_2.

This hypothesis is fully consistent with the PM6 calculations (**Figure 2.4**). First, the overall energy minimum for **2T′** is indeed much shallower than that of **3T′**. Secondly, there is a flexibility to **2T′**, manifested in φ_1 and φ_2, that is absent for **3T′**. For **2T′**, once one arm has rotated, it costs little additional energy to rotate the second (note the flat dependence of E on φ_1 once φ_2 = 90 °). In contrast, for **3T′**, rotation about the second arm is nearly as difficult as for the

first. This additional coupling between the tiers suggests that architectures of this basic form essentially become more rigid as their size increases.

2.3 Conclusion

In summary, we have developed a simple strategy for the synthesis of two- and three-tiered stacked architectures using DCC. While misaligned and incompletely assembled compounds have also been obtained, the method is efficient considering its brevity and the structural complexity of the products. Variable temperature NMR studies indicate that the conformational behavior of the two- and three-tiered structures is quite different, with the additional tier affording much slower conformational racemization. Computational results show that the additional tier deepens the energy wells for the most-stable conformers and increases conformational coupling between the subunits.

2.4 Experimental

2.4.1 Stack Assembly

***Rigid Two-Tiered Stack 2*T'**

To a scintillation vial containing **1** (11.3 mg, 0.024 mmol), **2** (11.8 mg, 0.028 mmol), and 3Å molecular sieves was added $CHCl_3$ (2 mL), followed by a solution of CF_3CO_2H (0.33 mg, 0.0029 mmol) in $CHCl_3$ (0.2 mL). After stirring for 5 h at rt, $NaBH(OAc)_3$ (31 mg,0.15 mmol) was added and stirring was continued for 3h. The reaction mixture was then quenched with sat. $NaHCO_3$(aq). The resulting suspension was diluted with $CHCl_3$, washed with water (2×), dried ($MgSO_4$), filtered, and concentrated. Purification by flash chromatography (4:1 toluene/hexanes) gave **2T′** as a light yellow solid (16 mg, 0.019 mmol, 78%): mp 123 ° C dec; ^{1}H NMR (500 MHz, C_6D_6,) δ 7.69 (s, 2H), 7.41 (d, J = 7.3 Hz, 2H), 7.35–7.30 (m, 4H), 7.09 (t, J = 7.6 Hz, 2H), 6.98 (d, J = 7.3 Hz, 2H), 6.87 (t, J = 7.0 Hz, 2H), 6.80 (t, J = 7.2 Hz, 2H), 6.74 (d, J = 8.4 Hz, 2H), 6.51 (t, J = 7.4 Hz, 2H), 6.33(t, J = 7.4 Hz, 2H), 4.38 (d, J = 7.4 Hz, 4H); ^{13}C NMR (125 MHz, C_6D_6,) δ 148.7, 142.0, 134.5, 133.8, 133.5, 132.3, 130.0, 129.4, 128.5, 127.3, 124.2, 123.8, 122.1, 116.9, 110.4, 108.6, 93.5, 93.4, 89.8, 87.2, 46.8; HRMS (MALDI) calcd for $C_{63}H_{40}N_3$ ([M+H$^+$]) 838.32167, found 838.32214.

Rigid Three-Tiered Stacks 3T′ and $3T_{iso}$′

To a scintillation vial containing **2** (18 mg, 0.043 mmol), **3** (10.9 mg, 0.020 mmol), and 3Å molecular sieves was added $CHCl_3$ (3 mL), followed by a solution of CF_3CO_2H (0.55 mg, 0.0048 mmol) in $CHCl_3$ (0.3 mL). After stirring for 5 h at rt, $NaBH(OAc)_3$ (51 mg, 0.24 mmol) was added and stirring was continued for 3 h. The reaction mixture was then quenched with sat. $NaHCO_3$ (aq). The resulting suspension was diluted with $CHCl_3$, washed with water (2×), dried ($MgSO_4$), filtered, and concentrated. Purification by flash chromatography (toluene) gave **3T′** as a light yellow solid (10.0 mg, 0.0077 mmol, 39%): mp 120 ℃ dec; ^{1}H NMR (500 MHz, C_6D_6) δ 7.70 (s, 3H) 7.33 (dd, J = 7.6, 1.5 Hz, 6H), 7.28 (s, 6H), 7.08 (ddd, J = 8.4,7.5, 1.2 Hz, 6H), 6.8–6.7 (m, 9H), 6.63 (d, J = 8.3 Hz, 6H), 6.53 (td, J = 7.5, 0.9 Hz, 6H), 6.16 (m, 6H), 4.58 (dd, J = 15.0, 3.2 Hz, 6H), 4.03 (dd, J = 14.6, 11.7 Hz, 6H); ^{13}C NMR (126 MHz, C_6D_6) δ 149.0, 143.5, 134.8, 133.4, 132.6, 130.4, 128.9, 127.6, 124.1, 123.0, 121.7, 117.0, 110.6, 108.3, 98.6, 93.4, 88.8, 87.7, 46.8; HRMS (MALDI) calcd for $C_{96}H_{61}N_6$ ([M+H$^+$]) 1297.49522, found1297.49407.

Compound **$3T_{iso}$′** was also isolated (13.3 mg, 51%): mp 111 ℃ dec; ^{1}H NMR (500 MHz, C_6D_6) δ 7.51 (t, J = 1.6 Hz, 1H), 7.50 (dd, J = 7.2,1.4 Hz, 2H), 7.33 (dd, J = 7.5, 1.4 Hz, 2H), 7.29 (d, J = 1.5 Hz, 2H), 7.23 (ddd, J = 7.6, 7.6, 0.4 Hz, 2H), 7.18 (t, J = 1.5 Hz, 2H), 7.15 (dd, 2H), 7.12 (dd, J = 7.6, 1.4 Hz, 2H), 7.05 (dd, J = 7.5, 1.1 Hz, 2H), 7.01 (ddd, J = 7.5, 7.5, 0.5 Hz, 2H), 6.99 (dd, J = 7.5, 1.0 Hz, 2H), 6.94 (dd, J = 7.5, 7.5 Hz, 2H), 6.87 (d, J = 6.9 Hz, 2H), 6.86 (t, J = 1.5 Hz, 2H), 6.75 (d, J = 7.8 Hz, 2H), 6.74 (t, 1H), 6.69 (t, J = 1.5 Hz, 2H), 6.68 (ddd, J = 7.4, 7.4, 0.4 Hz, 2H), 6.66 (d, J = 7.8 Hz, 2H), 6.62 (d, J = 8.2 Hz, 2H), 6.53 (dd, J = 7.4, 7.4 Hz, 2H), 6.43 (dd, J = 7.5, 7.5 Hz, 2H), 5.87 (dd, J = 11.3, 2.4 Hz, 2H), 5.59 (d, J = 10.4 Hz, 2H), 5.59 (d, J = 10.4 Hz, 2H), 4.78 (dd, J = 14.2, 2.4 Hz, 2H), 4.38 (dd, J = 13.7, 1.8 Hz, 2H), 4.26 (dd, J = 13, 13 Hz, 2H), 4.11 (dd, J = 12 Hz, 2H), 4.04 (dd, 2H), 4.04 (d, 2H); ^{13}C NMR (125 MHz, C_6D_6) δ 149.9, 149.3, 143.6, 142.3, 141.7, 137.0, 136.4, 132.8, 132.6, 131.8, 131.7, 131.5, 130.7, 130.4, 130.2, 130.1, 129.8, 124.1, 123.8, 123.6, 122.9, 122.8, 122.5, 121.6, 117.1, 116.9, 111.7, 111.2, 110.7, 108.8, 108.3, 107.8, 98.7, 98.2, 95.05, 95.02, 93.3, 89.4, 89.1, 88.0, 87.4, 87.2, 47.9, 47.6, 47.2; HRMS (MALDI) calcd for $C_{96}H_{61}N_6$ ([M+H$^+$]) 1297.49522, found 1297.49389.

Two-Tiered Stack $2T_B$′

To a scintillation vial containing **1** (13 mg, 0.028 mmol), **4** (10.5 mg, 0.016 mmol), and 3Å molecular sieves was added $CHCl_3$ (3 mL), followed by a solution of CF_3CO_2H (0.225 mg,

0.0020 mmol) in $CHCl_3$ (0.3 mL). After stirring for 5 h at r.t., $NaBH(OAc)_3$ (105 mg, 0.5 mmol) was added and stirring was continued for 3 h. The reaction mixture was then quenched with sat. $NaHCO_3$(aq). The resulting suspension was diluted with $CHCl_3$ (10 mL), washed with water (2×), dried ($MgSO_4$), filtered, and concentrated. Purification by flash chromatography (toluene) gave **$2T_B'$** as a light yellow solid (9.0 mg, 0.0086 mmol, 52%): ^{1}H NMR (500 MHz, $CDCl_3$) δ 7.65–7.60 (m, 3H), 7.47 (s, 3H), 7.40–7.35 (m, 3H), 7.33 (s, 3H), 7.29–7.24 (m, 6H), 6.36 (d, J = 1.5 Hz, 3H), 6.10 (d, J = 1.5 Hz, 3H), 4.64 (s, 6H), 4.12(brs, 6H), 1.29(s, 27H); ^{13}C NMR spectroscopy was not performed because of difficulties in purification, isolation, and stability; HRMS (MALDI) calcd for $C_{75}H_{67}N_6$ ([M+H$^+$]) 1051.54217, found 1051.54237.

2.4.2 Monomer Synthesis

Synthesis of monomer 1

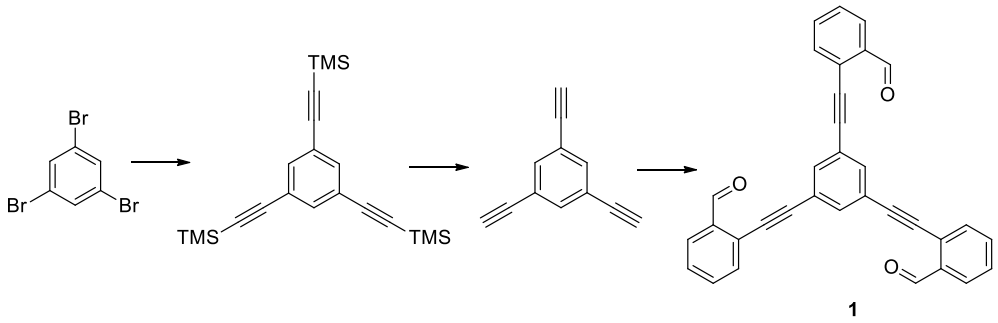

Scheme 2.4 Synthesis of monomer **1**.

Compound (1) Sonogashira coupling of **1,3,5-tribromobenzene** (4.00 g, 12.7 mmol) with **ethynyltrimethylsilane** (9 mL, 63.5 mmol) yield brown oil **1,3,5-tris((trimethylsilyl)ethynyl)benzene** [4] (3.41 g, 73%) which was deprotected with potassium carbonate to give brow solid **1,3,5-triethynylbenzene** [27]. **1,3,5-triethynylbenzene** was further purified with recrystallization from hexanes to yield a white crystal (1.17 g, 34%). A Schlenk tube containing $PdCl_2PPh_2$ (14 mg, 0.02 mmol), CuI (3.8 mg, 0.02 mmol), PPh_3 (5.2 mg, 0.02 mmol) and 2-bromobenzaldehyde (1.00 g, 0.4 mmol) was evacuated and backfilled with argon (3×). To this solid mixture was added a solution of **1,3,5-triethynylbenzene** (20 mg, 0.133 mmol) in NEt_3 (25 mL) and THF (5 mL). The suspension was degassed by three freeze-pump-thaw cycles and heated with stirring at 90 ℃ for 18 h. The resulting suspension was diluted with DCM (30 mL), washed with water (2 × 15 mL), dried ($MgSO_4$), filtered, and concentrated. Purification by flash chromatography (7:3 hexanes/EtOAc) gave **1** as white solid (34 mg, 54%);

mp 185.1 ℃; ^{1}H NMR (500 MHz, $CDCl_3$) δ 10.65 (s, 3H), 7.98 (d, *J* = 7.8 Hz, 3H), 7.78 (s, 3H), 7.69 (d, *J* = 7.5 Hz, 3H), 7.63 (dd, *J* = 10.8, 4.3 Hz, 3H), 7.52 (t, *J* = 7.5 Hz, 3H); ^{13}C NMR (126 MHz, $CDCl_3$) δ 191.3, 136.2, 134.8, 134.0, 133.6, 129.3, 127.8, 125.9, 123.8, 94.0, 86.8; HRMS (MALDI) calcd for $C_{33}H_{19}O_3$ ([M+H$^+$]) 463.13287, found: 463.13288.

Synthesis of monomer 2

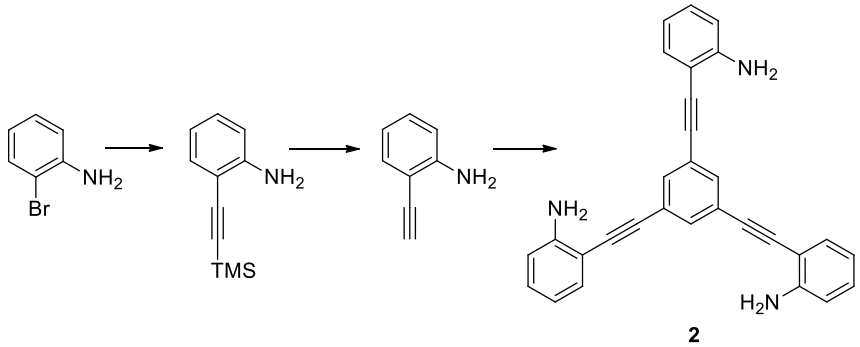

Scheme 2.5 Synthesis of monomer **2**.

Compound (2) Sonogashira coupling of **2-bromoaniline** (1.72 g, 10 mmol) with **trimethylsilyacetylene** (2.00 g, 20 mmol) yield brown oil **2-((trimethylsilyl)ethynyl)aniline** [28] (3.11 g, 82%) which was deprotected with **potassium carbonate** without further purification to give brow gel **2-ethynylaniline** [29] (1.30 g, 68%). A Schlenk tube containing $Pd(OAc)_2$ (21.4 mg, 0.789 mmol), CuI (13.5 mg, 0.07 mmol), PPh_3 (137 mg, 0.52 mmol) and **1,3,5-tribromobenzene** (248 mg, 0.789 mmol) was evacuated and backfilled with argon (3×). To this solid mixture was added a solution of **2-ethynylaniline** (301.5 mg, 2.57 mmol) in **diisopropylamine** (15 mL) and THF (5 mL). The suspension was degassed by three freeze-pump-thaw cycles and heated with stirring at 75 ℃ for 18 h. The resulting suspension was diluted with EtOAc (30 mL), washed with water (2 × 15 mL), dried ($MgSO_4$), filtered, and concentrated. Purification by flash chromatography (19:1 hexanes/EtOAc) gave **2** as a brown solid. Recrystallization with $CHCl_3$ gave a yellow crystal(187 mg, 56%); ^{1}H NMR (500 MHz, Acetone) δ 7.74 (s, 3H), 7.32 (dd, *J* = 7.6, 1.2 Hz, 3H), 7.17 – 7.09 (m, 3H), 6.81 (d, *J* = 8.3 Hz, 3H), 6.62 (t, *J* = 7.5 Hz, 3H), 5.27 (s, 4H); Spectroscopic characterization of this compound was in agreement with the literature.[30]

Synthesis of monomer 3

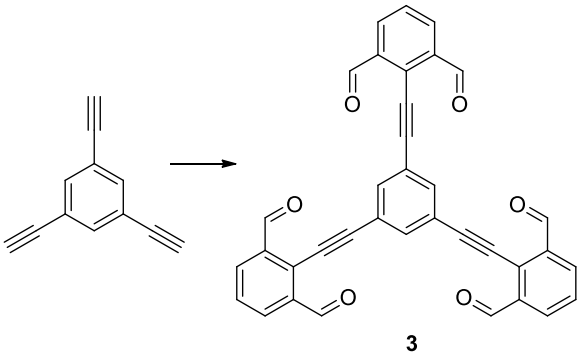

3

Scheme 2.6 Synthesis of monomer **3**.

Compound (3) A Schlenk tube containing $PdCl_2PPh_2$ (14 mg, 0.02 mmol), CuI (4 mg, 0.02 mmol), PPh_3 (5 mg, 0.02 mmol) and **2-bromoisophthalaldehyde** (85 mg, 0.4 mmol) was evacuated and backfilled with argon (3×). To this solid mixture was added a solution of **1,3,5-triethynylbenzene** (20 mg, 0.13 mmol) in NEt_3 (25 mL) and THF (5 mL). The suspension was degassed by three freeze-pump-thaw cycles and heated with stirring at 90 ℃ for 18 h. The resulting suspension was diluted with DCM (30 mL), washed with water (2 × 15 mL), dried ($MgSO_4$), filtered, and concentrated. Purification by flash chromatography (DCM) gave **3** as white solid(31 mg, 45%); mp 88 ℃ dec; ^{1}H NMR (500 MHz, $CDCl_3$) δ 10.74 (s, 6H), 8.24 (d, *J* = 7.7 Hz, 6H), 7.91 (s, 3H), 7.68 (t, *J* = 7.7 Hz, 3H); ^{13}C NMR (126 MHz, $CDCl_3$) δ 190.0, 136.9, 135.5, 133.2, 129.6, 127.7, 123.4, 100.1, 82.9; HRMS (MALDI) calcd for $C_{36}H_{18}O_6$ (M^+) 546.11034, found 546.10979.

Synthesis of monomer 4

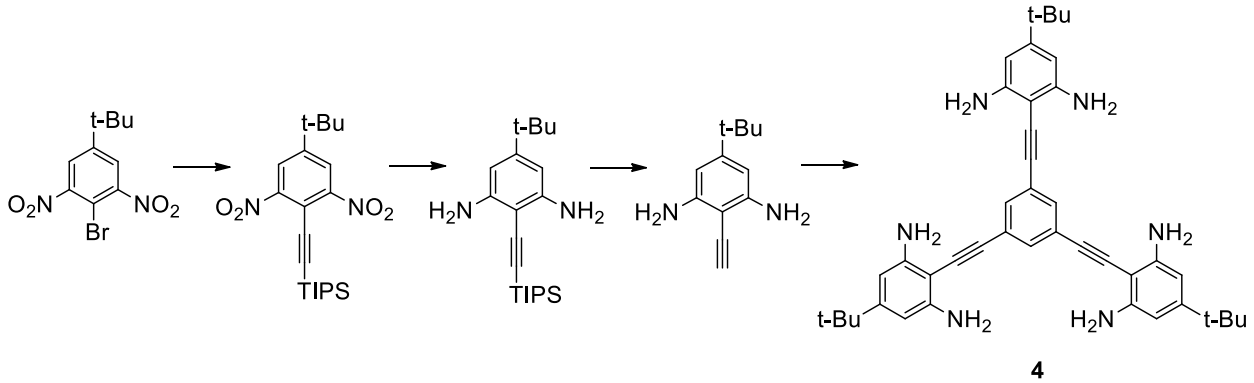

4

Scheme 2.7 Synthesis of monomer **4**.

((4-(tert-butyl)-2,6-dinitrophenyl)ethynyl)triisopropylsilane

A Schlenk tube containing $PdCl_2(PPh_3)_2$ (242 mg, 0.35 mmol), CuI (22 mg, 0.11 mmol), and **2-bromo-5-(tert-butyl)-1,3-dinitrobenzene** **2-bromo-5-(tert-butyl)-1,3-dinitrobenzene**[31] (3.5 g, 11.5 mmol) was evacuated and backfilled with argon (3×). To this solid mixture was added a solution of **(triisopropylsilyl)acetylene** (5 mL, 22 mmol) in diisopropylamine (25 mL) and THF (5 mL). The suspension was degassed by three freeze-pump-thaw cycles and heated with stirring at 70 ℃ for 18 h. The resulting suspension was diluted with DCM (100 mL), washed with water (2 × 50 mL), dried ($MgSO_4$), filtered, and concentrated. Purification by flash chromatography (19:1 hexanes/EtOAc) and recrystallized from (19:1 hexanes/EtOAc) to give **((4-(tert-butyl)-2,6-di-nitro-phenyl)ethynyl)tri-isopropyl-silane** as yellow crystal (3.0 g, 65%); m.p. 154.1 ℃; ^{1}H NMR (500 MHz, $CDCl_3$) δ 8.07 (s, 2H), 1.38 (s, 10H), 1.25 – 1.05 (m, 21H). ^{13}C NMR (126 MHz, $CDCl_3$) δ 153.9, 152.5, 124.5, 110.3, 110.1, 93.6, 35.8, 30.7, 18.5, 11.2; HRMS (MALDI) calcd for $C_{21}H_{32}N_2O_4Si$ (M^+) 404.21313, found 404.21221.

5-(*tert*-Butyl)-2-ethynylbenzene-1,3-diamine

To a round bottom flask charged with **((4-(tert-butyl)-2,6-di-nitro-phenyl)ethynyl)tri-isopropylsilane** (2.73 g, 6.75 mmol) was added CH_2Cl_2 (150 mL) and DMF (100 mL). Solid $SnCl_2{\cdot}2H_2O$ (76.3 g, 338 mmol) was added slowly. The reaction mixture was stirred at r.t. for 3 h, then poured into sat. $NaHCO_3$ (aq) (1 L). The resulting suspension was filtered through Celite, washing with DCM (1 L), then washed with brine (4×), dried ($MgSO_4$), filtered, and concentrated to give **5-(tert-butyl)-2-((tri-isopropyl-silyl)ethynyl)benzene-1,3-diamine** as a brown oil (1.67 g, 4.85 mmol, 72%) which was used in the next step without further purification: ^{1}H NMR (500 MHz, $CDCl_3$) δ 6.15 (s, 2H), 4.13 (s, 4H), 1.22 (s, 9H), 1.13 (s, 21H).

Compound **5-(tert-butyl)-2-((tri-isopropyl-silyl)ethynyl)benzene-1,3-diamine** (0.86 g, 2.5 mmol) was dissolved in THF (10 mL), then treated with a 1 M solution of TBAF in THF (2.74 mL, 3 mmol) and stirred for 30 min. The reaction mixture was then diluted with DCM, washed with brine (3×), dried ($MgSO_4$), filtered, and concentrated. Purification by flash chromatography (8:2 hexanes/EtOAc) gave **5-(*tert*-butyl)-2-ethynylbenzene-1,3-diamine** as a clear oil (0.46 g, 2.4 mmol, 98%, 71% over two steps): ^{1}H NMR (500 MHz, $CDCl_3$) δ 6.15 (s, 2H), 4.13 (s, 4H), 3.66 (s, 1H), 1.23 (s, 9H); ^{13}C NMR (125 MHz, $CDCl_3$) δ 154.5, 149.0, 101.8, 91.2, 87.4, 78.1, 34.8, 31.2.

Compound (4) A Schlenk tube containing $Pd(OAc)_2$ (37 mg, 0.09 mmol), CuI (23 mg, 0.07 mmol), PPh_3 (227 mg, 0.5 mmol) and 1,3,5-tribromobenzene (428 mg, 0.76 mmol) was evacuated and backfilled with argon (3×). To this solid mixture was added a solution of **5-(*tert*-butyl)-2-ethynylbenzene-1,3-diamine** (1281 mg, 3.0 mmol) in diisopropylamine (25 mL) and THF (5 mL). The suspension was degassed by three freeze-pump-thaw cycles and heated with stirring at 90 ℃ for 18 h. The resulting suspension was diluted with EtOAc (30 mL), washed with water (2 × 15 mL), dried ($MgSO_4$), filtered, and concentrated. Purification by flash chromatography (8:2 hexanes/EtOAc) gave **4** as brown solid crystal (417 mg, 48%); mp 162 ℃ dec. ^{1}H NMR (500 MHz, $CDCl_3$) δ 7.55 (s, 3H), 6.20 (s, 6H), 4.18 (s, 12H), 1.25 (s, 32H); ^{13}C NMR (126 MHz, $CDCl_3$) δ 154.7, 148.4, 132.8, 124.5, 102.0, 98.2, 92.0, 84.5, 34.8, 31.1; HRMS (MALDI) calcd for $C_{42}H_{49}N_6$ ([M+H$^+$]) 637.40132, found 637.40182.

Reference

(1) S. J. Rowan, S. J. Cantrill, G. R. L. Cousins, J. K. M. Sanders, J. F. Stoddart, *Angew. Chem. Int. Ed.* **2002**, *41*, 898.

(2) Y. Jin, Q. Wang, P. Taynton, W. Zhang, *Acc. Chem. Res.* **2014**, *47*, 1575.

(3) M. Mastalerz, *Angew. Chem. Int. Ed.* **2010**, *49*, 5042.

(4) J. Sun, J. L. Bennett, T. J. Emge, R. Warmuth, *J. Am. Chem. Soc.* **2011**, *133*, 3268.

(5) T. Mitra, K. E. Jelfs, M. Schmidtmann, A. Ahmed, S. Y. Chong, D. J. Adams, A. I. Cooper, *Nature Chem.* **2013**, *5*, 276.

(6) A. Granzhan, C. Schouwey, T. Riis-Johannessen, R. Scopelliti, K. Severin, *J. Am. Chem. Soc.* **2011**, *133*, 7106.

(7) C. D. Pentecost, K. S. Chichak, A. J. Peters, G. W. V. Cave, S. J. Cantrill, J. F. Stoddart, *Angew. Chem. Int. Ed.* **2007**, *46*, 218.

(8) C. S. Hartley, E. L. Elliott, J. S. Moore, *J. Am. Chem. Soc.* **2007**, *129*, 4512.

(9) T. Wei, J. H. Jung, T. F. Scott, *J. Am. Chem. Soc.* **2015**, *137*, 16196.

(10) N. Sakai, S. Matile, *J. Am. Chem. Soc.* **2011**, *133*, 18542.

(11) T. Otsubo, S. Mizogami, I. Otsubo, Z. Tozuka, A. Sakagami, Y. Sakata, S. Misumi, *Bull. Chem. Soc. Jpn.* **1973**, *46*, 3519.

(12) W. Grimme, H. T. Kämmerling, J. Lex, R. Gleiter, J. Heinze, M. Dietrich, *Angew. Chem. Int. Ed.* **1991**, *30*, 205.

(13) S. Mataka, K. Shigaki, T. Sawada, Y. Mitoma, M. Taniguchi, T. Thiemann, K. Ohga, N. Egashira, *Angew. Chem. Int. Ed.* **1998**, *37*, 2532.

(14) J. K. Klosterman, Y. Yamauchi, M. Fujita, *Chem. Soc. Rev.* **2009**, *38*, 1714.

(15) X. Xu, L. Wang, G. Wang, J. Lin, G. Li, X. Jiang, Z. Li, *Chem. Eur. J.* **2009**, *15*, 5763.

(16) S. Fujii, T. Tada, Y. Komoto, T. Osuga, T. Murase, M. Fujita, M. Kiguchi, *J. Am. Chem. Soc.* **2015**, *137*, 5939.

(17) T. Murase, K. Otsuka, M. Fujita, *J. Am. Chem. Soc.* **2010**, *132*, 7864.

(18) J. Stojaković, A. M. Whitis, L. R. MacGillivray, *Angew. Chem. Int. Ed.* **2013**, *52*, 12127.

(19) G. C. Bazan, *J. Org. Chem.* **2007**, *72*, 8615.

(20) M. Fujitsuka, S. Tojo, M. Shibahara, M. Watanabe, T. Shinmyozu, T. Majima, *J. Phys. Chem. A* **2010**, *115*, 741.

(21) Y. Wu, M. Frasconi, D. M. Gardner, P. R. McGonigal, S. T. Schneebeli, M. R. Wasielewski, J. F. Stoddart, *Angew. Chem. Int. Ed.* **2014**, *53*, 9476.

(22) D. Sakamaki, A. Ito, K. Tanaka, K. Furukawa, T. Kato, M. Shiro, *Angew. Chem. Int. Ed.* **2012**, *51*, 8281.

(23) Y. Yamada, T. Kubota, M. Nishio, K. Tanaka, *J. Am. Chem. Soc.* **2014**, *136*, 6505.

(24) C. Zhang, Q. Wang, H. Long, W. Zhang, *J. Am. Chem. Soc.* **2011**, *133*, 20995.

(25) R. Katoono, T. Suzuki, *Chem. Commun.* **2016**, *52*, 1029.

(26) S. E. Wheeler, J. W. G. Bloom, *J. Phys. Chem. A* **2014**, *118*, 6133.

(27) N. Sakai, K. Annaka, A. Fujita, A. Sato, T. Konakahara, *J. Org. Chem.* **2008**, *73*, 4160.

(28) C. Xu. *Org. Lett.* **2014**, *16*, 948.

(29) S. H. Lim, Y. Su, S. M. Cohen, *Angew. Chem. Int. Ed.* **2012**, *51*, 5106.

(30) S. W. Youn, S. R. Lee, *Org. Biomol. Chem.* **2015**, *13*, 4652.

(31) P. R. Ashton, K. D. M. Harris, B. M. Kariuki, D. Philp, J. M. A. Robinson, N. Spencer, *J. Chem. Soc. Perkin Trans.2* **2001**, 2166.

Spectral Data

NMR Assignments for 2T′

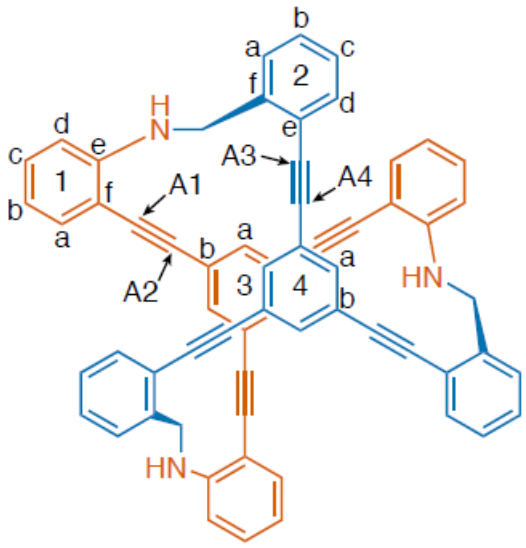

Position	^{1}H δ (ppm)	^{13}C δ (ppm)
1a	7.31	132.3
1b	6.51	116.8
1c	7.09	129.8
1d	6.74	110.4
1e		148.7
1f		108.6
2a	6.98	129.3
2b	6.87	128.5
2c	6.80	127.3
2d	7.41	133.5
2e		122.1

Position	^{1}H δ (ppm)	^{13}C δ (ppm)
2f		142.0
3a	7.31`	134.4
3b		123.9
4a	7.69	133.8
4b		124.0
NH	6.33	
CH_2	4.38	46.8
A1		87.2
A2		93.5
A3		89.8
A4		93.3

NMR Assignments for 3T′

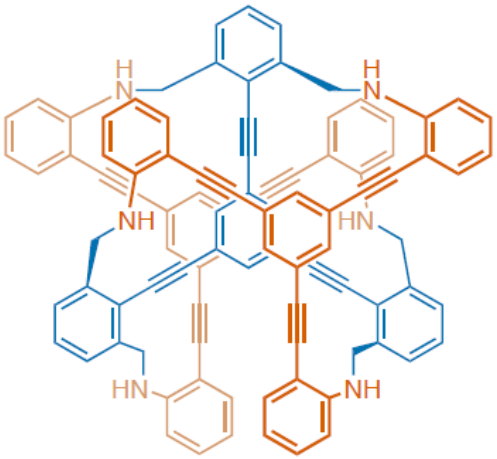

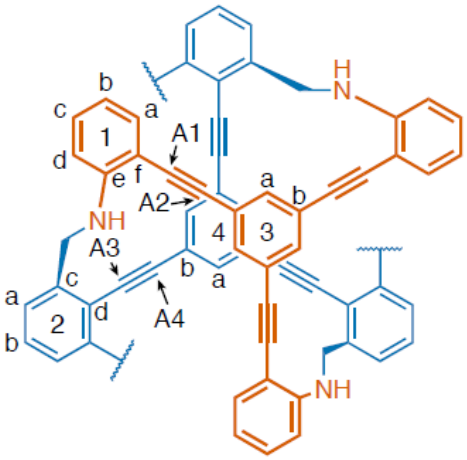

Position	^{1}H δ (ppm)	^{13}C δ (ppm)
1a	7.33	132.2
1b	6.53	116.7
1c	7.08	130.0
1d	6.64	110.3
1e		148.5
1f		108.3
2a	6.77	128.7
2b	6.74	127.7
2c		143.6
2d		121.8
3a	7.29	134.5

Position	^{1}H δ (ppm)	^{13}C δ (ppm)
3b		n/d
4a	7.68	133.3
4b		n/d
NH	6.15	
CH_2	4.05	46.5
	4.59	
A1		87.6
A2		93.4
A3		n/d
A4		98.5

NMR Assignments for 3Tiso'

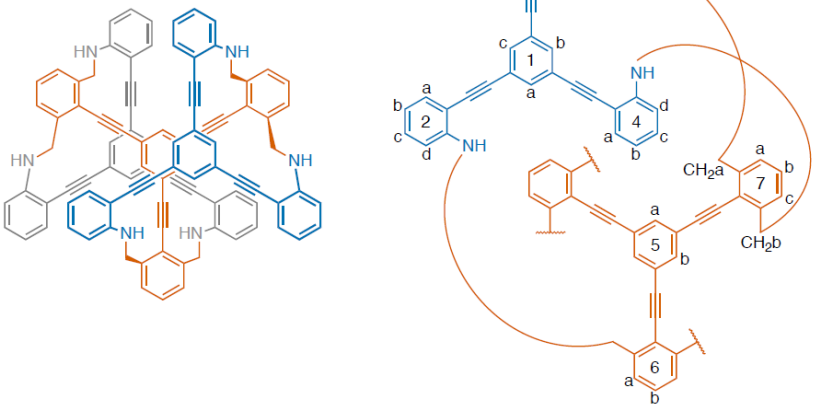

Position	^{1}H δ (ppm)	^{13}C δ (ppm)	ROESY
1a	7.18	132.4	6(CH_2)
1b	6.69	136.7	3(NH)
			4(NH)
1c	6.86	131.5	2(NH)
			3(NH)
2a	7.12	131.6	
2b	6.43	116.8	
2c	7.01	129.9	
2d	6.66	110.5	
2(NH)	5.87		1c
3a	7.33	131.6	
3b	6.53	116.8	
3c	7.23	130.2	
3d	6.75	111.4	7(CH_2a)
3(NH)	5.59		1b
			1c
4a	7.50	131.3	
4b	6.68	116.3	

Position	^{1}H δ (ppm)	^{13}C δ (ppm)	ROESY
4c	7.15	130.3	
4d	6.62	110.5	7(CH_2b)
4(NH)	5.59		1b
5a	7.51	136.1	7(CH_2a)
5b	7.29	132.6	6(CH_2)
			7(CH_2B)
6a	6.87	128.5	
6b	6.74	128.5	
6(CH_2)	4.26	47.3	1a
	4.78		5b
7a	7.05	129.8	
7b	6.94	129.6	
7c	6.99	129.8	
7(CH_2a)	4.04	47.7	3d
			5a
	4.11		3d
7(CH_2b)	4.04	46.9	4d
	4.38		5b

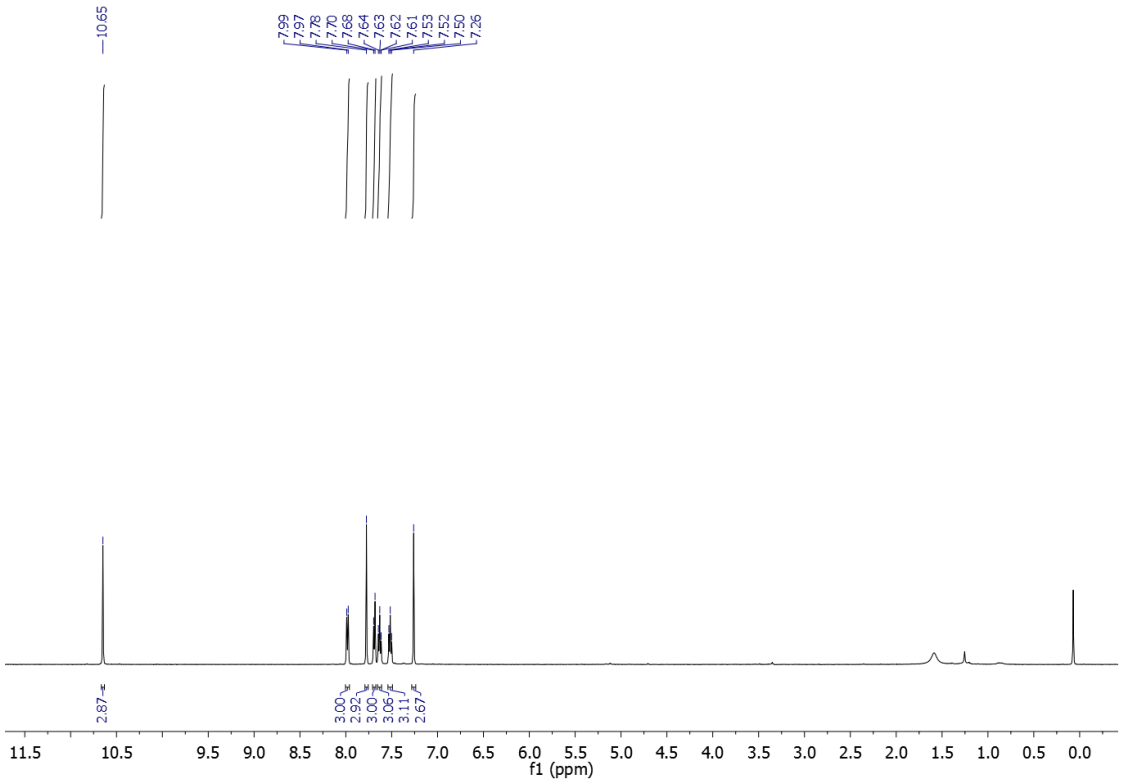

^{1}H NMR spectrum (500 MHz, $CDCl_3$) of compound **2**.

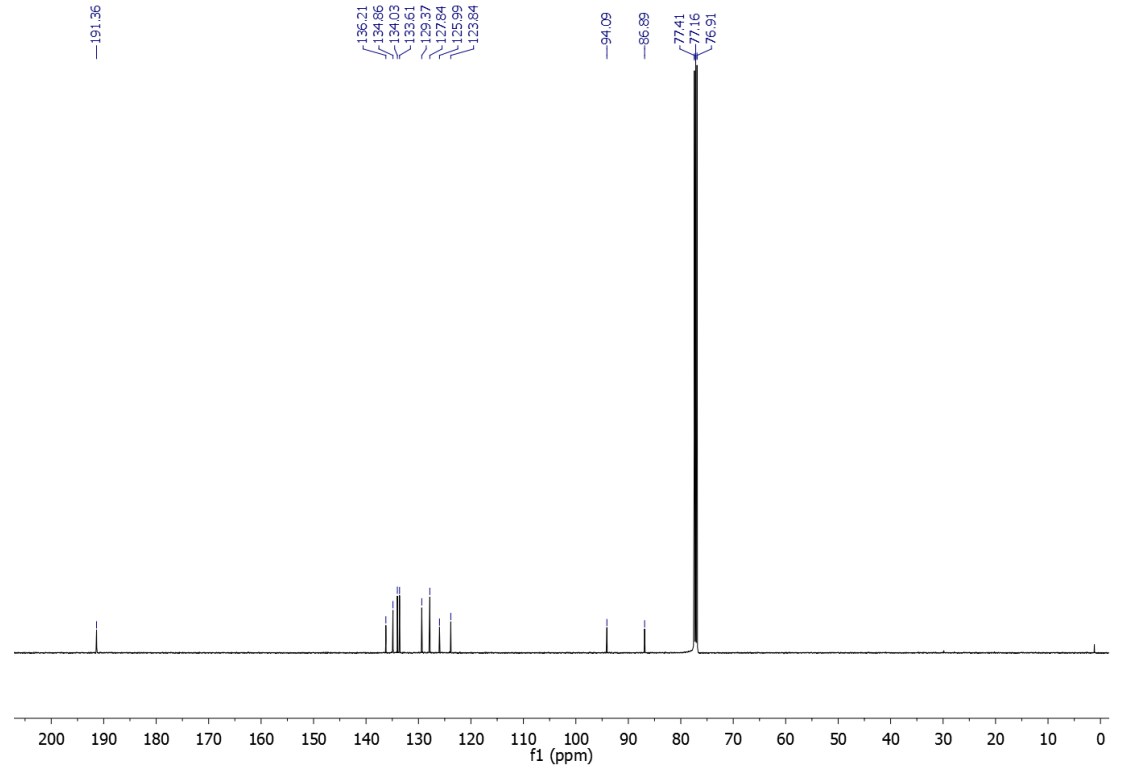

^{13}C NMR spectrum (126 MHz, $CDCl_3$) of compound **2**.

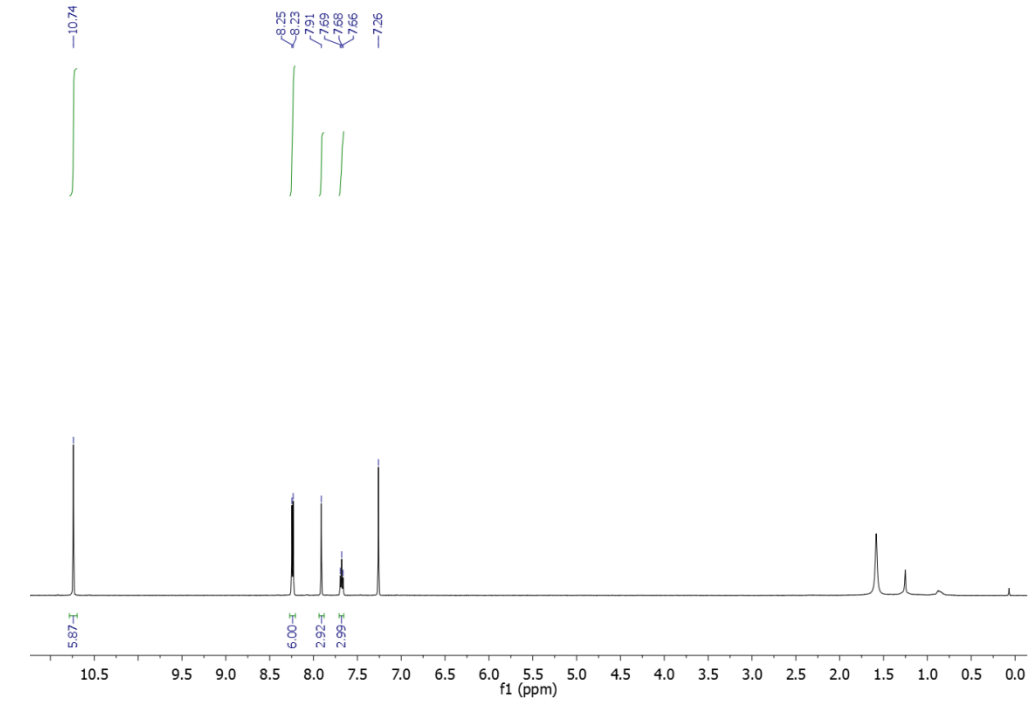

^{1}H NMR spectrum (500 MHz, $CDCl_3$) of compound **3**.

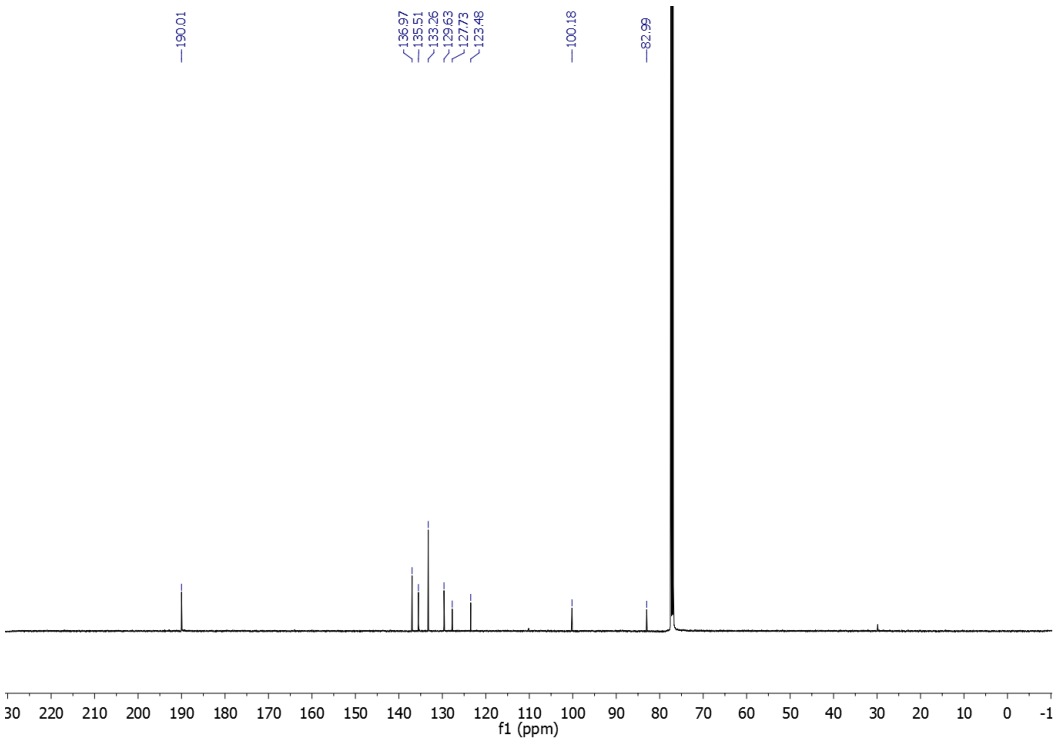

^{13}C NMR spectrum (126 MHz, $CDCl_3$) of compound **3**.

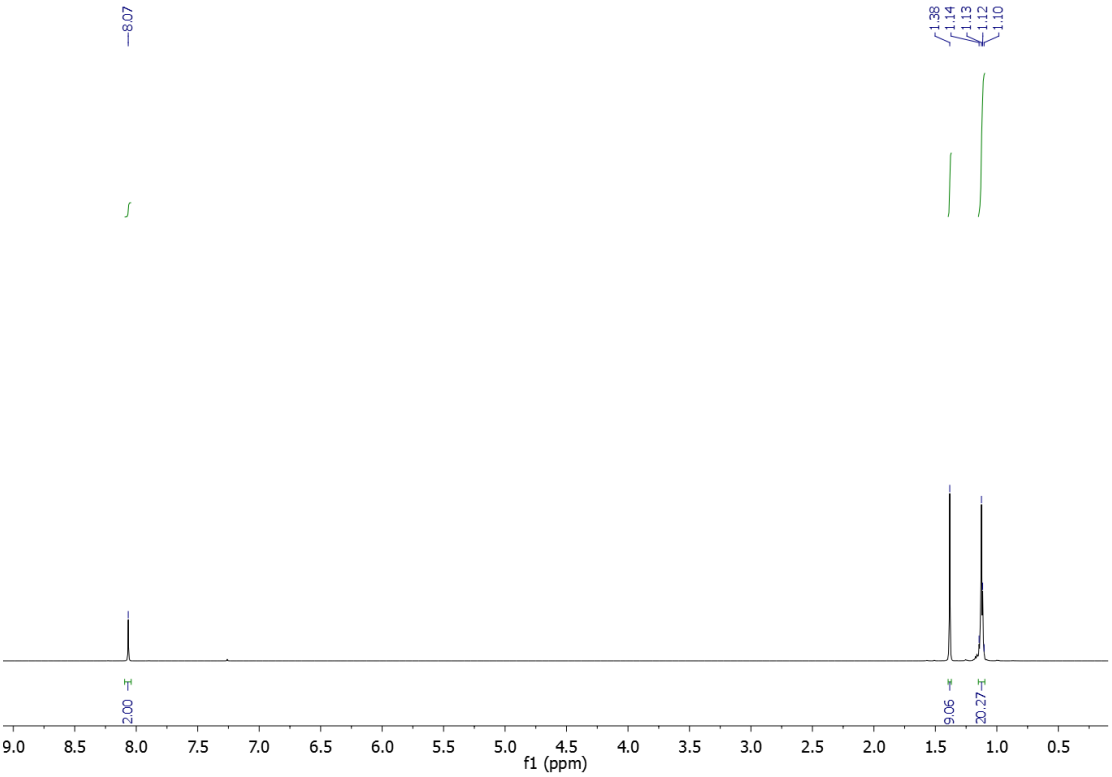

^{1}H NMR spectrum (500 MHz, $CDCl_3$) of compound **S8**.

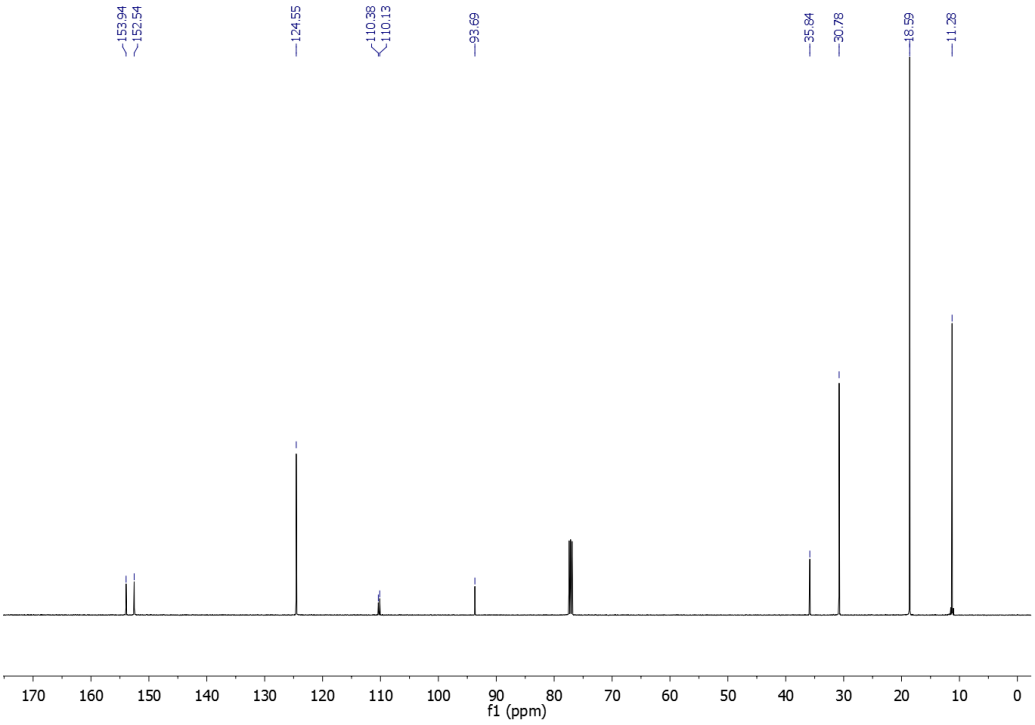

^{13}C NMR spectrum (126 MHz, $CDCl_3$) of compound **S8**

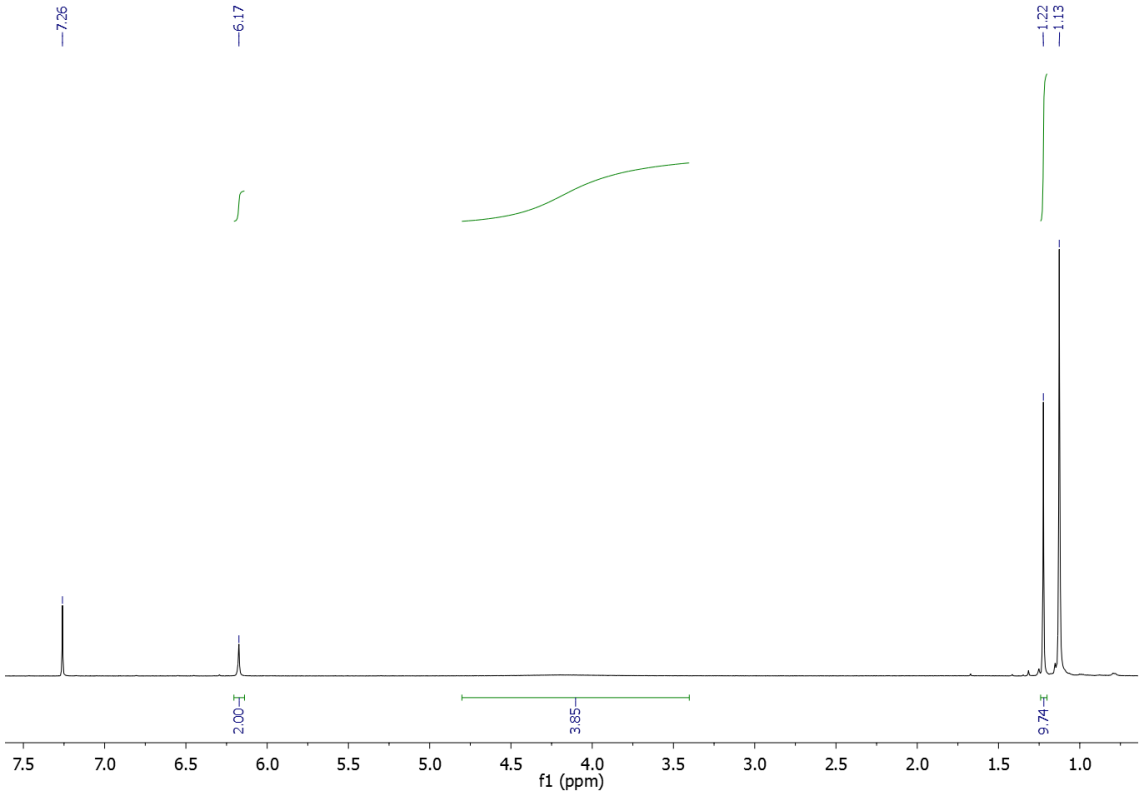

^{1}H NMR spectrum (500 MHz, $CDCl_3$) of compound **S9**.

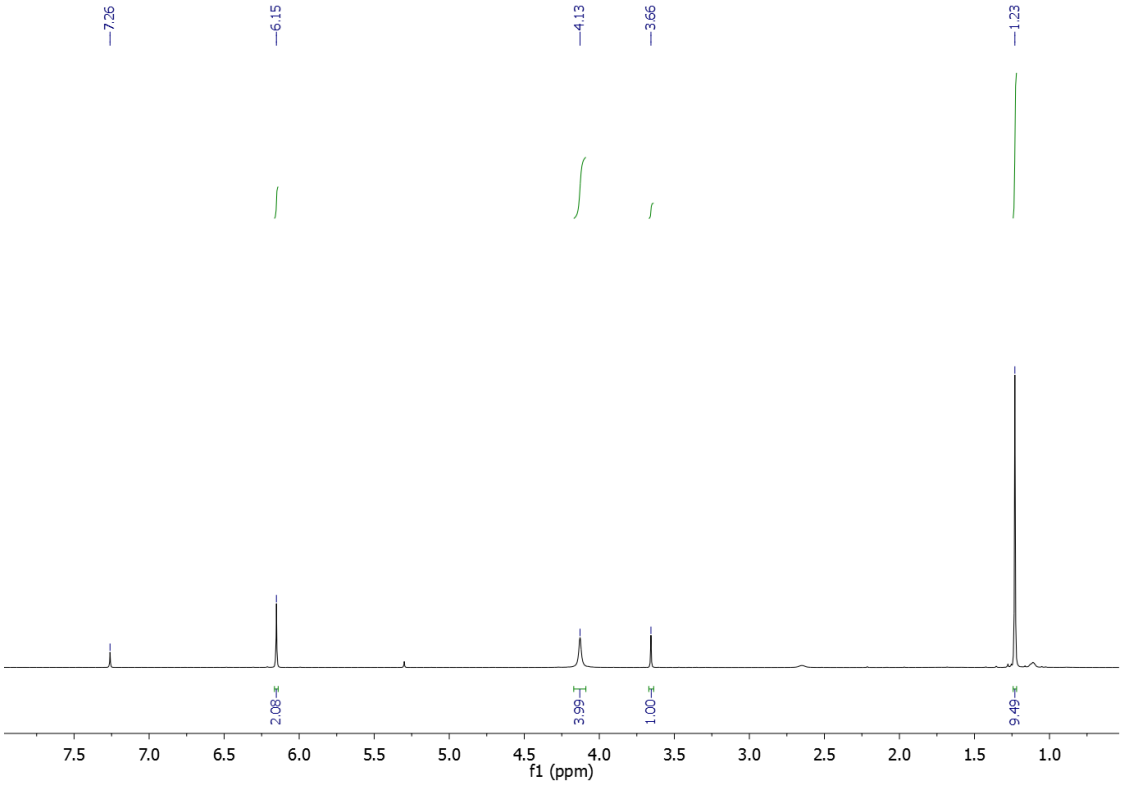

^{1}H NMR spectrum (500 MHz, $CDCl_3$) of compound **S10**.

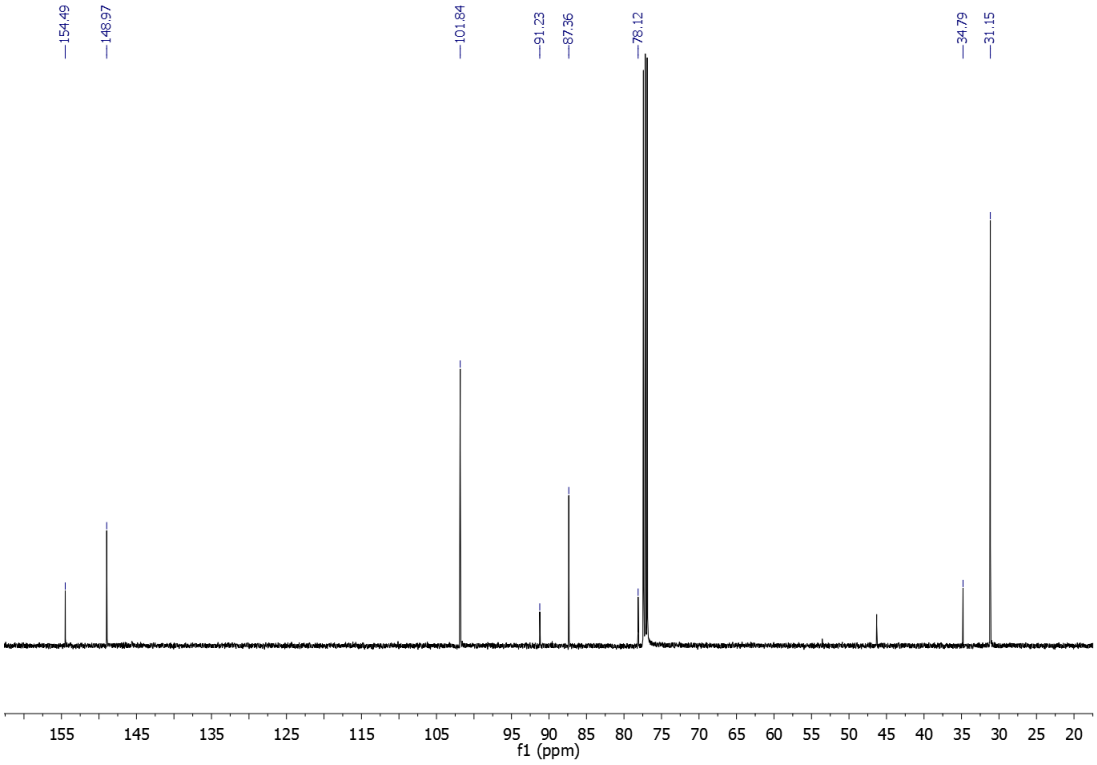

^{13}C NMR spectrum (126 MHz, $CDCl_3$) of compound **S10**.

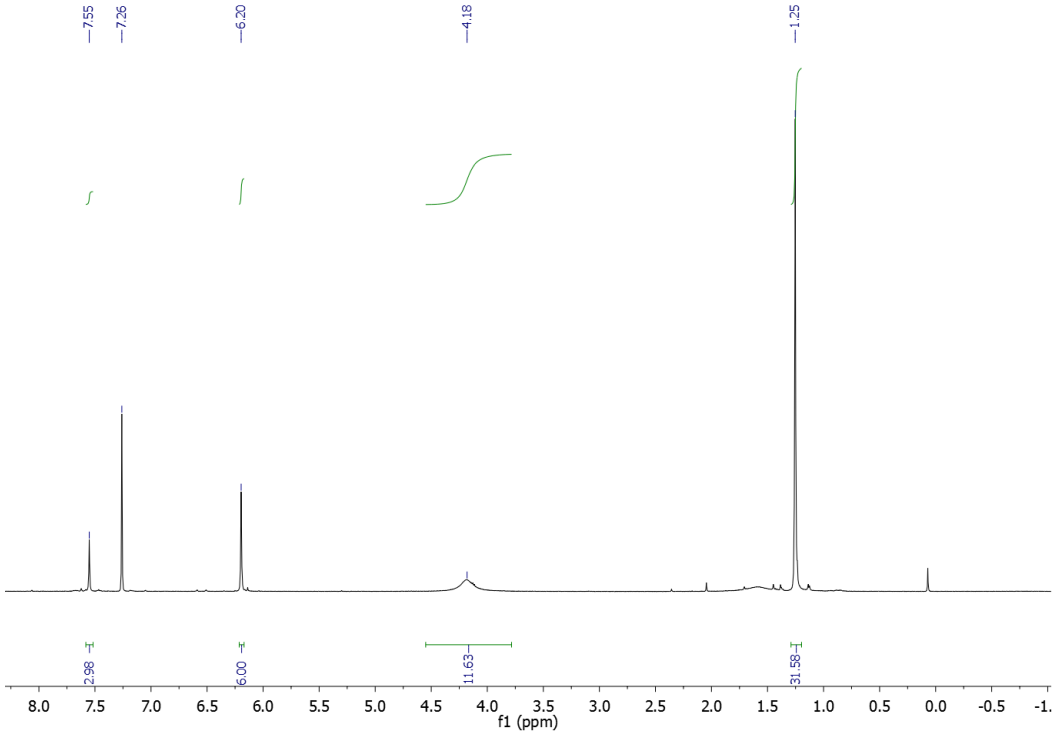

^{1}H NMR spectrum (500 MHz, $CDCl_3$) of compound **4**.

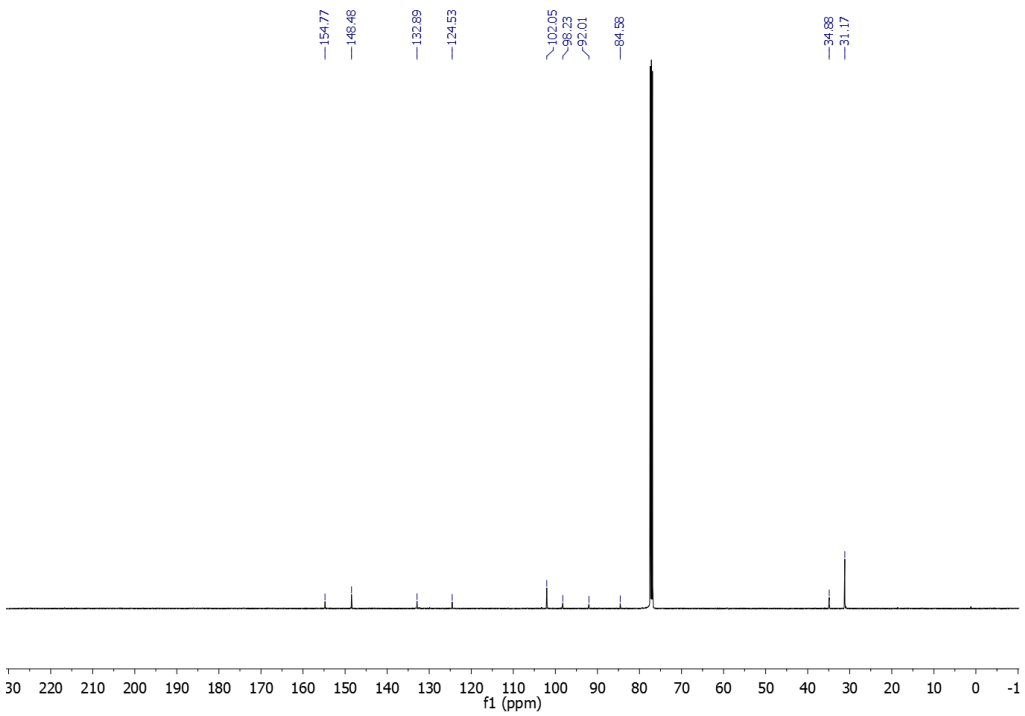

^{13}C NMR spectrum (126 MHz, $CDCl_3$) of compound **4**.

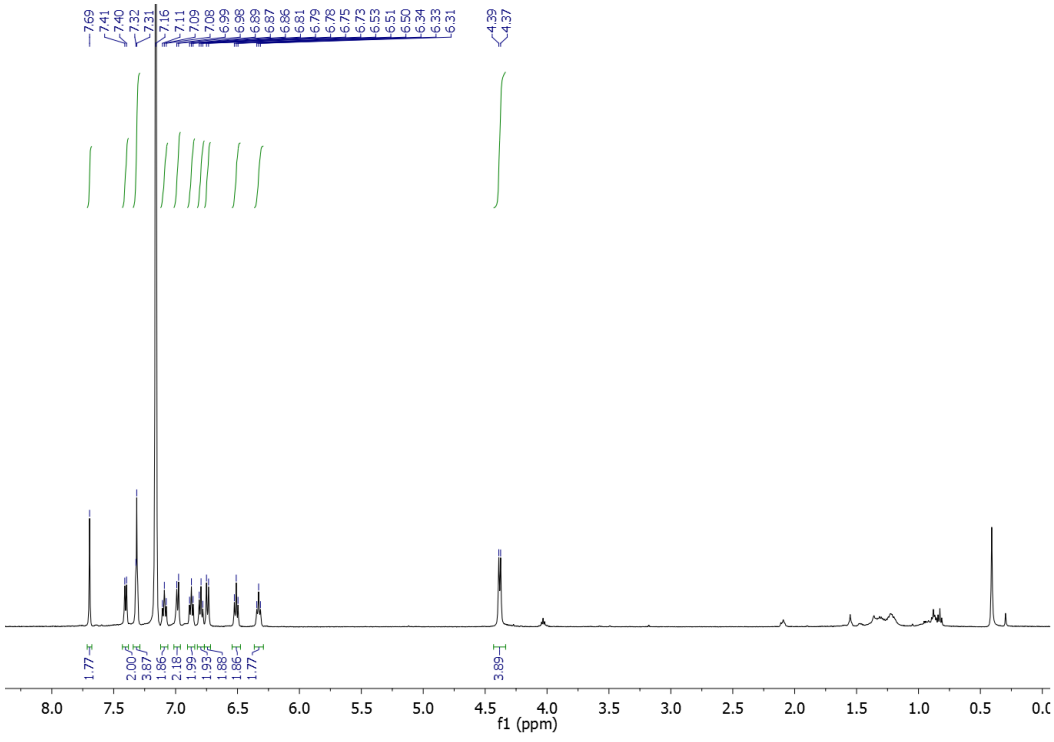

^{1}H NMR spectrum (500 MHz, C_6D_6) of compound **2T′**.

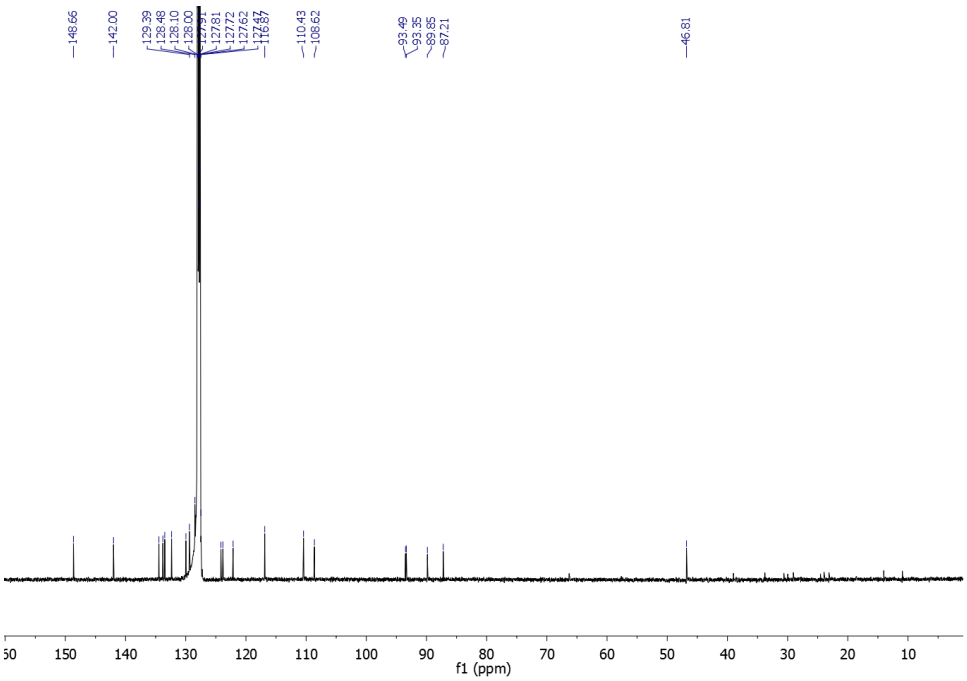

^{13}C NMR spectrum (126 MHz, C_6D_6) of compound **2T′**.

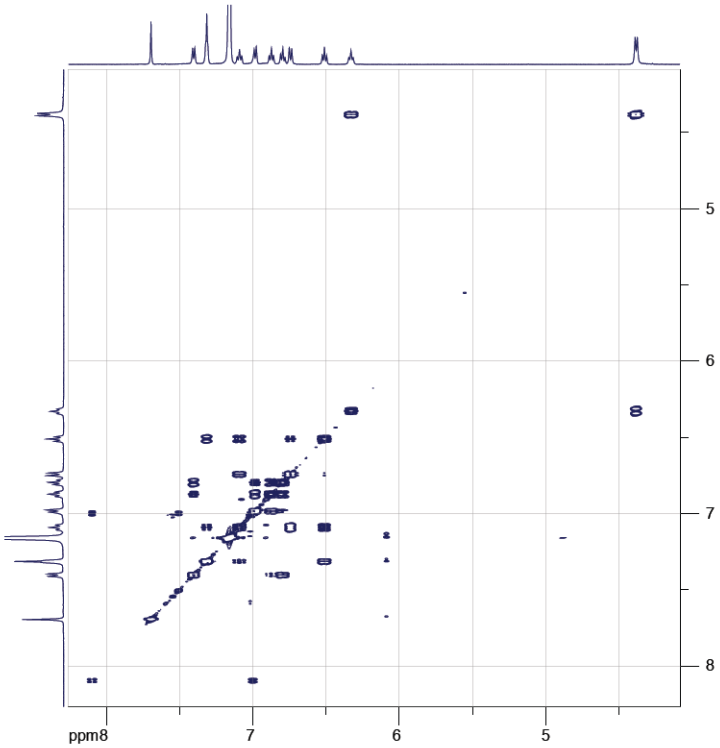

COSY NMR spectrum (500 MHz, C_6D_6) of **2T′**.

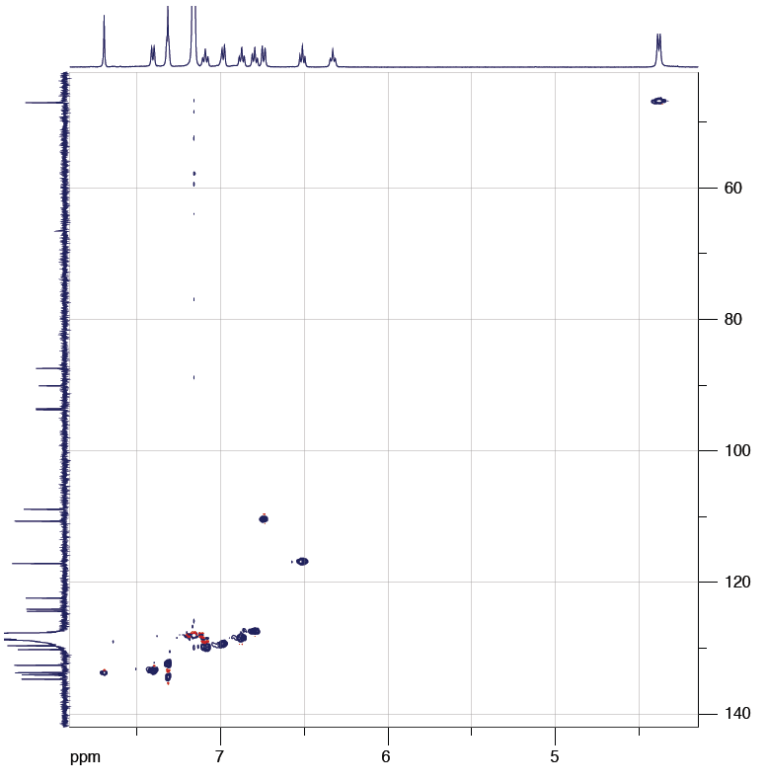

HSQC NMR spectrum (500 MHz, C_6D_6) of **2T′**.

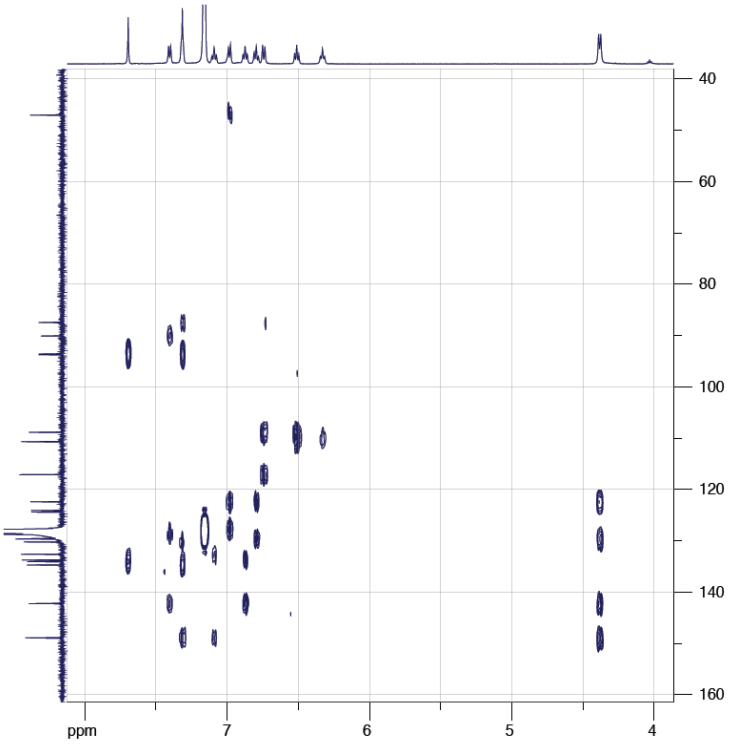

HMBC NMR spectrum (500 MHz, C_6D_6) of **2T′**.

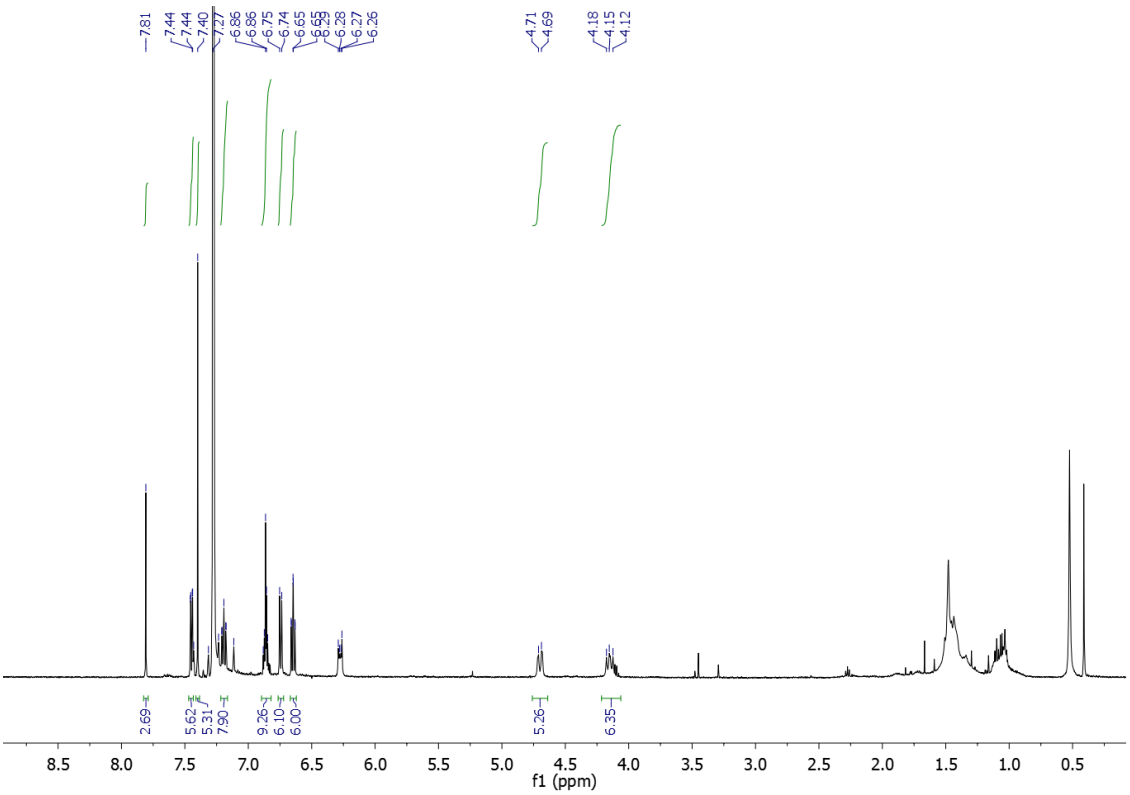

^{1}H NMR spectrum (500 MHz, C_6D_6) of compound **3T′**.

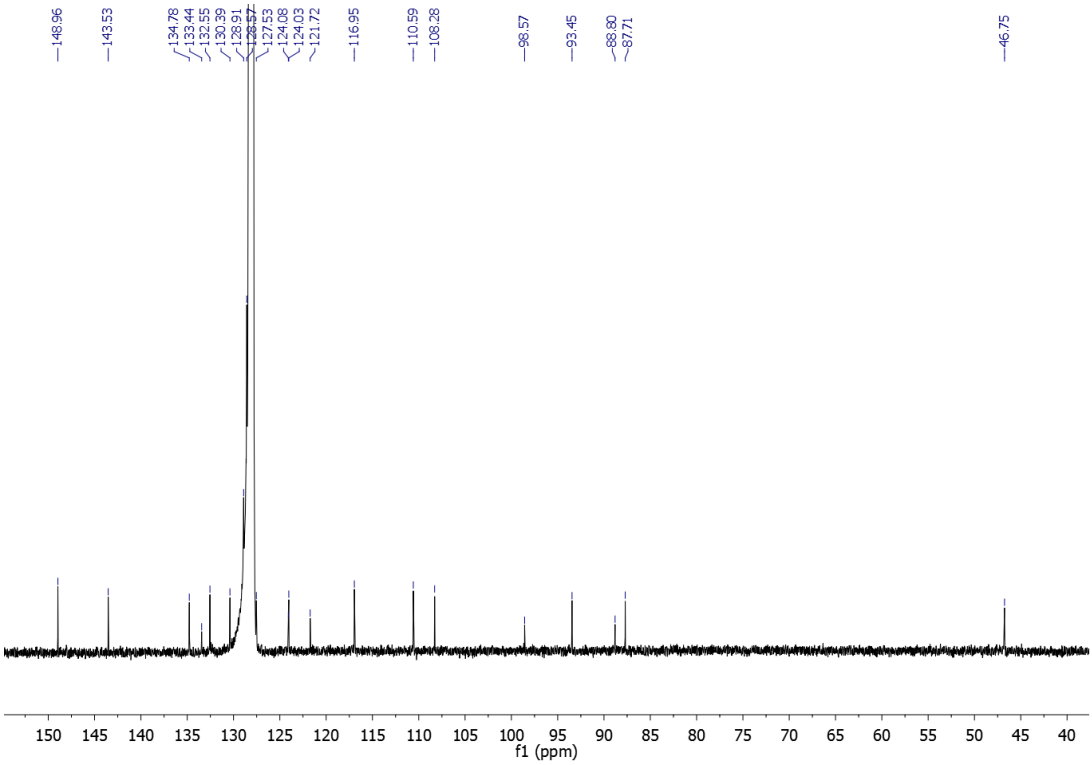

^{13}C NMR spectrum (126 MHz, C_6D_6) of compound **3T′**.

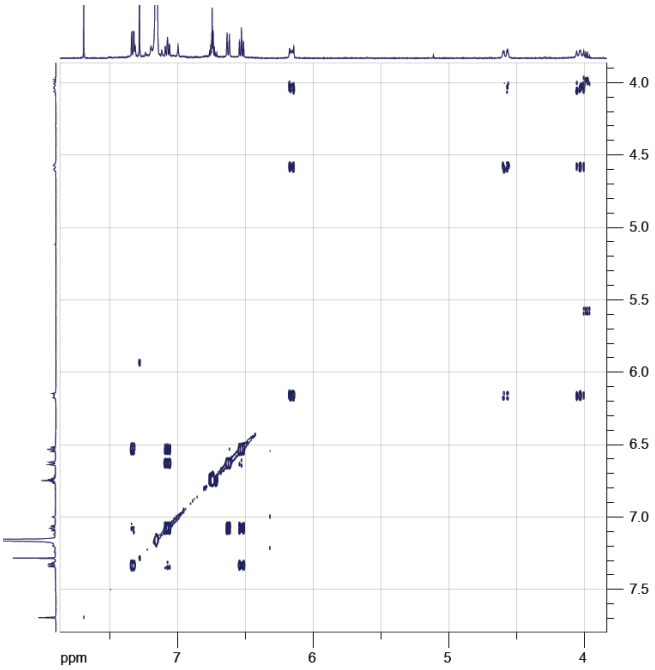

COSY NMR spectrum (500 MHz, C_6D_6) of **3T′**.

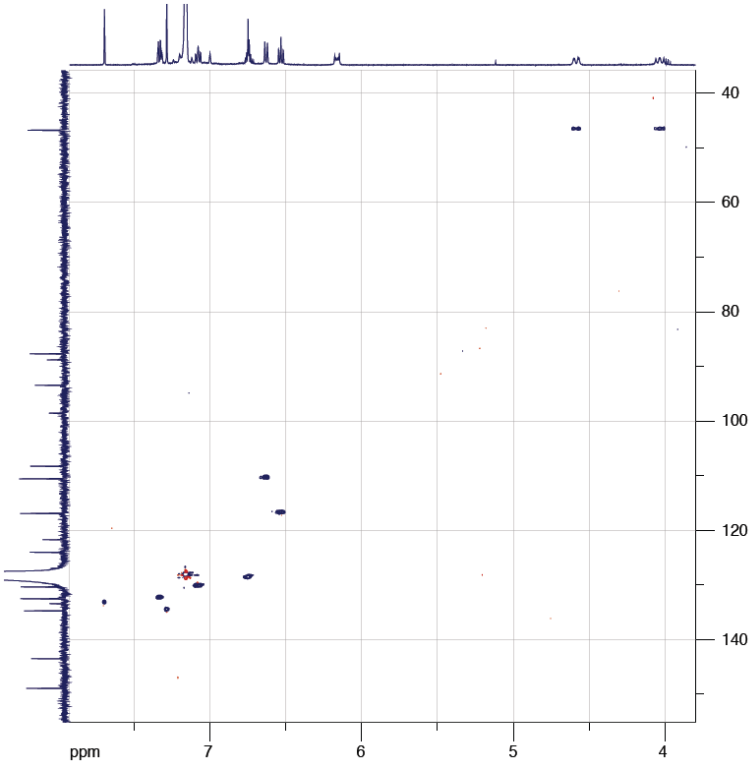

HSQC NMR spectrum (500 MHz, C_6D_6) of **3T′**.

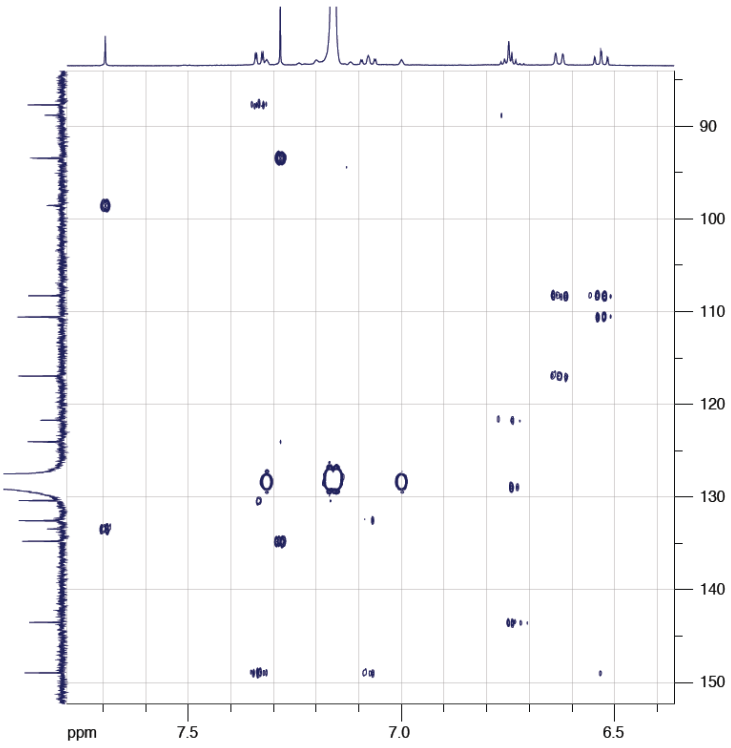

HMBC NMR spectrum (500 MHz, C_6D_6) of **3T′**.

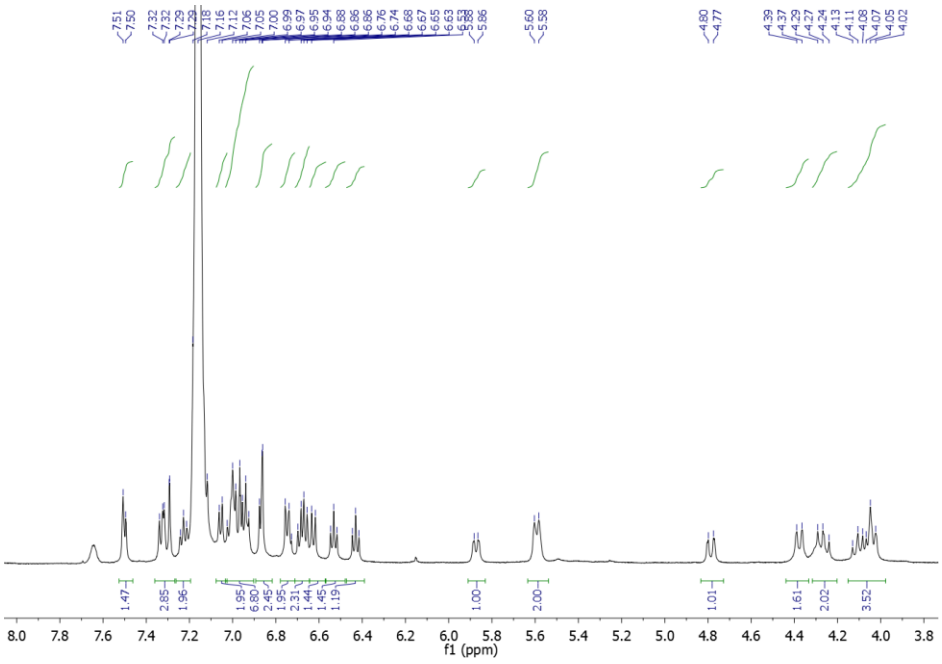

^{1}H NMR spectrum (500 MHz, C_6D_6) of compound **3T$_{iso}$**.

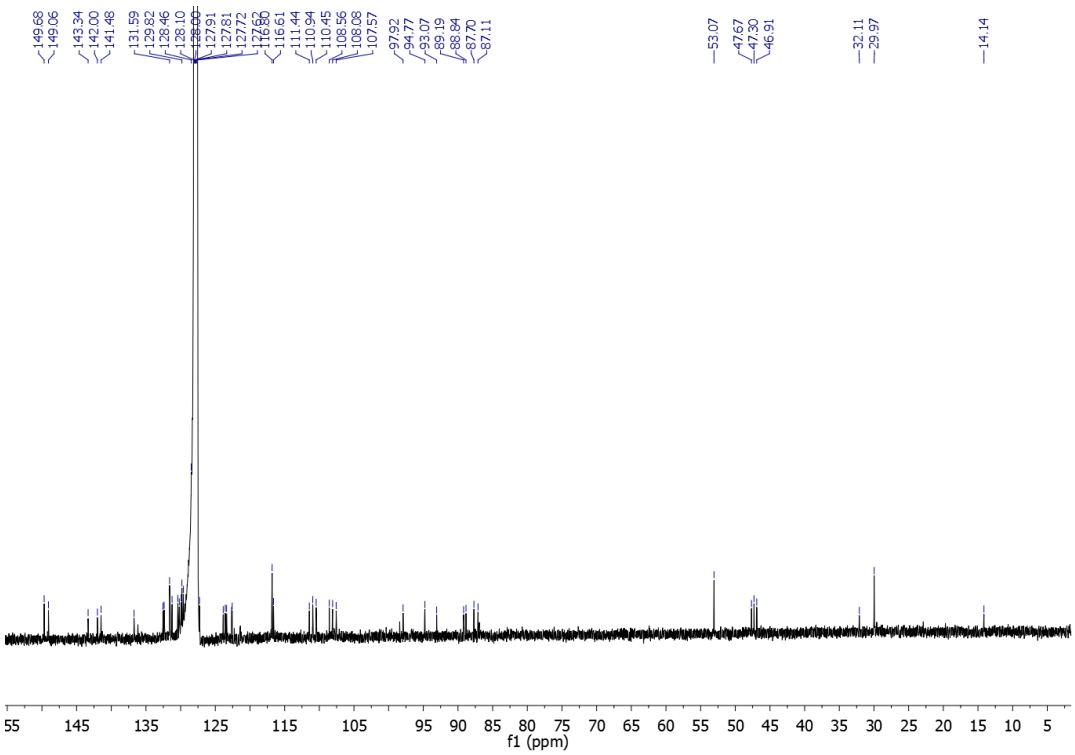

^{13}C NMR spectrum (126 MHz, C_6D_6) of compound **3T$_{iso}$**.

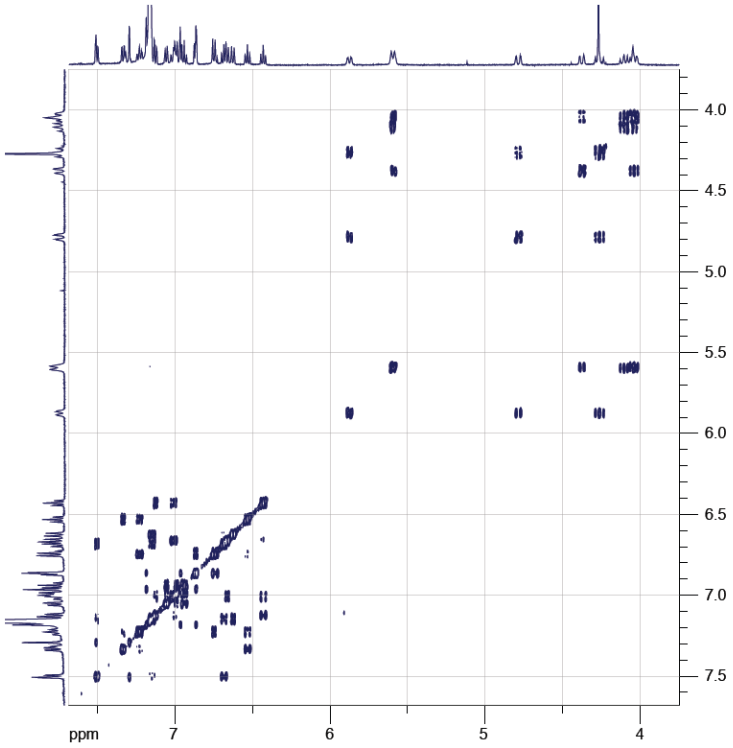

COSY NMR spectrum (500 MHz, C_6D_6) of **3T$_{iso}$′**.

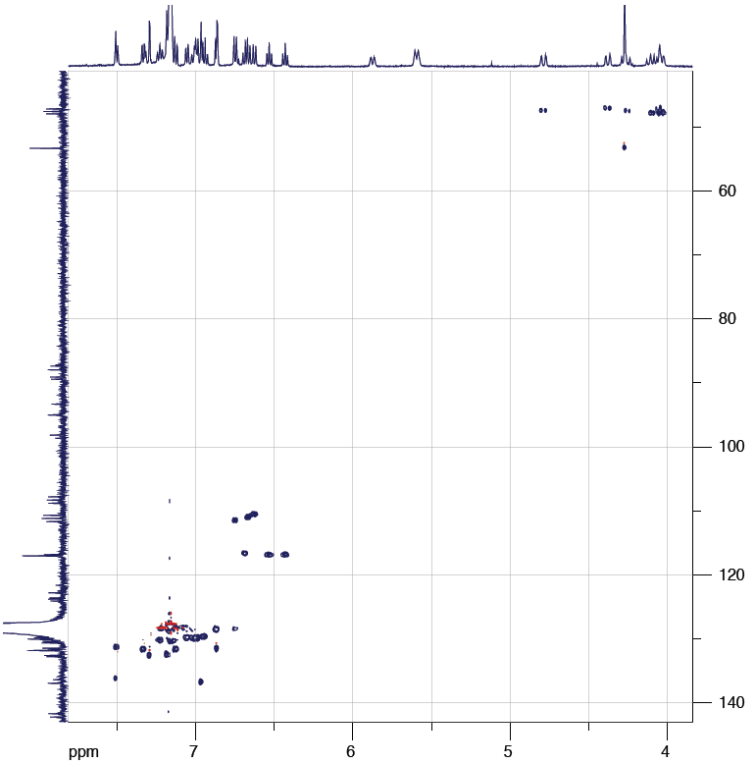

HSQC NMR spectrum (500 MHz, C_6D_6) of **$3T_{iso}'$**.

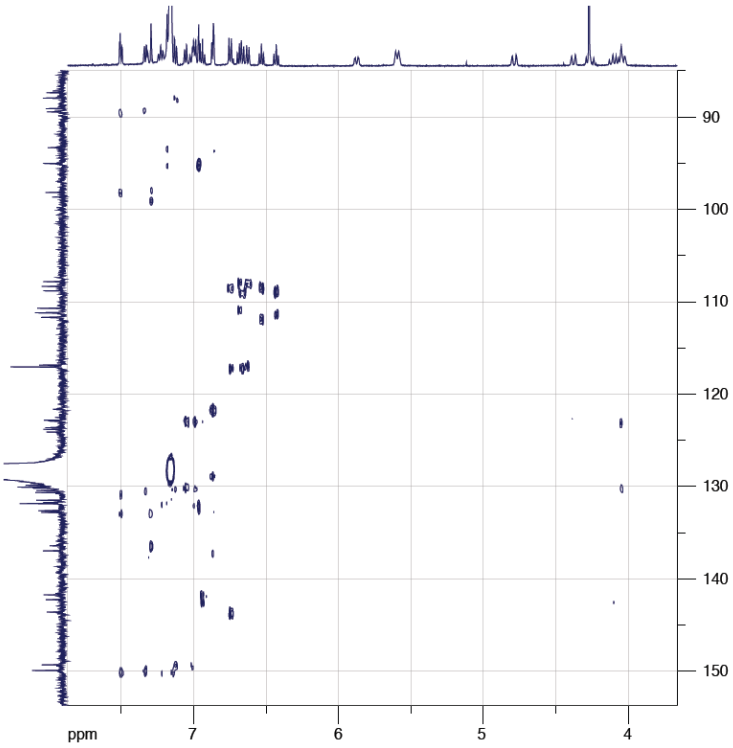

HMBC NMR spectrum (500 MHz, C_6D_6) of **$3T_{iso}'$**.

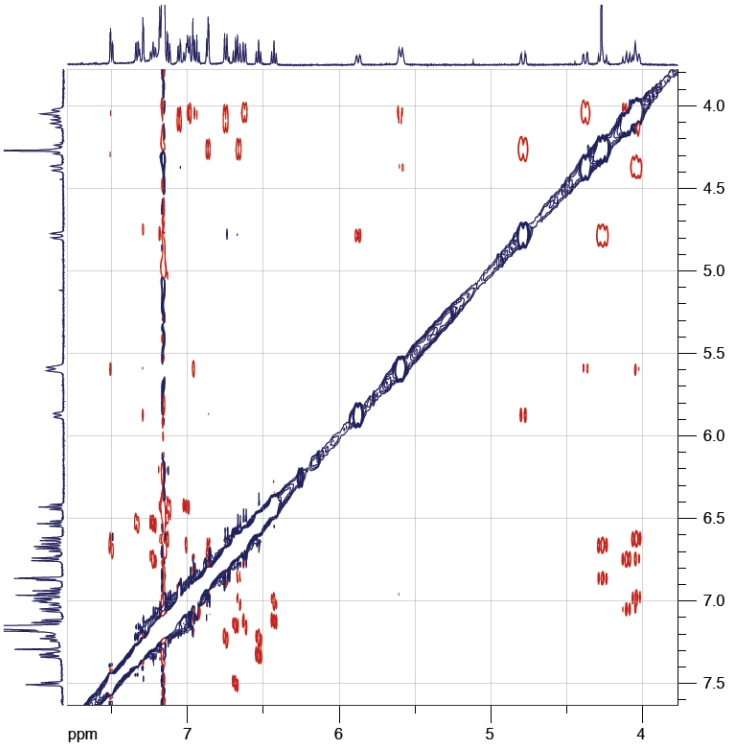

ROESY NMR spectrum (500 MHz, C_6D_6) of **$3T_{iso}'$.**

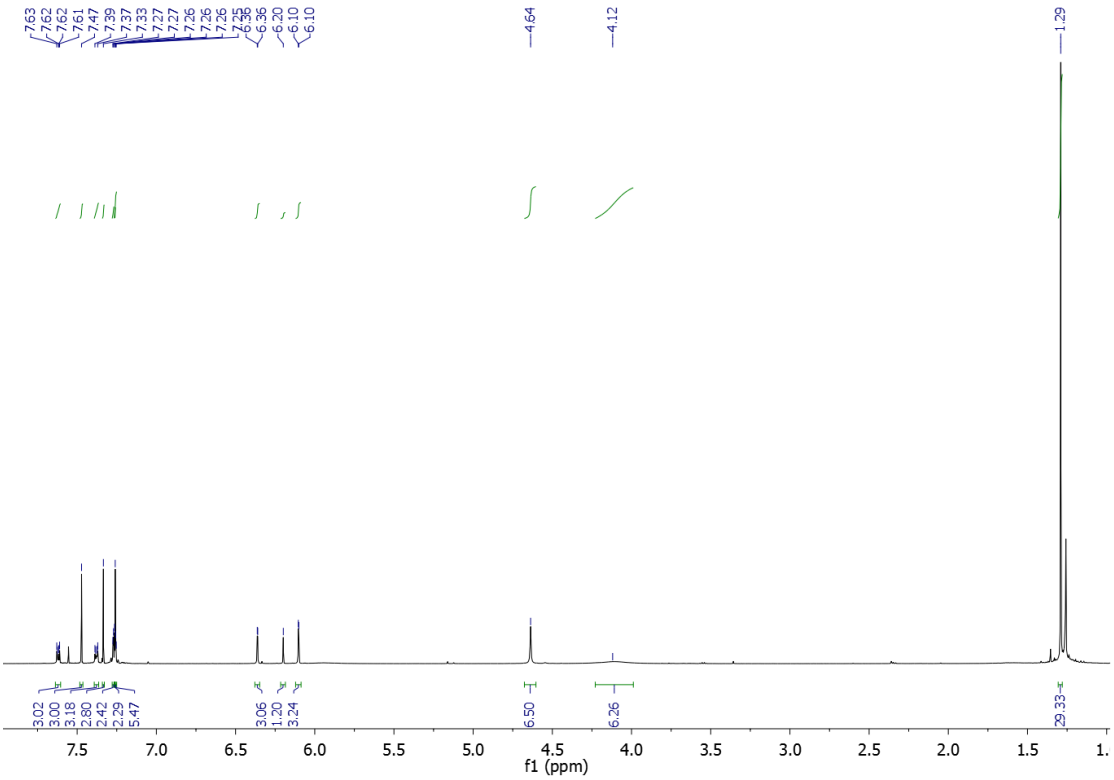

^{1}H NMR spectrum (500 MHz, $CDCl_3$) of compound **$2T_B$**.

Chapter 3 Studies Toward Alternate Assembly Strategies

3.1 Introduction

Our project focuses on combining the error-correction character of supramolecular chemistry with the robustness of covalent bonding. Dynamic covalent chemistry (DCC) deals with reversible covalent reactions that allow the exchange of molecular components to achieve a target structure at equilibrium.[1] The challenge for our research is precision design of monomers for complex three-dimensional architectures. Equilibrium product structures are affected dramatically by monomer design, and a number of external factors such as temperature, concentration and impurities. Thus, adjustments should be done to the monomers to change the thermodynamic favorability of the products. As mentioned in Chapter 2, we observed competing formation of misaligned three-tiered stack and a halting assembly at $\mathbf{2T_B}$ when we tried to prepare the desired rigid three-tiered stack.[2] In order to suppress the formation of misaligned three tiered stack we tried several approaches, described in this chapter: 1) The introduction of solubilizing and stabilizing groups to the aldehyde monomers. This strategy was intended to address the decreased solubility of dialdehyde monomer **3** compared with aldehyde monomer **1** (Chapter 2). 2) The introduction of more space between the monomers during self-assembly (longer linkers). Our analysis of the previous stacks suggested that they were modestly strained; longer linkers could help alleviate this strain.

3.2 Results and Discussion

3.2.1 Alternate Aldehyde Monomers

As we mentioned in Chapter 2, a competing misaligned 3-tiered stack $\mathbf{3T_{iso}}$ was observed when self-assembly of monomer **1** and dialdehyde monomer **3** was performed. In order to suppress the formation of misaligned 3-tiered stack $\mathbf{3T_{iso}}$, modification of the dialdehyde monomer was first attempted. A *tert*-butyl group was first installed to increase the solubility of the dialdehyde monomer (dialdehyde **3** was found to have only limited solubility in the original experiments). Following the standard procedures, monomer **5** was successfully synthesized as shown in **Scheme 3.1**. This synthesis of monomer **5** was performed in a small scale and monomer **5** was hard to purify with silica chromatography.

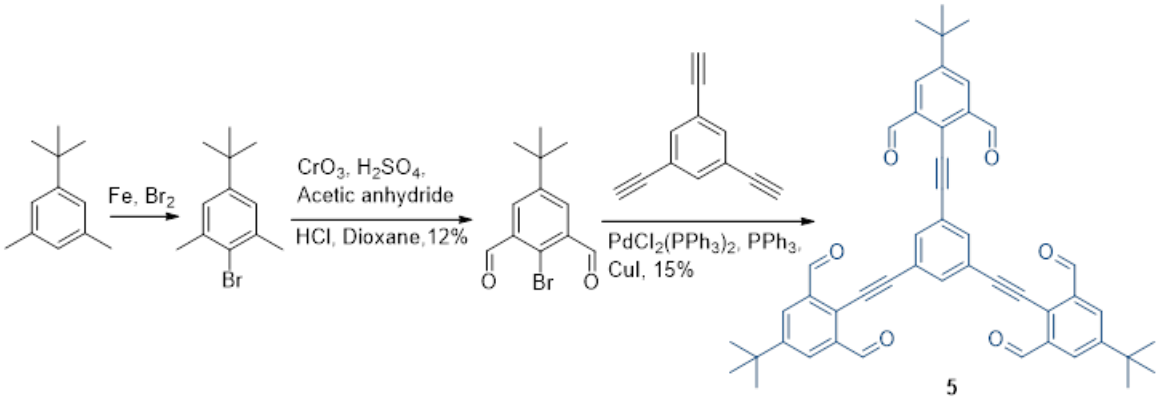

Scheme 3.1 Synthesis of monomer **5**.

We then attempted to prepare the three-tiered structure with monomer **5** and monomer **2** as shown in **Scheme 3.2**. The GPC trace actually showed there was promising product fitting the size of 3-tiered stacks. However, ^{1}H NMR analysis showed only a complex mixture of products and this direction was abandoned（**Figure 3.1**）.

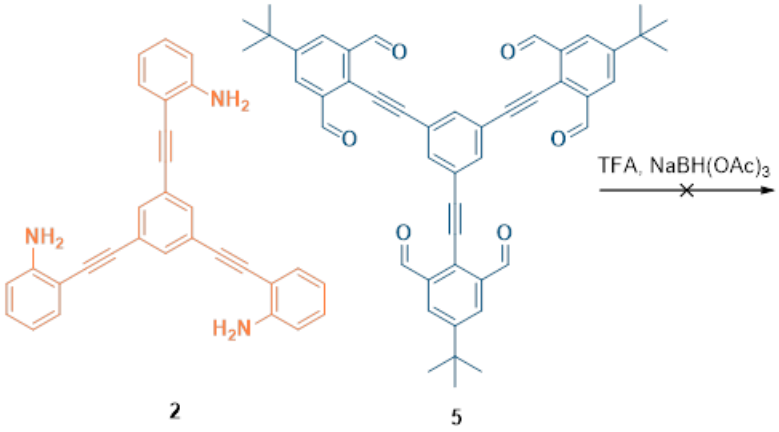

Scheme 3.2 Self-assembly of monomer **2** and monomer **5**.

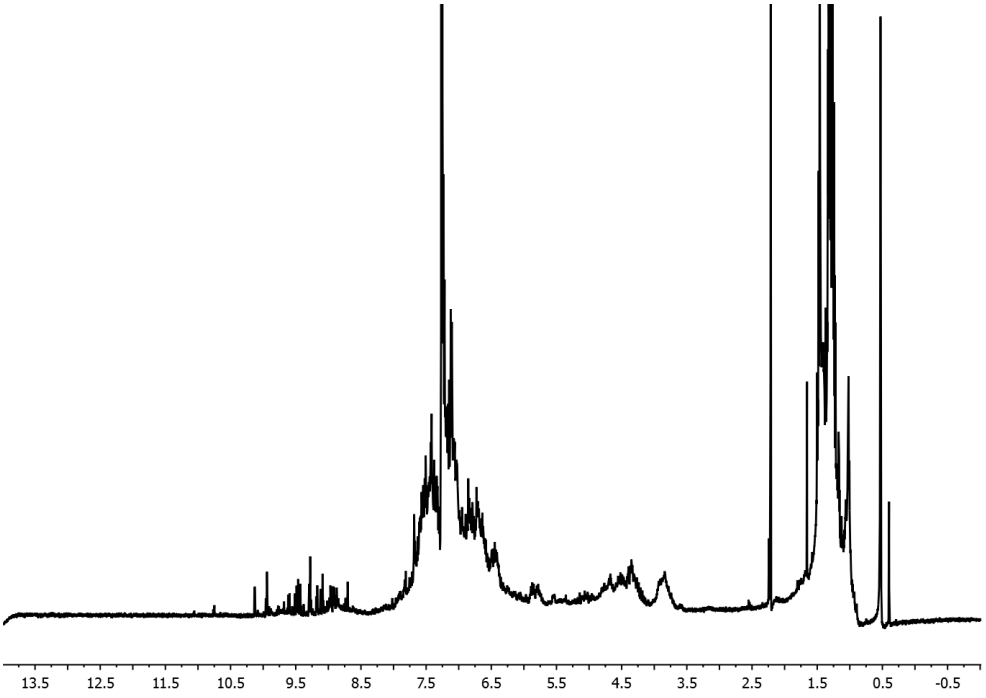

Figure 3.1 ^{1}H NMR of self-assembly product of monomer **2** and monomer **5**.

Further modification of the dialdehyde monomer then focused on adding longer alkyl chains, such as hexyloxy groups **(Scheme 3.3).** Unfortunately, as indicated in **Scheme 3.3**, the Sonogashira coupling of 2-bromo-5-(hexyloxy)isophthalaldehyde with 1,3,5-triethynylbenzene was unsuccessful and the route was abandoned because of the lengthy synthesis.

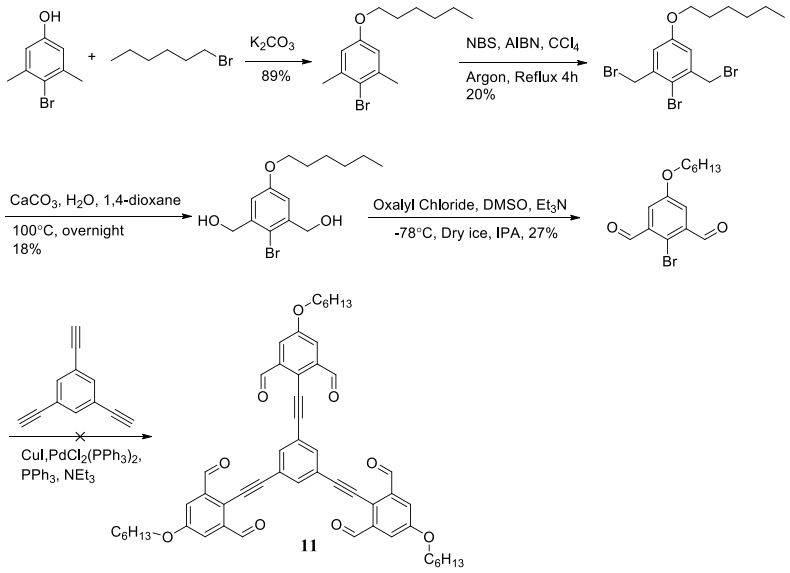

Scheme 3.3 Proposed synthesis route for soluble dialdehyde monomer **11**.

3.2.2 Alternate Amine Monomers

Instead of the unsuccessful modification of dialdehyde monomers, we then turned our focus to the adjustment of amine monomers. We proposed that the formation of the desired 3-tiered stacks would benefit from the introduction of more space between monomers. Hydrazone-based self-assembly has been explored and reported by Sanders' group.[3,4] The modularity, straightforward synthesis, and stability towards hydrolysis is one reason for their popularity. In addition, hydrazine-based supramolecular chemistry exhibits various applications, such as molecular switches[5], metallo-assemblies[6,7], and sensing tools[8]. Inspired by this research, we proposed to change from imine condensation to hydrazone-based self-assembly between monomers as shown in **Scheme 3.4.** However, the reaction led to complex outcome without evidence (NMR) for the formation hydrozone-based monomer **12**.[9]

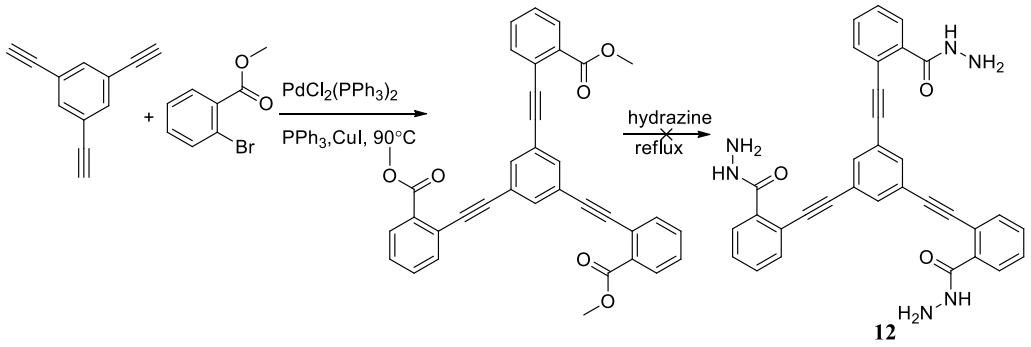

Scheme 3.4 Attempt to synthesis of monomer **12**.

Cooper's group has reported that different chain lengths of diamines result in different porous imine cage structures.[10] Thus, we decided that replacing the aniline-based monomers with benzylamine monomers could be a good solution to the problems encountered in Chapter 2 by increasing flexibility. Further, additional symmetry could be introduced into the reduced 2-tiered stacks derived from benzylamine monomers, since the final dibenzylamine products would be twofold symmetric.

Screening conditions for the Sonogashira coupling of 2-bromobenzylamine with 1,3,5-triethynylbenzene is summarized in **Table 3.1**. Unfortunately, based on ^{1}H NMR analysis of the crude product, the formation of monomer **6** was not detected. Sonogashira coupling of 2-bromobenzylamine with triisopropylsilylacetylene was then carried out as an alternative.

(**Scheme 3.6**) The screening of conditions is summarized in **Table 3.2**. No desired product was obtained based on ^{1}H NMR analysis of the crude product.

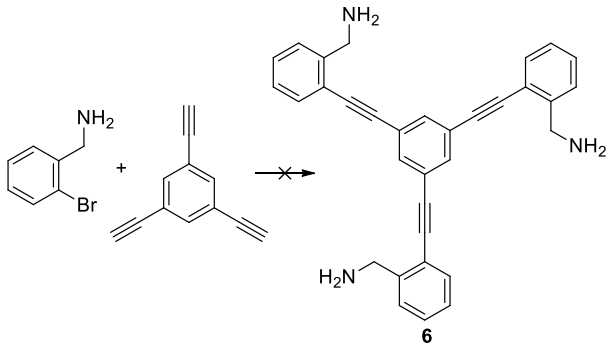

Scheme 3.5 Direct Sonogashira coupling for synthesis of monomer **6**.

entry number	catalysts	temperature	yield
1	$PdCl_2(PPh_3)_2$, CuI, NEt_3	90°C	n.a.
2	$PdCl_2(PPh_3)_2$, CuI, $NH(i\text{-}Pr)_2$	90°C	n.a.
3	$PdCl_2(PPh_3)_2$, CuI, $NH(i\text{-}Pr)_2$	70°C	n.a.
4	Pd(Pt-Bu3)2, Et3N	r.t.	n.a.

Table 3. 1 Conditions tried for direct Sonogashira coupling for synthesis of monomer 6.

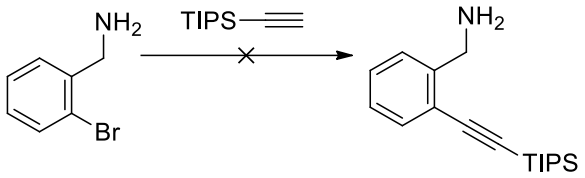

Scheme 3.6 Direct Sonogashira coupling for Synthesis of benzylamine arm.

entry number	catalysts	temperature	yield
1	$PdCl_2(PPh_3)_2$, CuI, NEt_3	90°C	n.a.
2	$PdCl_2(PPh_3)_2$, CuI, $NH(i\text{-}Pr)_2$	90°C	n.a.
3	$PdCl_2(PPh_3)_2$, CuI, $NH(i\text{-}Pr)_2$	70°C	n.a.
4	$Pd(Pt\text{-}Bu_3)_2$, Et_3N	r.t.	n.a.

Table 3. 2 Conditions tried for direct Sonogashira coupling for synthesis of benzylamine arm.

Eventually, monomer **6** was successfully synthesized through the synthesis route shown in **Scheme 3.7**. Unfortunately, monomer **6** does not dissolve in chloroform or dichloromethane. However, methanol and THF were identified as suitable solvents.

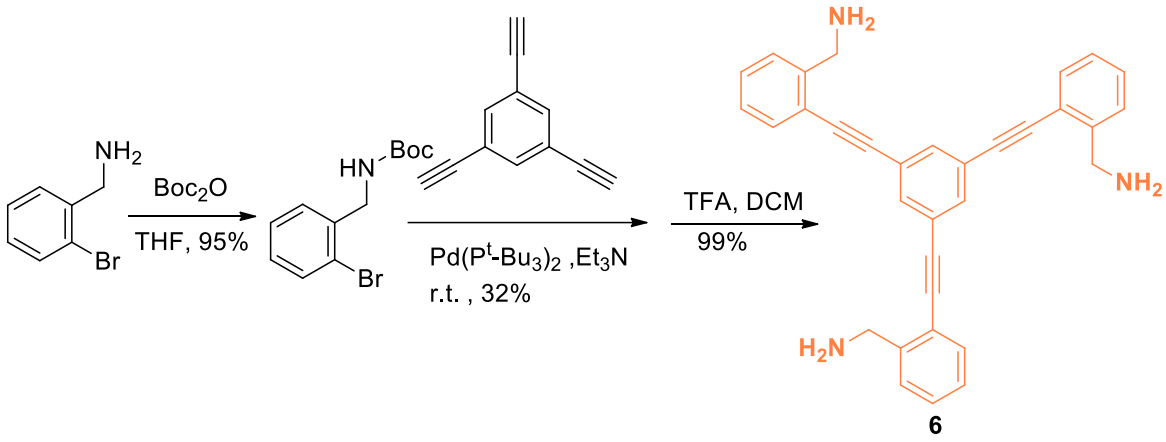

Scheme 3.7 Synthesis of monomer **6**.

With monomer **6** in hand, self-assembly of a 2-tiered stack with monomer **1** was then tested. (**Scheme 3.8**) The desired 2-tiered stack was not obtained under conditions shown in **Table 3.3**. We reasoned that the poor solubility of monomer **6** inhibited the formation of the desired 2-tiered stack. In order to understand the transformation better, ^{1}H NMR monitoring was then carried out in THF-*d8* and CD_3OD. As indicated in **Figure 3.2,** monomer **6** decomposed after 22 h while unreacted monomer **1** was remained in the reaction mixture (THF-*d8*). In order to rule out the possibility that monomer **6** was unstable under acidic condition, TFA was then replaced with scandium triflate.[11] Unfortunately, decomposition of monomer **6** was still observed after several hours. Self-assembly of monomer **1** and monomer **6** was also examined at higher temperature; however, no desired product was obtained.

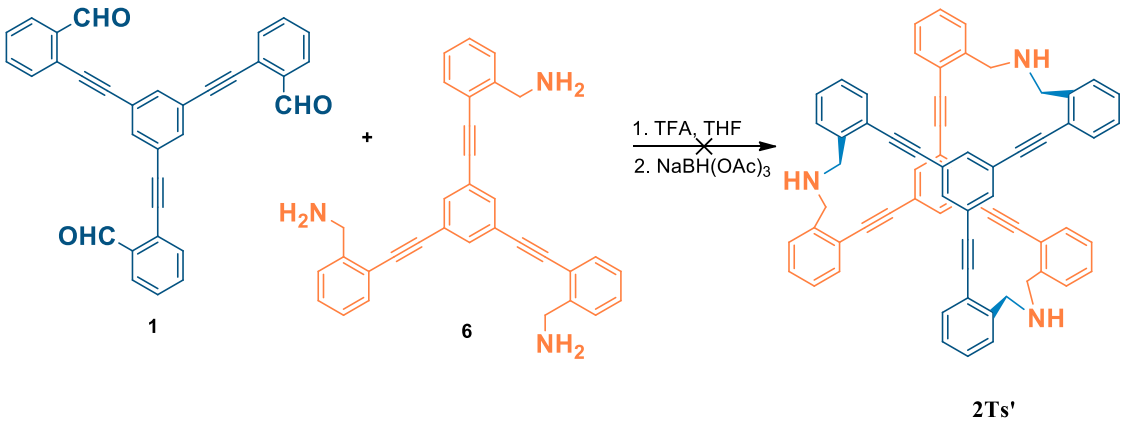

Scheme 3.8 Self-assembly of monomer **1** and monomer **6**.

entry number	catalyst	solvent	yield
1	TFA	$CDCl_3$	n.a.
2	TFA	THF-*d8*	n.a.
3	TFA	MeOD	n.a.
4	$Sc(OTf)_3$	THF-*d8*	n.a.

Table 3.3 Conditions tried for self-assembly of monomer **1** and monomer **6**.

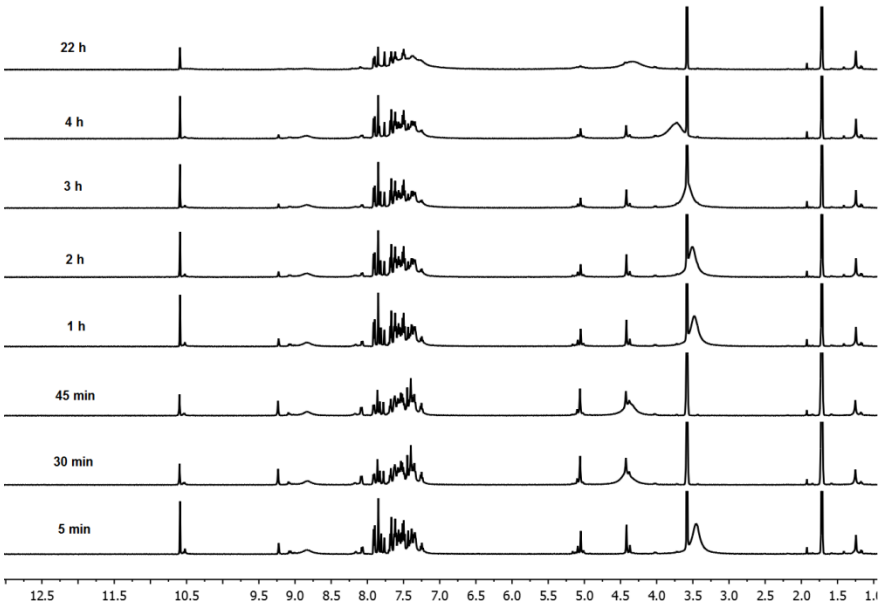

Figure 3.2 ^{1}H NMR monitoring of self-assembly of monomer **1** and monomer **6** in THF-*d8* with TFA as catalyst.

3.4 Experimental

3.4.1 General

Unless otherwise noted, all reagents and solvents were purchased from commercial sources and used without further purification. Anhydrous THF was obtained using an alumina-column solvent purification system. Flash column chromatography was performed using Silicycle SiliaFlash P60 (40–63 μm, 230–400 mesh). Melting points were determined using a Thermal Analysis Q20 differential scanning calorimeter at a heating rate of 5 ℃/min. NMR spectra were measured in deuterated solvents using Bruker Avance 300 or 500 MHz spectrometers. Chemical shifts are reported in δ (ppm) relative to TMS, with the residual solvent protons used as internal standards ($CDCl_3$: 7.26 for ^1H, 77.16 for ^{13}C).

3.4.2 Synthesis

Monomer 5

The synthesis of monomer **5** followed a reported literature procedure as described below.[12,13] To a round bottom flask containing 1-(tert-butyl)-3,5-dimethylbenzene and Fe was added Br_2 dropwise to give 2-bromo-5-(tert-butyl)-1,3-dimethylbenzene as white crystals. 2-bromo-5-(tert-butyl)-1,3-dimethylbenzene (1g, 4.0mmol) was then oxidized with CrO_3 (2.49 g, 0.025 mol) gave 2-bromo-5-(tert-butyl)isophthalaldehyde (0.13 g, 0.048 mmol) as a pale yellow solid. Sonogashira coupling of 2-bromo-5-(tert-butyl)isophthalaldehyde(0.11 g, 0.40 mmol) with 1,3,5-triethynylbenzene (0.18mg, 0.12 mmol) gave monomer **5** (0.013 g, 0.018 mmol) as a white solid, 15%. ^1H NMR (500 MHz, $CDCl_3$) δ 10.73 (s, 1H), 8.26 (s, 1H), 7.87 (s, 1H), 1.40 (s, 5H). ^{13}C NMR (126 MHz, $CDCl_3$) δ 190.4, 153.6, 136.7, 135.2, 130.2, 125.4, 123.5, 99.5, 83.0, 35.5, 31.0.

Self-assembly of monomer 2 with monomer 5

To a scintillation vial containing **2** (18 mg, 0.043 mmol), **3** (13.4 mg, 0.019 mmol), and 3 Å molecular sieves was added $CHCl_3$ (3 mL), followed by a solution of CF_3CO_2H (0.51 mg, 0.0045 mmol) in $CHCl_3$ (0.3 mL). After stirring for 5 h at r.t., $NaBH(OAc)_3$ (48 mg, 0.23 mmol) was added and stirring was continued for 3 h. The reaction mixture was then quenched with sat. $NaHCO_3$(aq). The resulting suspension was diluted with $CHCl_3$, washed with water (2×), dried

($MgSO_4$), filtered, and concentrated. Purification by GPC gave no desired product as judged by ^{1}H NMR spectroscopy of each fraction.

Monomer 11

The synthesis of monomer **11** followed reported literature procedure as described below.[14] 4-bromo-3,5-dimethylphenol was first alkylated with 1-bromohexane to form 2-bromo-5-(hexyloxy)-1,3-dimethylbenzene, then treated with NBS and AIBN to form 2-bromo-1,3-bis(bromomethyl)-5-(hexyloxy)benzene. Hydrolysis of the benzylic bromides gave (2-bromo-5-(hexyloxy)-1,3-phenylene)dimethanol, which was then oxidized with oxalyl chloride to form 2-bromo-5-(hexyloxy)isophthalaldehyde. ^{1}H NMR (500 MHz, $CDCl_3$) δ 10.49 (s, J = 0.5 Hz, 2H), 7.65 (s, 2H), 4.03 (t, J = 6.5 Hz, 2H), 1.84 – 1.75 (m, 2H), 1.46 (m, 2H), 1.38 – 1.28 (m, 4H), 0.91 (t, J = 6.7 Hz, 3H). Sonogashira coupling of 2-bromo-5-(hexyloxy)isophthalaldehyde with 1,3,5-triethynylbenzene was unsuccessful.

Monomer 12

A Schlenk tube containing $PdCl_2(PPh_3)_2$ (47 mg, 0.022 mmol), CuI (10 mg, 0.020 mmol), PPh_3 (34 mg, 0.020 mmol) and methyl 2-bromobenzoate (1.43 mL, 0.01 mmol) was evacuated and backfilled with argon (3×). To this mixture was added a solution of 1,3,5-triethynylbenzene (0.51g, 3.4 mmol) in NEt_3 (25 mL) and THF (5 mL). The suspension was degassed by three freeze-pump-thaw cycles and heated with stirring at 90 ℃ for 18 h. The resulting suspension was diluted with CH_2Cl_2, washed with water (2×), dried ($MgSO_4$), filtered, and concentrated. Purification by flash chromatography (3:1 hexanes/EtOAc) gave trimethyl 2,2',2"-(benzene-1,3,5-triyltris(ethyne-2,1-diyl))tribenzoate (**b**) as a white solid (1.7 g, 3 mmol, 95%). ^{1}H NMR (500 MHz, $CDCl_3$) δ 8.01 (d, J = 7.8 Hz, 1H), 7.75 (s, 1H), 7.67 (d, J = 7.7 Hz, 1H), 7.52 (t, J = 7.6 Hz, 1H), 7.42 (t, J = 7.6 Hz, 1H), 4.00 (s, 3H).

Monomer 6

To a 50 mL round bottom flask containing 2-bromobenzylamine (3 mL, 24 mmol) and THF (15 mL) was added di-tert-butyldicarbonate (6.93 g, 32 mmol). The reaction mixture was stirred for 6 h, then treated with diethyl ether. The organic layer was washed with water (2×), dried ($MgSO_4$), filtered, and concentrated. Purification by flash chromatography (2% EtOAc/hexanes) gave tert-butyl 2-bromobenzylcarbamate as a white solid (6.2 g, 95%). ^{1}H NMR

(500 MHz, $CDCl_3$) δ 7.54 (d, *J* = 7.8 Hz, 1H), 7.38 (d, 1H), 7.30 (t, *J* = 6.6 Hz, 1H), 7.14 (t, *J* = 6.9 Hz, 1H), 5.01 (s, 2H), 4.39 (s, 2H).

A Schlenk tube containing tert-butyl 2-bromobenzylcarbamate (3.7 g, 14 mmol) and $Pd(P^tBu_3)_2$ (0.15 g, 0.30 mmol) was evacuated and backfilled with argon (3×). To this mixture was added a solution of 1,3,5-triethynylbenzene (0.50 g, 3.3 mmol) in NEt_3 (40 mL). The suspension was degassed by three freeze-pump-thaw cycles and heated with stirring at r.t. for 18 h. The resulting suspension was diluted with CH_2Cl_2, washed with water (2×), dried ($MgSO_4$), filtered, and concentrated. Purification by flash chromatography (4:1 hexanes/EtOAc) gave tri-tert-butyl(((benzene-1,3,5-triyltris(ethyne-2,1-diyl))tris(benzene-2,1-diyl))-tris(methylene))-tri-carbamate as a brown solid (0.77 g, 1.0 mmol), 32%. ^{1}H NMR (500 MHz, $CDCl_3$) δ 7.69 (s, 1H), 7.55 (d, *J* = 7.5 Hz, 1H), 7.41 (d, *J* = 7.4 Hz, 1H), 7.35 (t, *J* = 7.5 Hz, 1H), 7.29 (t, *J* = 7.5 Hz, 1H), 5.01 (s, 2H), 4.58 (d, *J* = 4.8 Hz, 2H).

To a 250ml round bottom flask containing tri-tert-butyl (((benzene-1,3,5-triyltris(ethyne-2,1-diyl))tris(benzene-2,1-diyl))tris(methylene))tricarbamate (0.49 g, 0.64 mmol) and DCM (100 mL) was added TFA (5.2 g, 45 mmol) slowly in an ice bath. The reaction mixture was then removed from the ice bath and stirred at r.t. for 10 h. The reaction mixture was then extracted with water (2×) and the water layer basified with 1 M NaOH(aq). Precipitate was formed and isolated by vacuum filtration to give monomer **6** as a brown solid (0.29 g, 62 mmol), 99%. ^{1}H NMR (500 MHz, MeOD) δ 7.86 (s, 1H), 7.68 (dd, *J* = 7.5, 1.1 Hz, 1H), 7.57 (d, *J* = 7.5 Hz, 1H), 7.52 (td, *J* = 7.5, 1.4 Hz, 1H), 7.48 (td, *J* = 7.5, 1.4 Hz, 1H), 4.35 (s, 2H).

Reference

(1) S. J. Rowan, S. J. Cantrill, G. R. L. Cousins, J. K. M. Sanders, J. F. Stoddart, *Angew. Chem. Int. Ed.* **2002**, *41*, 898.

(2) F. Ren, K. J. Day, C. S. Hartley, *Angew. Chem. Int. Ed.* **2016**, *55*, 8620.

(3) S. R. Beeren, M. Pillelkow, J. K. M. Sanders, *Chem. Commun*. **2011**, *47*, 7359.

(4) S. R. Beeren, J. K. M. Sanders, *J. Am. Chem. Soc.* **2011**, *133*, 3804.

(5) A. C. Fahrenbach, S. C. Warren, J. T. Incorvati, A. J. Avestro, J. C. Barnes, J. F. Stoddart and B. A. Grzybowski, Adv. Mater., **2013**, *25*, 331.

(6) M. Ruben, J.-M. Lehn and P. Muller, *Chem. Soc. Rev.* **2006**, *35*, 1056.

(7) J. G. Hardy, *Chem. Soc. Rev.* **2013**, *42*, 7881.

(8) P. A. Gale, N. Busschaert, C. J. E. Haynes, L. E. Karagiannidis and I. L. Kirby, *Chem. Soc. Rev.* **2014**, *43*, 205.

(9) S. F. Vasilevsky, T. F. Mikhailovskaya, I. V. Alabugin, *J. Org. Chem.* **2009**, *74*, 8106.

(10) K. E. Jelfs, E. G. B. Eden, A. I. Cooper, *J. Am. Chem. Soc*. **2013**, *135*, 9307.

(11) N. Giuseppone, J. Schmitt, E. Schwartz, J. Lehn, *J. Am. Chem. Soc.* **2005**, *127*, 5528.

(12) S. Käss, T. Gregor, B. Kersting, *Angew. Chem. Int. Ed.* **2006**, *45*, 101.

(13) N. Sakai, K. Annaka, A. Fujita, A. Sato, T. Konakahara, *J. Org. Chem.* **2008**, *73*, 4160.

(14) W. Sun, L. D. Cama, E. T. Birzin, S. Warrier, L. Locco, R. Mosley, M. L. Hammond, S. P. Rohrer, *Bioorg. Med. Chem. Lett.* **2006**, *16*, 1468.

Spectral Data

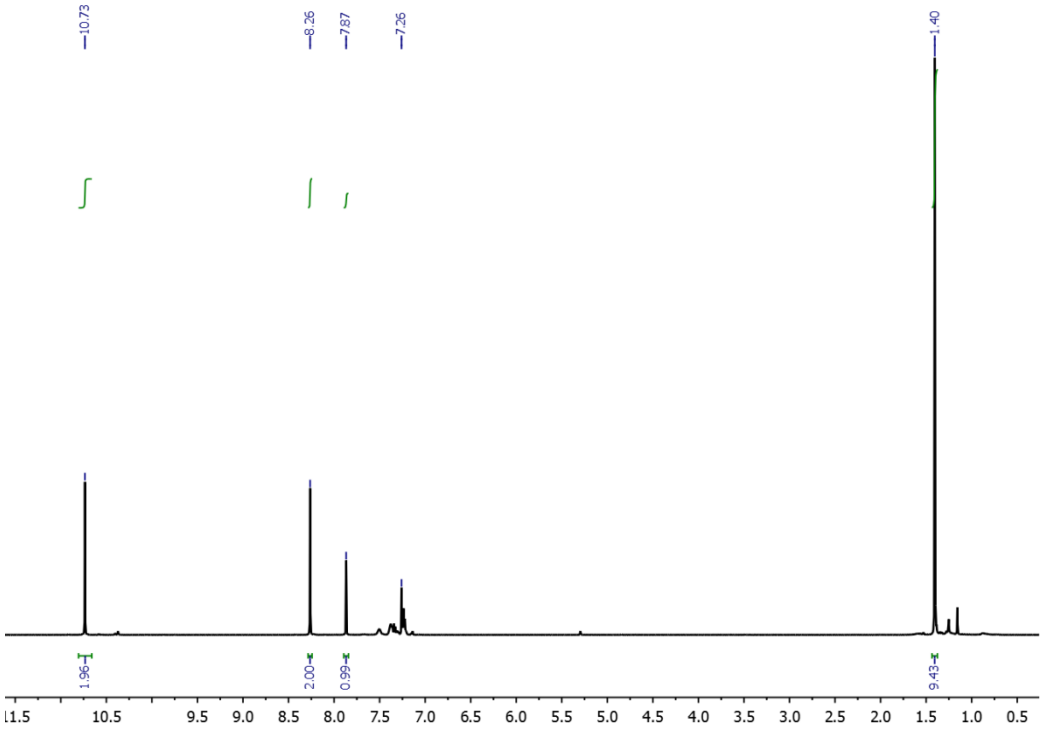

^{1}H NMR (500 MHz, $CDCl_3$) of monomer **5**

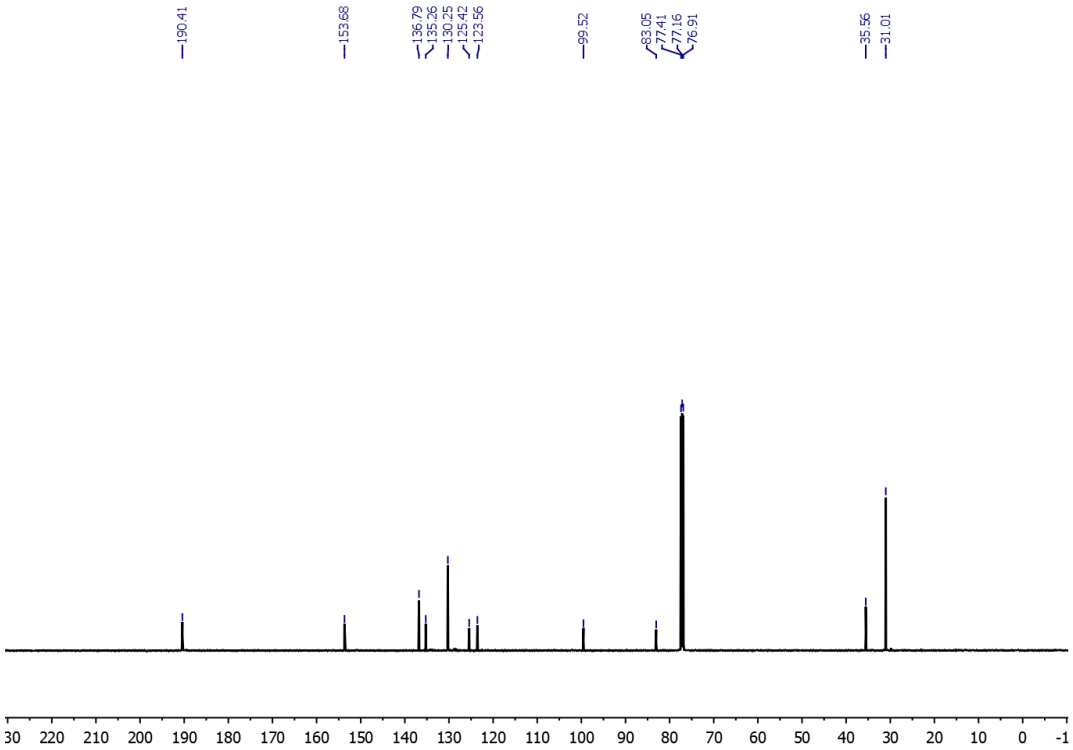

^{13}C NMR (126 MHz, $CDCl_3$) of monomer **5**

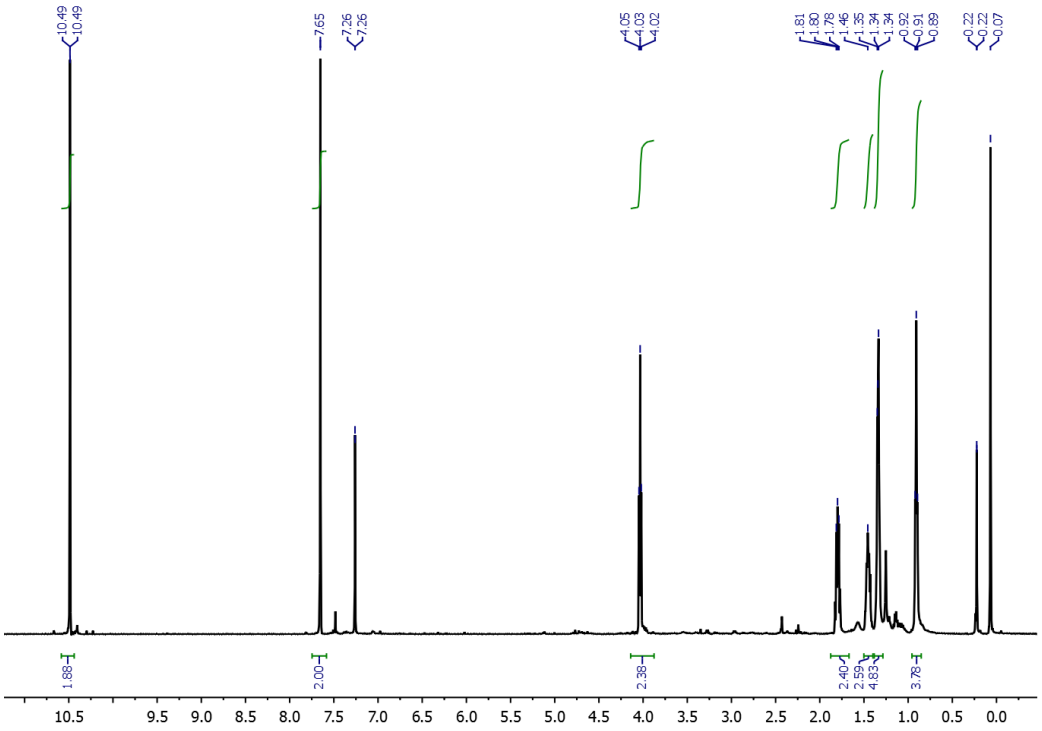

^{1}H NMR (500 MHz, $CDCl_3$) of 2-bromo-5-(hexyloxy)isophthalaldehyde

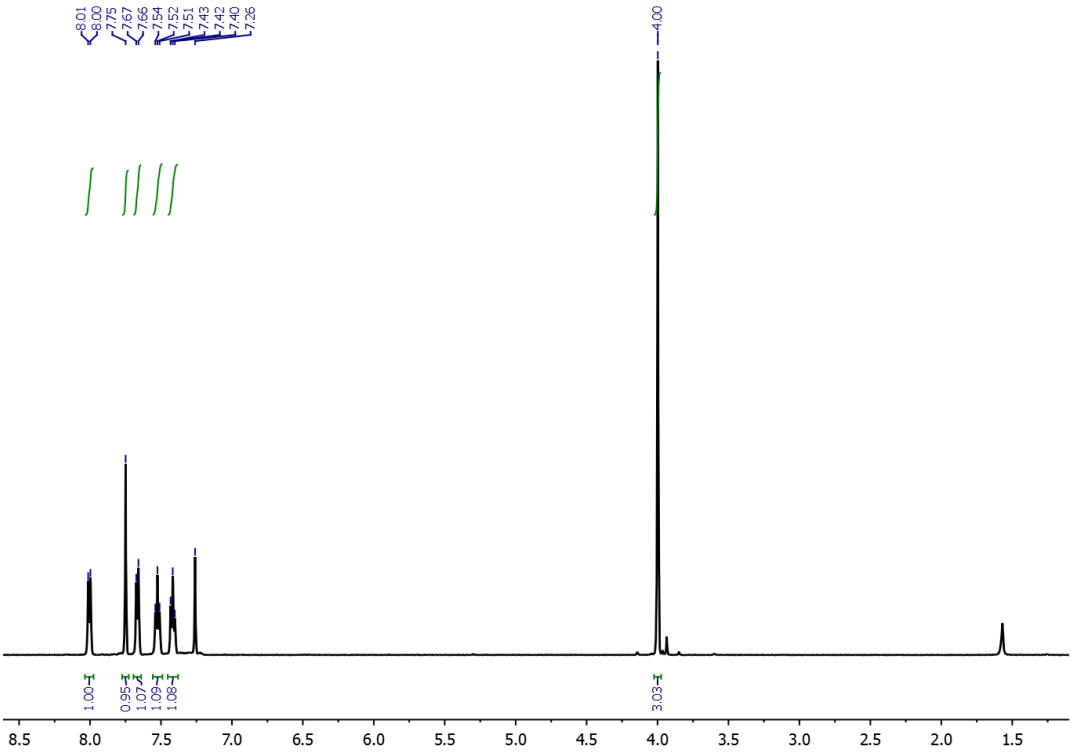

^{1}H NMR (500 MHz, $CDCl_3$) of trimethyl 2,2',2"-(benzene-1,3,5-triyltris(ethyne-2,1-diyl))tribenzoate

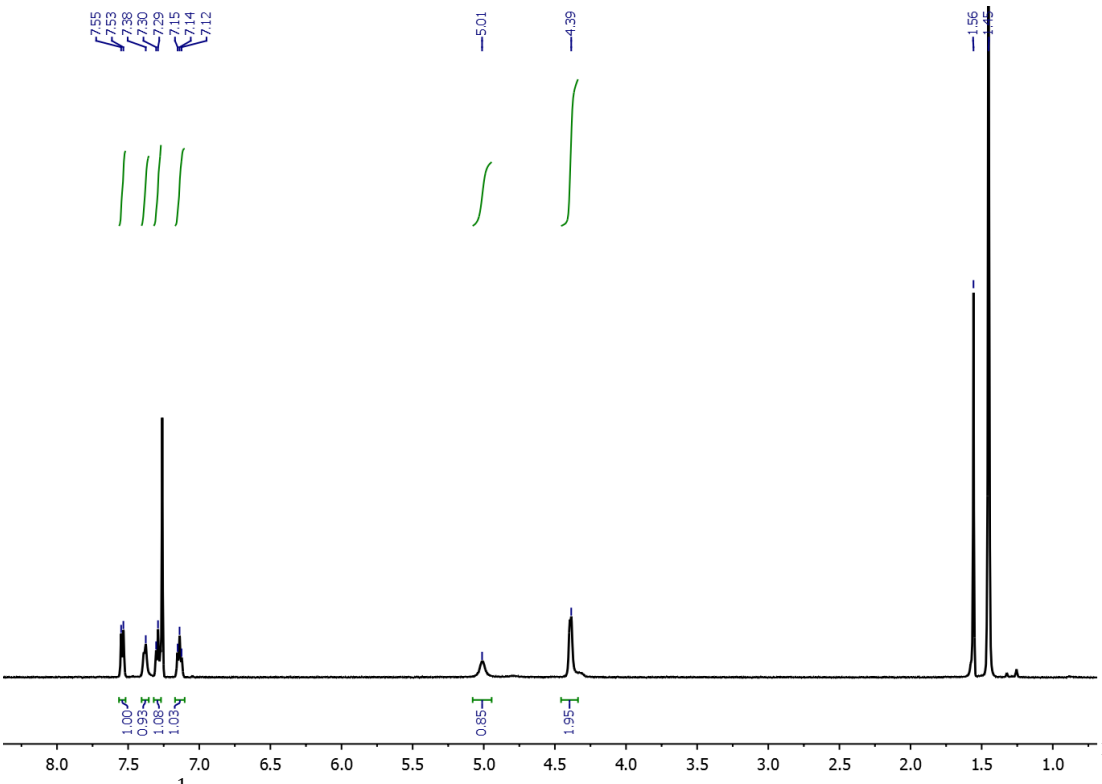

^{1}H NMR (500 MHz, $CDCl_3$) of tert-butyl 2-bromobenzylcarbamate

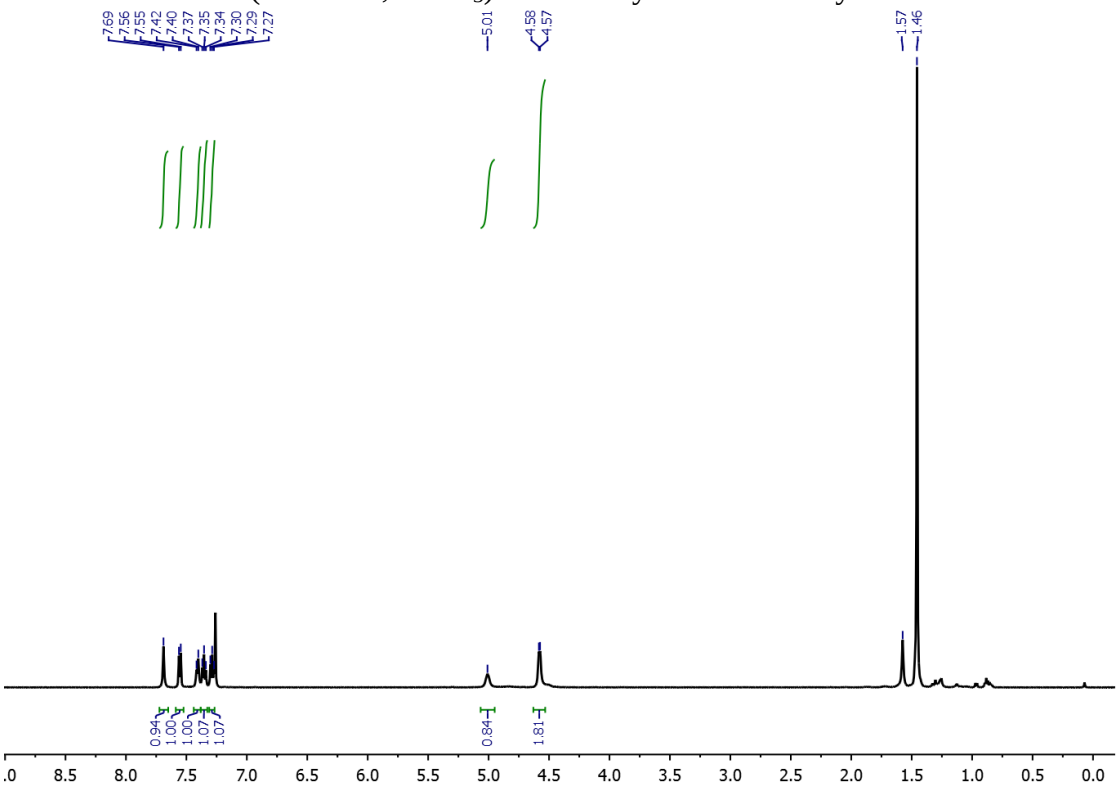

^{1}H NMR (500 MHz, $CDCl_3$) of tri-tert-butyl (((benzene-1,3,5-triyltris(ethyne-2,1-diyl))tris(benzene-2,1-diyl))tris(methylene))tricarbamate

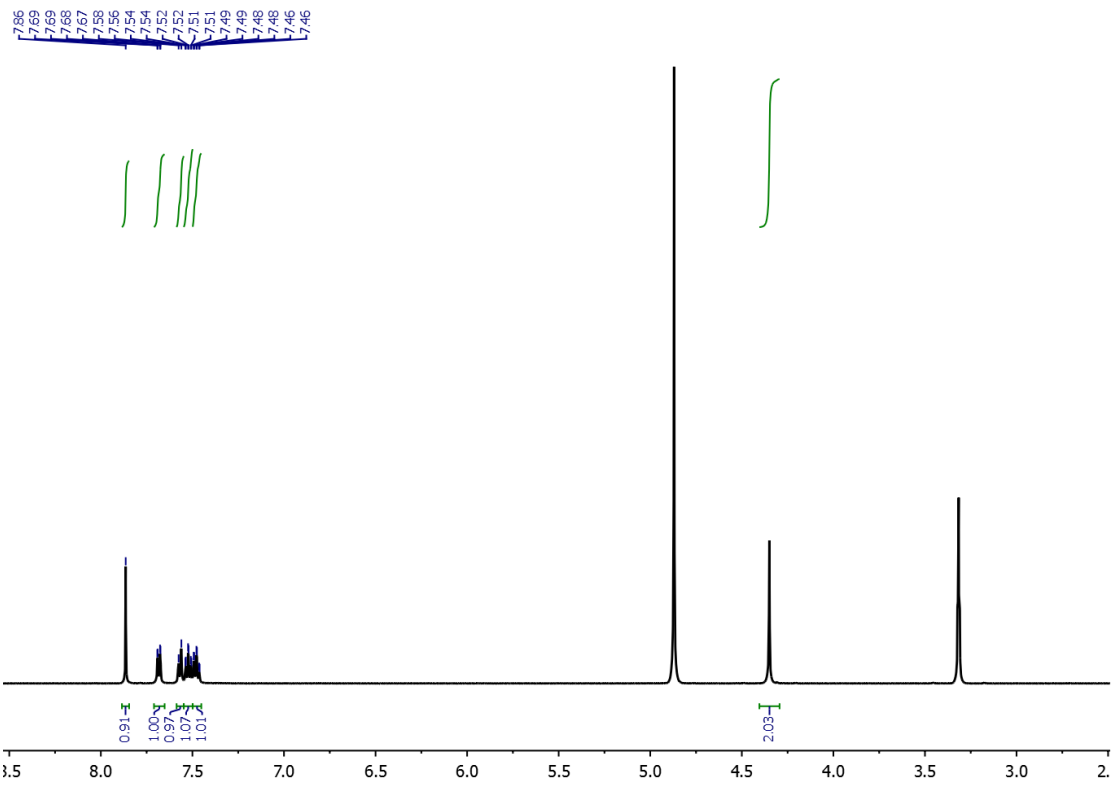

^{1}H NMR (500 MHz, MeOD-*d*4) of Monomer **6**

Chapter 4 Dynamic Covalent Self-Assembly of Flexible 2- and 3-tiered stacks

4.1 Introduction

Methodologies and strategies for the synthesis of small organic molecules have attracted enormous research interest due to their great importance in development of novel functional materials, such as liquid crystals, electronic devices, etc.[1-5] Dynamic covalent chemistry (DCC) has been used in the construction of covalently bound, 2-D and 3-D molecules in the past two decades.[6-10] It is its self-correction behavior that makes DCC a powerful tool for bottom-up materials synthesis.[11-13] Monomer design is tremendously important in the self-assembly process because it contains the information that determines product structure at equilibrium. Previously, we showed that stacked architectures could be assembled from discotic cores functionalized with reactive arms. In this work, we used acetylene as the connections between the reactive groups and the central core.[14] However, there was competing formation of mis-assembled byproducts in systems designed to yield 3-tiered stacks: in one cases a low-symmetry isomer was obtained, and in another we observed a stopped two-tiered stack with unreacted amino groups.

We reasoned that the formation of these byproducts suggests that our original stacked architectures are strained. In order to solve this problem, we decided to change our monomers to use flexible linkers: ethylene groups that connect the benzene core to the aldehyde and amino coupling partners. Of course, while the added flexibility could minimize strain it could also inhibit assembly through reduced pre-organization. Here, we show that it is possible to assemble covalent stacks in high yields using flexible building blocks.

4.2 Results and Discussion

4.2.1 Synthesis

All of the flexible monomers were synthesized through hydrogenation of the rigid monomers analogous to our previous work. Hydrogenation of amino-functionalized monomers **2** and **4** in DCM with Pd/C as catalyst for 16 hours gave flexible monomers **8** and **9** without difficulty (Scheme 4.1). However, for monomer **1** the aldehyde functional group was also hydrogenated when first attempted (entry **1**, **Table 4.1**). To solve this problem, we looked at protection of the aldehyde as the dimethyl acetal (entries **2**, **3** and **4**, **Table 4.1**), which required optimization. For entry **2** in **Table 4.1**, the yield was 40% but the product **7** was impure and

difficult to purify. The impure product contained hydrogenated aldehyde and uncomplete hydrogenated alkyne. No **7** was formed when the solvent was changed from ethyl acetate to DCM (entry **3**, **Table 4.1**). Pure monomer **7** was, however, isolated in 25% yield when the time was shortened to 1 hour (entry **4**, **Table 4.1**). Switching to the ethylene glycol acetal was unsuccessful, as the acetylene could no longer be hydrogenated (entry 5, table 4.1). Surprisingly, however, 78% pure monomer **7** was isolated when monomer **1** was hydrogenated with Pd/C as catalyst for with the time reduced to 1 h in DCM.

Hydrogenation of the dialdehyde monomer **3** was, however, more problematic. Protection of the aldehyde was first performed but conditions could not be identified for hydrogenation of the acetylenes. Following our success with monomer **1**, monomer **3** was then hydrogenated directly with different time and catalysts (**Table 4.2**). When monomer **3** was hydrogenated with Pd/C as catalyst for 1 h in DCM the acetylene was hydrogenated only to the alkene level (entry **1**, **Table 4.2**). The aldehydes were hydrogenated to methyl groups at longer reaction times (entries **2** and **3**, **Table 4.2**). Other conditions were attempted, notably Pd(0) EnCat 30NP and using diphenylsulfide as catalyst poison to Pd/C were also tried to hydrogenate monomer **3**; however, no desired product was obtained (entries **4**,**5** and **6**, **Table 4.2**).[15-17]

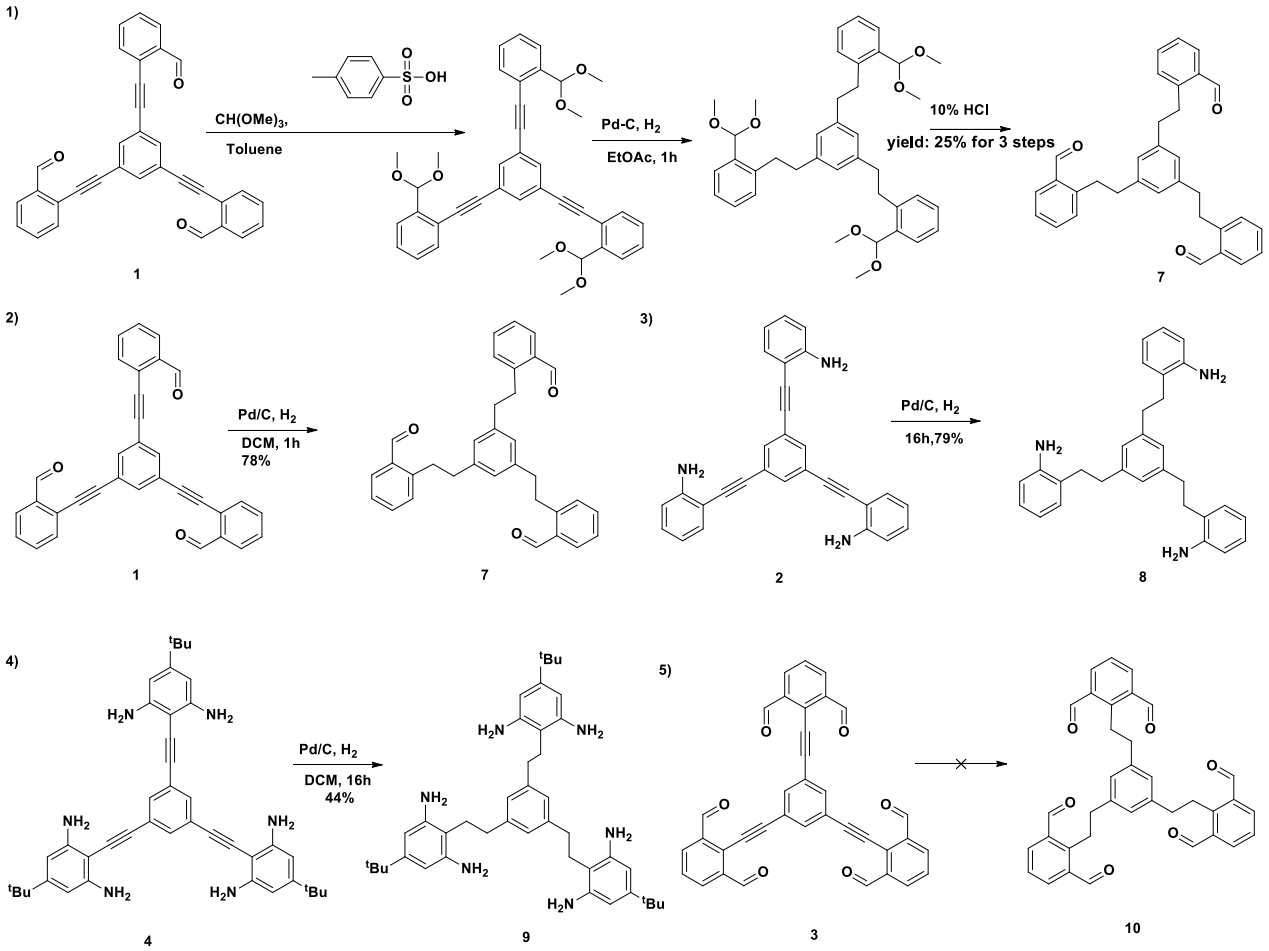

Scheme 4.1 Hydrogenation of rigid monomers to flexible monomers.

Entry Number	Protection Group	Catalyst	time/h	solvent	yield
1	n.a.	Pd/C	4	EtOAc	n.a.
2	acetal	Pd/C	4	EtOAc	40% not pure
3	acetal	Pd/C	4	DCM	n.a.
4	acetal	Pd/C	1	EtOAc	25%
5	ethylene glycol acetal	Pd/C	4	EtOAc	n.a.
6	n.a.	Pd/C	1	DCM	78%

Table 4.1 Conditions for hydrogenation of monomer 1 to monomer 7.

Entry Number	Catalysts	time/h	yield
1	Pd/C	1	n.a.
2	Pd/C	4	n.a.
3	Pd/C	16	n.a.
4	Pd(0) EnCat 30NP	16	n.a.
5	Pd(0) EnCat 30NP	48	n.a.
6	Pd(0) EnCat 30NP	72	n.a.
7	Pd/C, diphenylsulfide	24	n.a.
8	Pd/C, diphenylsulfide	48	n.a.
9	Pd/C, diphenylsulfide	72	n.a.

Table 4.2 Conditions for hydrogenation of monomer 3 to monomer 10. (DCM was the solvent used for all conditions because of the solubility of monomer 3.)

With the flexible monomers in hand, we first tested the assembly of flexible 2-tiered stack **F-2TPh**, as shown in **Scheme 2**. In the presence of trifluoroacetic acid (12 mol%) in chloroform-d, monomers **7** and **8** assemble to **F-2TPh**. ^{1}H NMR monitoring (**Figure 4.1**) showed that the reaction proceeded quickly, with 59% of starting material converted to **F-2TPh** in about 25 min. Approximately 81% **F-2TPh** was formed after 110 min. A plot of relative concentration of imine vs time also showed that the reaction reaches equilibrium after 1 h as shown in **Figure 4.2**. **F-2TPh** was isolated in 35% yield by flash chromatography (directly as the imine).

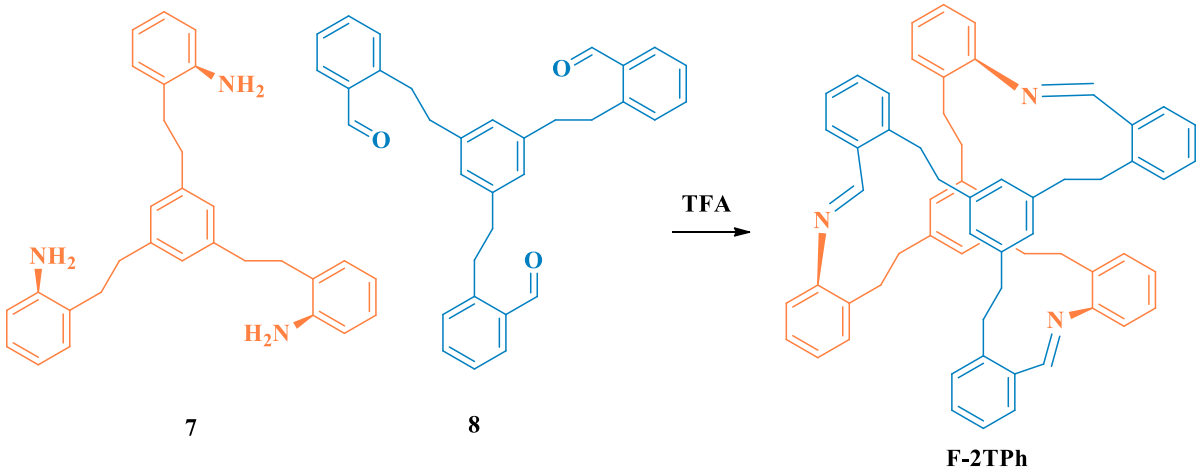

Scheme 4.2 Synthesis of **F-2TPh**.

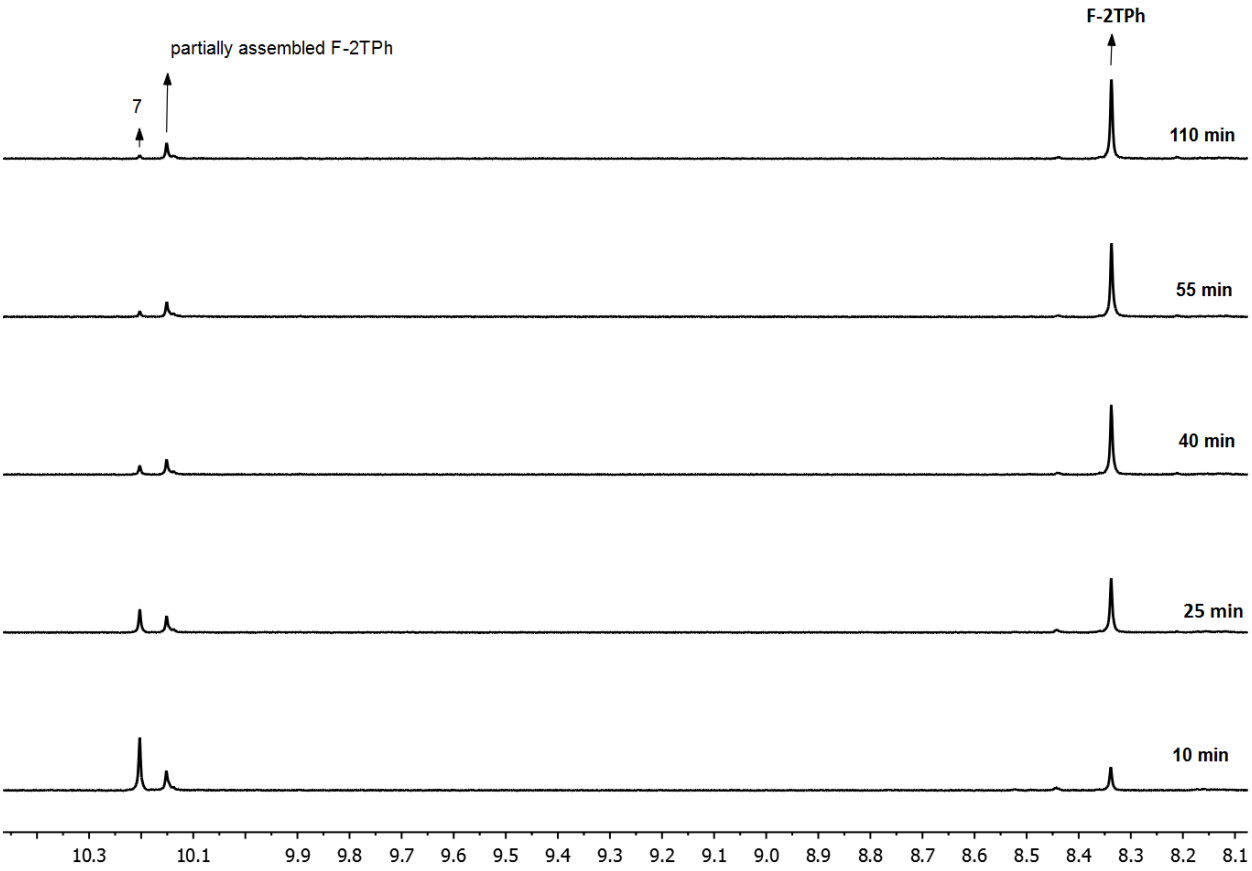

Figure 4.1 ^{1}H NMR monitoring of the assembly of **F-2TPh**($CDCl_3$, 500 MHz).

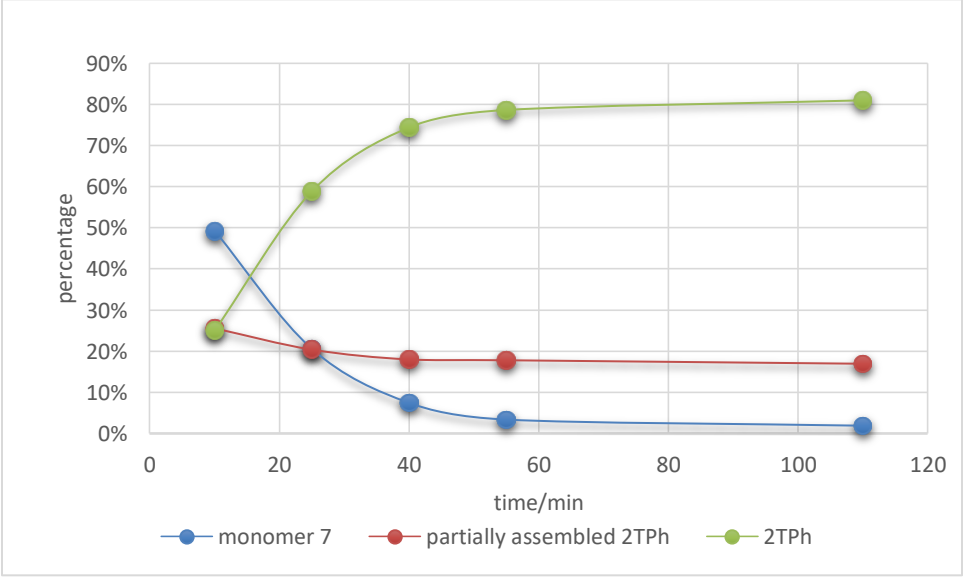

Figure 4.2 Relative concentration of imine vs Time for **F-2TPh**.

We then attempted to prepare the flexible three-tiered stack **F-3TPh** as shown in **Scheme 4.3**. Monomer **9**, with six pendant amino groups, was combined with two equivalents of monomer **7**. As shown in ^{1}H NMR monitoring (**Figure 4.3**), **F-3TPh** was not formed very quickly compared with ^{1}H NMR monitoring of **F-2TPh**. The assembly system for **F-3TPh** is more complex than **F-2TPh**, and equilibration takes more time, with concurrent formation of polymeric byproducts that slowly decompose. The imine peak of **F-3TPh** showed up in around 1 h, highlighting the importance of the reversibility of these dynamic systems. 90% of monomer **7** was consumed at 3.5 h relative to the imine peak. The target **F-3TPh** was isolated in 66% yield by flash chromatography.

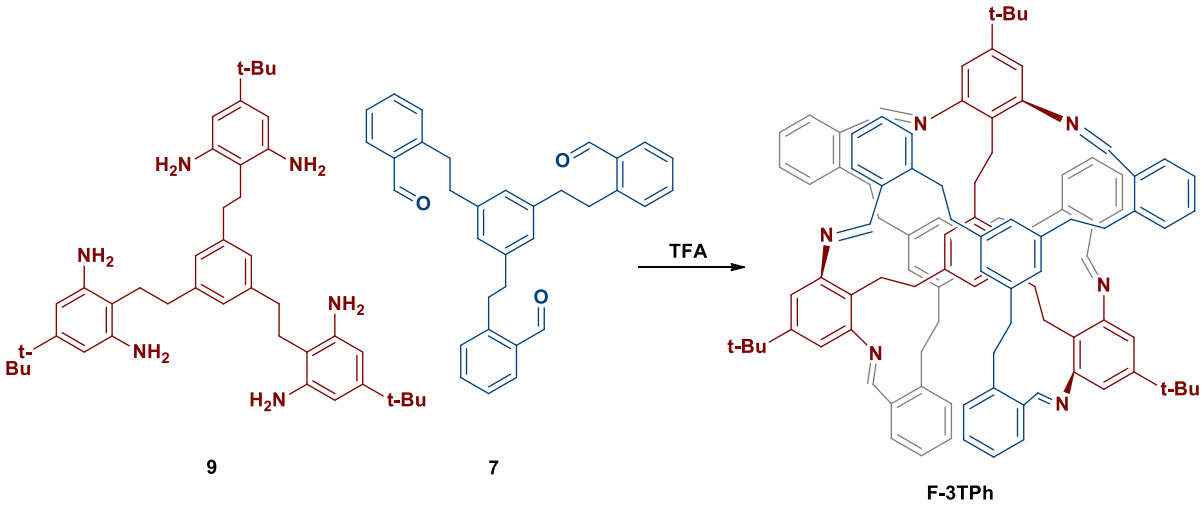

Scheme 4.3 Synthesis of **F-3TPh.**

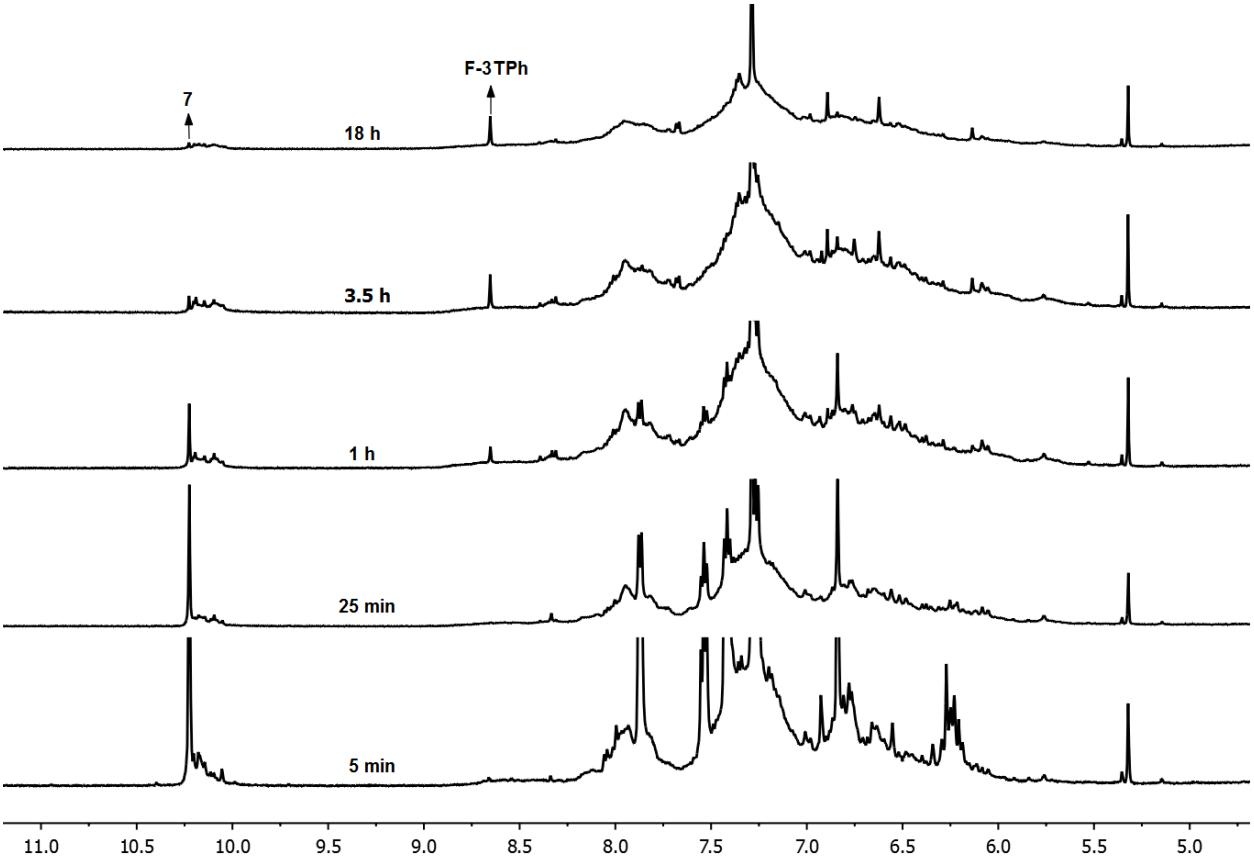

Figure 4.3 ^{1}H NMR monitoring of the assembly of **F-3TPh** ($CDCl_3$, 500 MHz).

This result is particularly significant because in our previous work we saw the competing formation of an isomeric byproduct $\mathbf{3T_{iso}}$ formed during self-assembly of rigid three-tiered stack which was only twofold symmetric. However, in the ^{1}H NMR spectra of **F-3TPh** only one imine peak is observed. The ^{13}C spectrum of **F-3TPh** also confirmed the D_3 structural symmetry of **F-3TPh**. Thus, the added flexibility of the system allows the desired higher-symmetry product to be formed exclusively, presumably because it minimizes strain. Flexible amines and aldehydes have also assembled into different cages by Cooper.[18]

4.2.2 Conformational Analysis

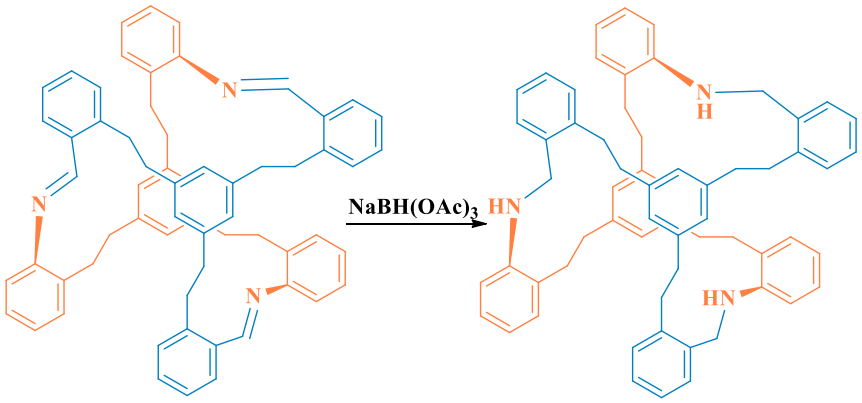

F-2TPh **F-2T'**

Scheme 4.4 Reduction of **F-2TPh** to **F-2T′**.

F-2TPh was reduced with $NaBH(OAc)_3$ (6 eq) to form **F-2T′**. For these stacked architectures, racemization should occur via twisting of overall structure.[4] For **F-2T′** at room temperature (toluene-*d8*), only one ^1H NMR signal was observed for the diastereotopic methylene protons (-C$\underline{H}_2$NH-). Variable temperature ^1H NMR was performed, no change has been observed before all peaks started to broaden at around 233 K. This behavior is qualitatively similar to that of the rigid stack **2T′**.

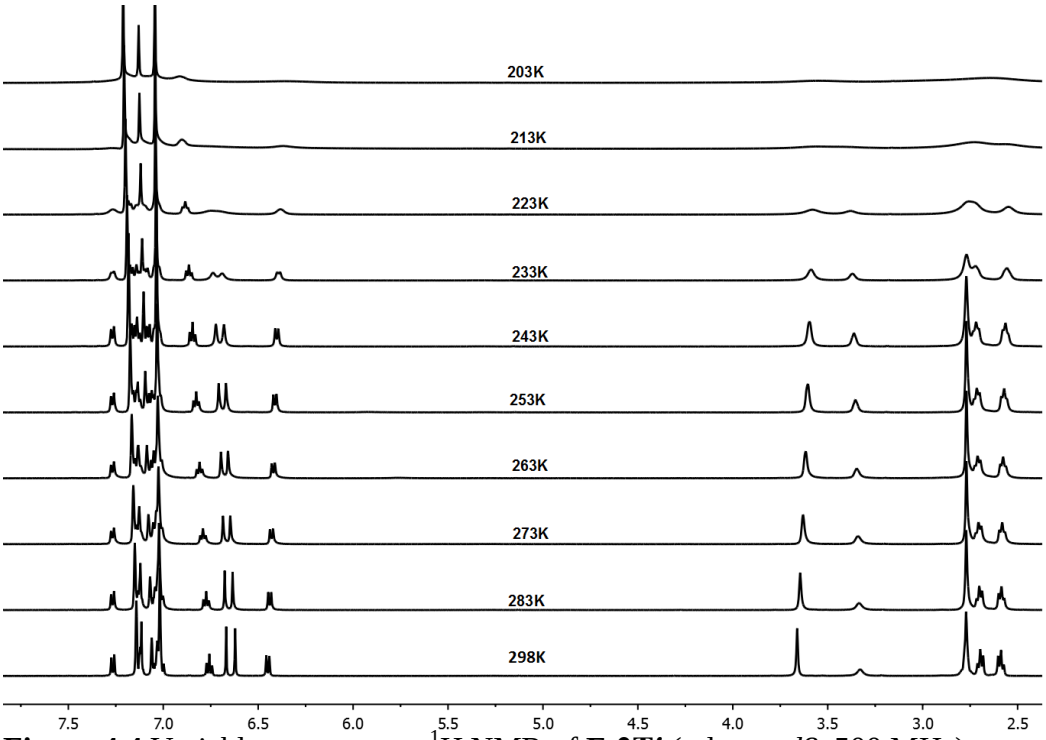

Figure 4.4 Variable temperature ^{1}H NMR of **F-2T′** (toluene-*d8*, 500 MHz).

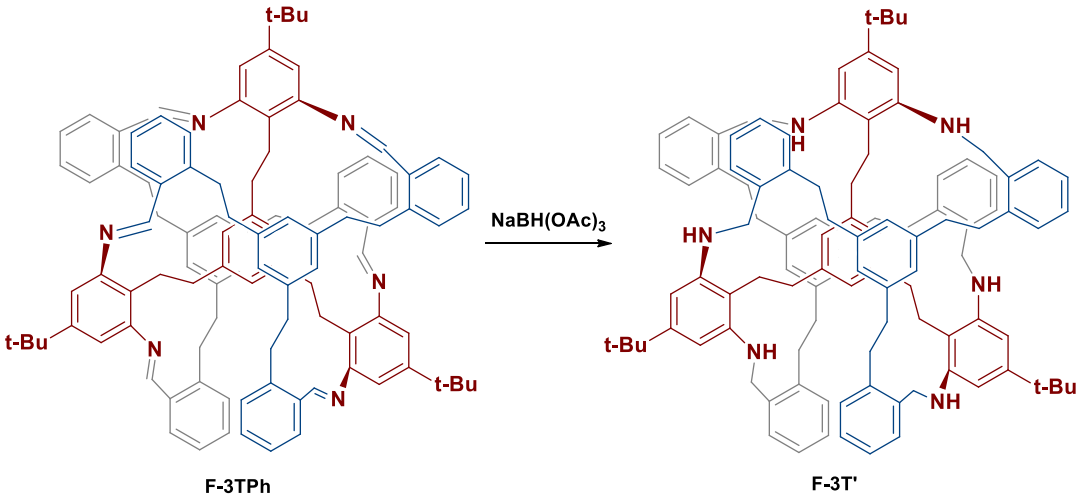

Scheme 4.5 Reduction of **F-3TPh** to **F-3T′**.

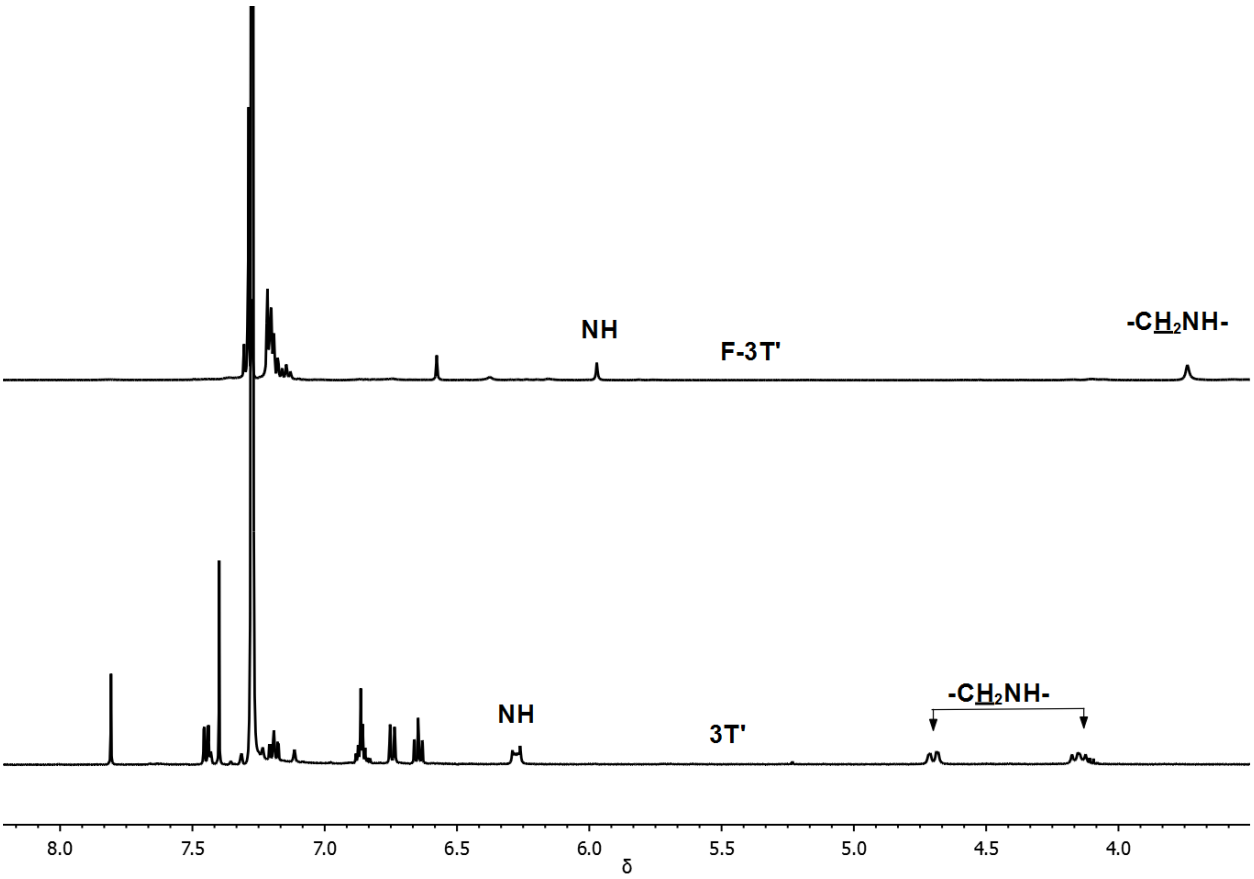

Figure 4.5 ^{1}H NMR of **F-3T′** vs **3T′**.

F-3T′ was also synthesized through reduction of **F-3TPh** with $NaBH(OAc)_3$ (12 eq). The conformational dynamics of **F-3T′** and **3T′** are different. As we discussed in our previous paper, the two methylene protons of **3T′** are clearly distinguishable by ^{1}H NMR at room temperature; In contrast, **F-3T′** as shown in **Figure 4.5** only one ^{1}H NMR signal is observed for the diastereotopic methylene protons (**-C<u>H</u>$_2$NH-**); Thus, after hydrogenation of acetylene, interconversion between the (M)- and (P)-enantiomers of **F-3T′** is much faster than for **3T′**.

4.4 Experimental

4.4.1 General

Unless otherwise noted, all reagents and solvents were purchased from commercial sources and used without further purification. Anhydrous THF was obtained using an alumina-column solvent purification system. Flash column chromatography was performed using Silicycle SiliaFlash P60 (40–63 μm, 230–400 mesh). Melting points were determined using a

Thermal Analysis Q20 differential scanning calorimeter at a heating rate of 5 ℃/min. NMR spectra were measured in deuterated solvents using Bruker Avance 300 or 500 MHz spectrometers. Chemical shifts are reported in δ (ppm) relative to TMS, with the residual solvent protons used as internal standards ($CDCl_3$: 7.26 for ^1H, 77.16 for ^{13}C). High resolution mass spectra were obtained from the Ohio State University mass spectrometry facility.

4.4.2 Synthesis

Monomer (8)

To a 100 mL round bottom flask containing **2** (99.8 mg, 0.24 mmol) and Pd/C (70.4 mg, 3 mol%) was added DCM (15 mL). After stirring for 16 h at rt under H_2, the resulting suspension was filtered through Celite. The filtrate was concentrated to give **8** as a brown oil (80.6 mg, 0.19 mmol, 79%). ^1H NMR (500 MHz, $CDCl_3$) δ 7.09 – 6.99 (m, 1H), 6.84 (s, 1H), 6.75 (td, J = 7.4, 1.1 Hz, 1H), 6.68 (dd, J = 7.8, 0.9 Hz, 1H), 2.86 (dd, J = 9.4, 6.5 Hz, 1H), 2.73 (dd, J = 9.2, 6.6 Hz, 1H). ^{13}C NMR (126 MHz, $CDCl_3$) δ 144.1 , 142.0 , 129.5 , 127.0 , 126.3 , 126.0 , 118.8 , 115.6 , 35.1 , 33.4 ; HRMS (MALDI) calcd for $C_{30}H_{33}N_3$ ($[M+H^+]$) 436.2747, found: 436.2758.

Monomer (7)

To a scintillation vial containing **1** (41.1 mg, 0.090 mmol) and Pd/C (28.8 mg, 3 mol%) was added DCM (10 mL). After stirring for 1 h at r.t. under H_2, the resulting suspension was filtered through Celite. The filtrate was concentrated to give **7** as a colorless oil (33.2 mg, 0.070 mmol, 78%). ^1H NMR (500 MHz, $CDCl_3$) δ 10.20 (s, 1H), 7.97 – 7.71 (m, 1H), 7.51 (td, J = 7.5, 1.1 Hz, 1H), 7.39 (t, J = 7.5 Hz, 1H), 7.24 (d, J = 7.6 Hz, 1H), 6.82 (s, 1H), 3.33 – 3.18 (t, 2H), 2.92 – 2.76 (t, 2H).^{13}C NMR (126 MHz, $CDCl_3$) δ 192.3, 144.6, 141.5, 133.9, 132.1, 131.4, 126.9, 126.8, 38.4, 35.0; HRMS (MALDI) calcd for $C_{33}H_{30}O_3$ ($[M+H^+]$) 475.2268, found: 475.2274.

Monomer (9)

To a 100 mL round bottom flask containing **4** (83.0 mg, 0.13 mmol) and Pd/C (41.6 mg, 3 mol%) was added DCM (15 mL). After stirring for 16 h at r.t. under H_2, the resulting suspension was filtered through Celite. The filtrate was concentrated to give **9** as a brown oil (37.0 mg, 0.057 mmol, 44%). ^1H NMR (500 MHz, $CDCl_3$) δ 7.26 (s, 6H), 6.91 (s, 3H), 6.21 (s,

6H), 3.43 (s, 12H), 2.78 (t, J = 7.8 Hz, 6H), 2.65 (t, J = 7.8 Hz, 6H), 1.24 (s, 30H). ^{13}C NMR (126 MHz, $CDCl_3$) δ 150.9, 144.9, 142.8, 126.5, 109.2, 104.7, 34.4, 33.9, 31.4, 27.9; HRMS (MALDI) calcd for $C_{42}H_{60}N_6$ ([M+H$^+$]) 649.4952, found: 649.4966.

F-2TPh Stack

To a scintillation vial containing **8** (37.4 mg, 0.086 mmol), **7** (36.6 mg, 0.077 mmol), and 3 Å molecular sieves was added $CHCl_3$ (10 mL), followed by a solution of CF_3CO_2H (1.05 mg, 0.0092 mmol) in $CHCl_3$ (0.2 mL). After stirring for 16 h at rt, the reaction mixture was quenched with triethylamine. The solution was concentrated directly. Purification by flash chromatography (10:5:85 DCM/triethylamine/hexanes) gave **F-2TPh** as a colorless oil (22.9 mg, 0.027 mmol, 35%). ^{1}H NMR (500 MHz, $CDCl_3$) δ 8.35 (s, 1H), 7.78 (d, J = 7.2 Hz, 1H), 7.35 (p, J = 7.1 Hz, 2H), 7.26 (m, J = 7.9 Hz, 2H), 7.16 (dt, J = 14.6, 7.2 Hz, 2H), 6.94 (d, J = 7.7 Hz, 1H), 6.68 (s, 1H), 6.48 (s, 1H), 3.32 (m, 2H), 2.98 (m, 2H), 2.76 (m, 2H), 2.59 (m, 2H). ^{13}C NMR (126 MHz, $CDCl_3$) δ 160.6, 151.6, 142.8, 141.1, 135.9, 134.1, 131.7, 131.1, 130.7, 129.6, 127.1, 126.4, 126.3, 125.9, 125.8, 118.0, 37.5, 36.9, 34.8, 33.2; HRMS (MALDI) calcd for $C_{63}H_{57}N_3$ ([M+H$^+$]) 856.4625, found: 856.4633.

F-3TPh stack

To a scintillation vial containing **7** (18.3 mg, 0.039 mmol), **9** (11.4 mg, 0.018 mmol), and 3 Å molecular sieves was added $CHCl_3$ (2 mL), followed by a solution of CF_3CO_2H (0.48 mg, 0.0042 mmol) in $CHCl_3$ (0.2 mL). After stirring for 3.5 h at rt, the reaction mixture was quenched with triethylamine. The solution was concentrated directly. Purification by flash chromatography (10:5:85 DCM/triethylamine/hexanes) gave **F-3TPh** as a clear oil (17.4 mg, 0.012mmol, 66%).^{1}H NMR (500 MHz, $CDCl_3$) δ 8.63 (s, 4H), 7.66 (m, 2H), 7.34 (m, 6H), 6.86 (s, 2H), 6.60 (s, 2H), 6.11 (s, 1H), 3.50 (dd, J = 5.96, 11.46 Hz, 4H), 3.06 (m, 2H), 2.68 (m, 4H), 2.45 (br. s., 2H), 1.40 (s, 9H). ^{13}C NMR (126 MHz, $CDCl_3$) δ 162.7, 152.2, 150.6, 143.5, 140.7, 139.3, 134.1, 133.7, 131.0, 130.6, 126.5, 126.1, 125.3, 124.4, 113.1, 37.3, 36.2, 35.1, 33.6, 31.6, 26.6; HRMS (MALDI) calcd for $C_{108}H_{108}N_6$ ([M+H$^+$]) 1489.8708, found: 1489.8721.

Reference

(1) T. Gaich, P. S. Baran, *J. Org. Chem.* **2010**, *75*, 4657.

(2) C. D. Dimitrakopoulos, P. R. L. Malenfant, *Adv. Mater.* **2002**, *14*, 99.

(3) S. R. Forrest, *Nature* **2004**, *428*, 911.

(4) G. Malliaras, R. Friend, *Phys. Today* **2005**, *58*, 53.

(5) X. Fu, L. Chen, J. Choo, *Anal. Chem.* **2016**.

(6) W. Zhang, J. S. Moore, *Angew. Chem. Int. Ed.* **2006**, *45*, 4416.

(7) M. J. MacLachlan, *Pure Appl. Chem.* **2006**, *78*.

(8) Y. Jin, A. Zhang, Y. Huang, W. Zhang, *Chem. Commun.* **2010**, *46*, 8258;

(9) X.-N. Xu, L. Wang, G.-T. Wang, J.-B. Lin, G.-Y. Li, X.-K. Jiang, Z.-T. Li, *Chem. Eur. J.* **2009**, *15*, 5763.

(10) Y. Jin, Q. Wang, P. Taynton, W. Zhang, *Acc. of Chem. Res.* **2014**, *47*, 1575.

(11) R. S. Forgan, J.-P. Sauvage, J. F. Stoddart, *Chem. Rev.* **2011**, *111*, 5434.

(12) J.-M. Lehn, *Science* **2002**, *295*, 2400.

(13) S. J. Rowan, S. J. Cantrill, G. R. L. Cousins, J. K. M. Sanders, J. F. Stoddart, *Angew. Chem. Int. Ed.* **2002**, *41*, 898.

(14) F. Ren, K. J. Day, C. S. Hartley, *Angew. Chem. Int. Ed.* **2016**, *55*, 8620.

(15) X.-N. Xu, L. Wang, G.-T. Wang, J.-B. Lin, G.-Y. Li, X.-K. Jiang, Z.-T. Li, *Chem. Eur. J.* **2009**, *15*, 5763.

(16) S. V. Ley, A. J. P. Stewart-Liddon, D. Pears, R. H. Perni, K. Treacher, *Beilstein J. Org. Chem.* **2006**, *2*, 15.

(17) A. Mori, Y. Miyakawa, E. Ohashi, T. Haga, T. Maegawa, H. Sajiki, *Org. Lett.* **2006**, *8*, 3279.

(18) M. E. Briggs, K. E. Jelfs, S. Y. Chong, C. Lester, M. Schmidtmann, D. J. Adams, A. I. Cooper, *Cryst. Growth Des.* **2013**, *13*, 4993.

Spectral Data

NMR assignment for F-2TPh

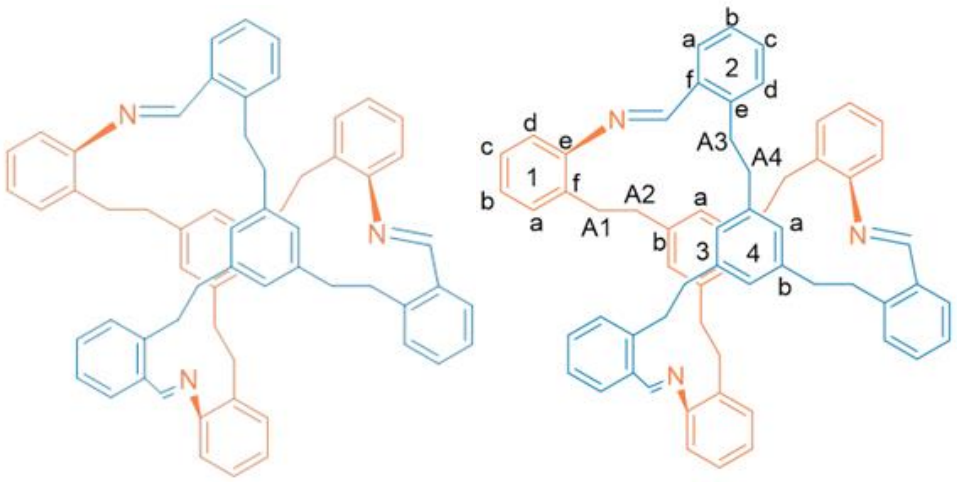

Position	^{1}H (ppm)	^{13}C(ppm)
1a	7.16	129.6
1b	7.16	125.8
1c	7.25	127.1
1d	6.94	118.0
1e		151.6
1f		135.9
2a	7.78	131.7
2b	7.35	126.3
2c	7.35	130.7
2d	7.25	131.1
2e		134.1

Position	^{1}H (ppm)	^{13}C(ppm)
2f		142.8
3a	6.48	125.9
3b		141.1
4a	6.68	126.4
4b		141.1
A1	2.98	33.2
A2	2.59	36.9
A3	3.32	34.8
A4	2.76	37.5
CH	8.35	160.6

NMR assignment for F-3TPh

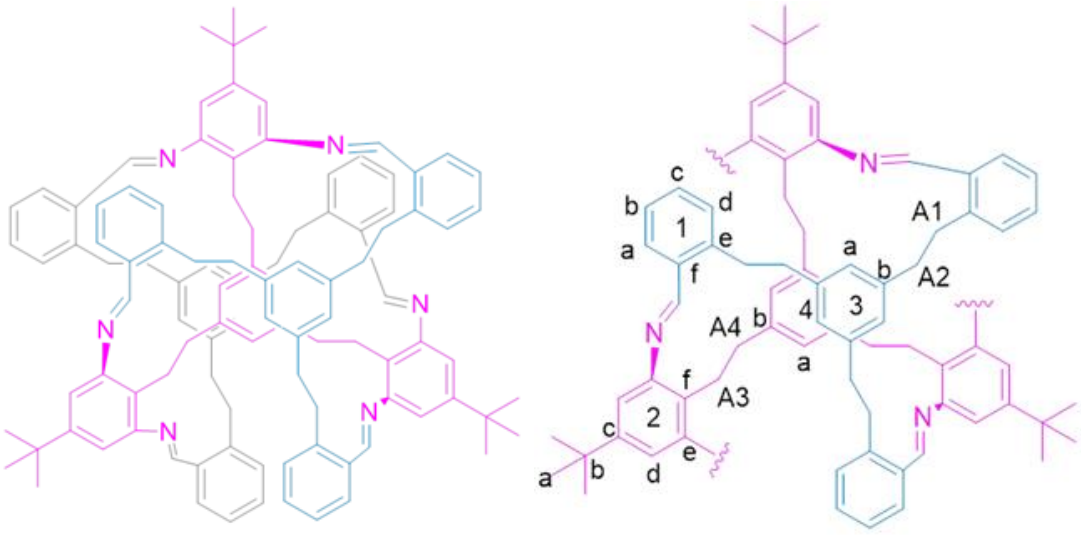

Position	^{1}H (ppm)	^{13}C(ppm)
1a	7.66	134.1
1b	7.34	133.7
1c	7.34	126.5
1d	7.34	131.0
1e		130.6
1f		143.5
2a	1.40	31.6
2b		35.1
2c		150.6
2d	6.86	113.1
2e		152.2

Position	^{1}H (ppm)	^{13}C(ppm)
2f		126.1
3a	6.60	125.3
3b		140.7
4a	6.11	124.4
4b		139.3
A1	2.68	37.3
A2	3.50	33.6
A3	2.45	36.2
A4	3.06	26.6
CH	8.63	162.7

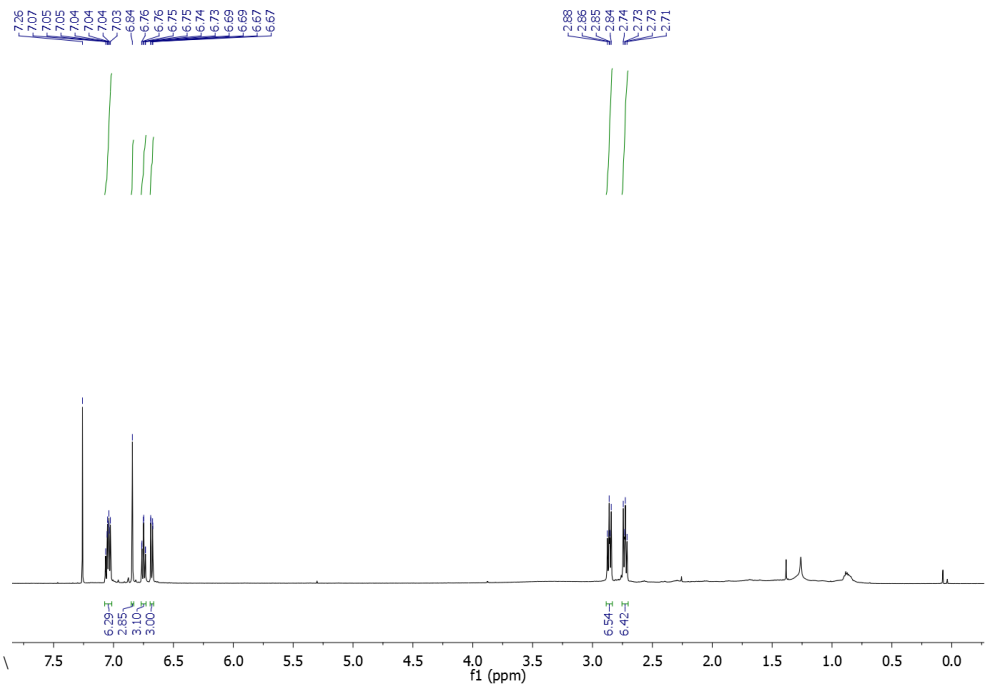

^{1}H NMR spectrum (500 MHz, $CDCl_3$) of monomer **8**

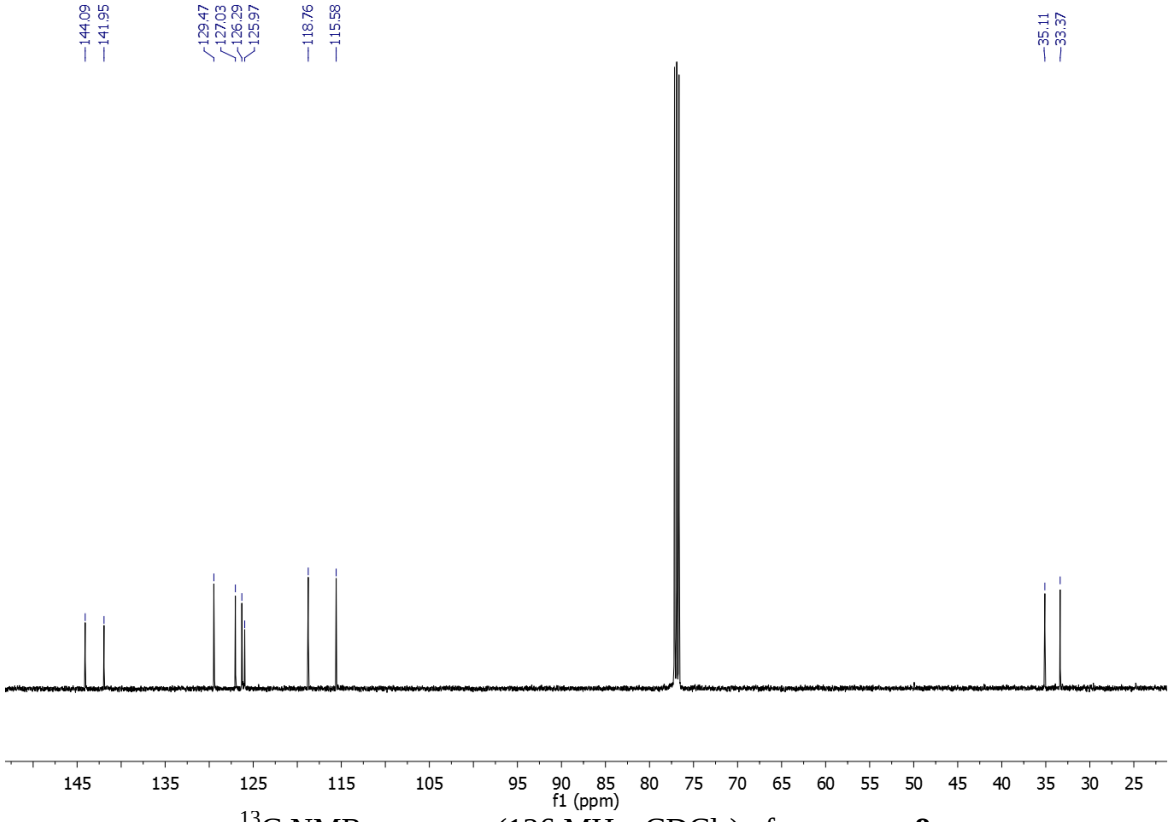

^{13}C NMR spectrum (126 MHz, $CDCl_3$) of monomer **8**

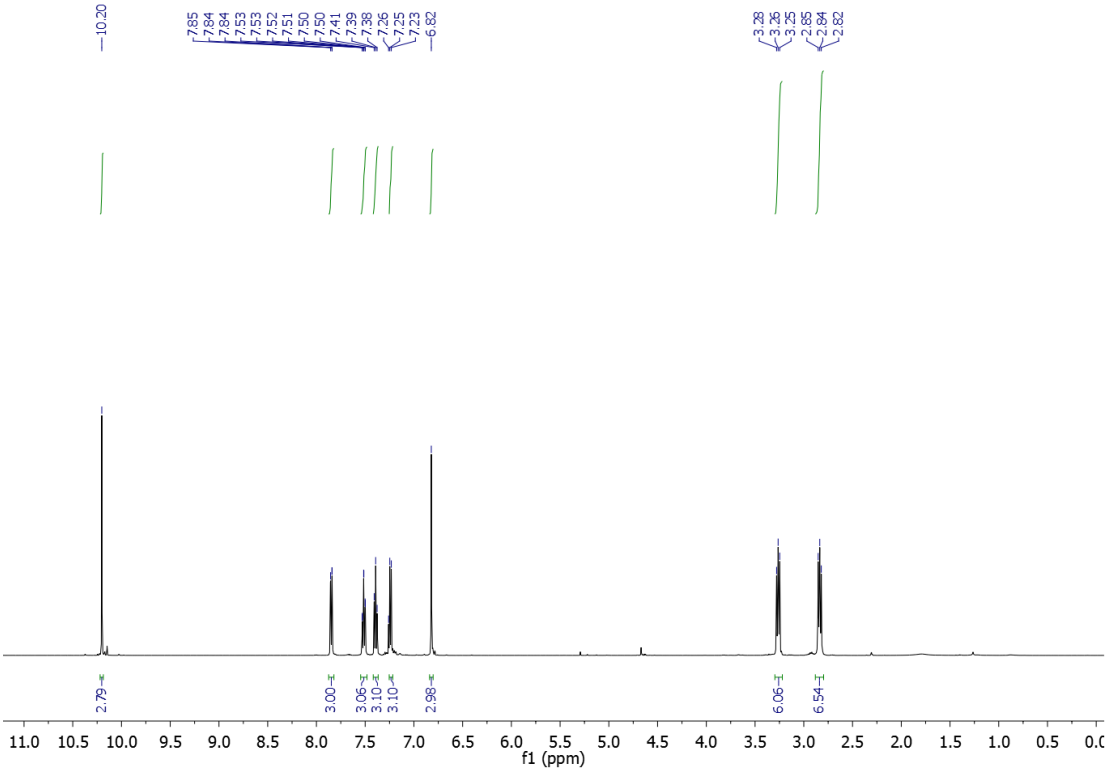

^{1}H NMR spectrum (500 MHz, $CDCl_3$) of monomer 7

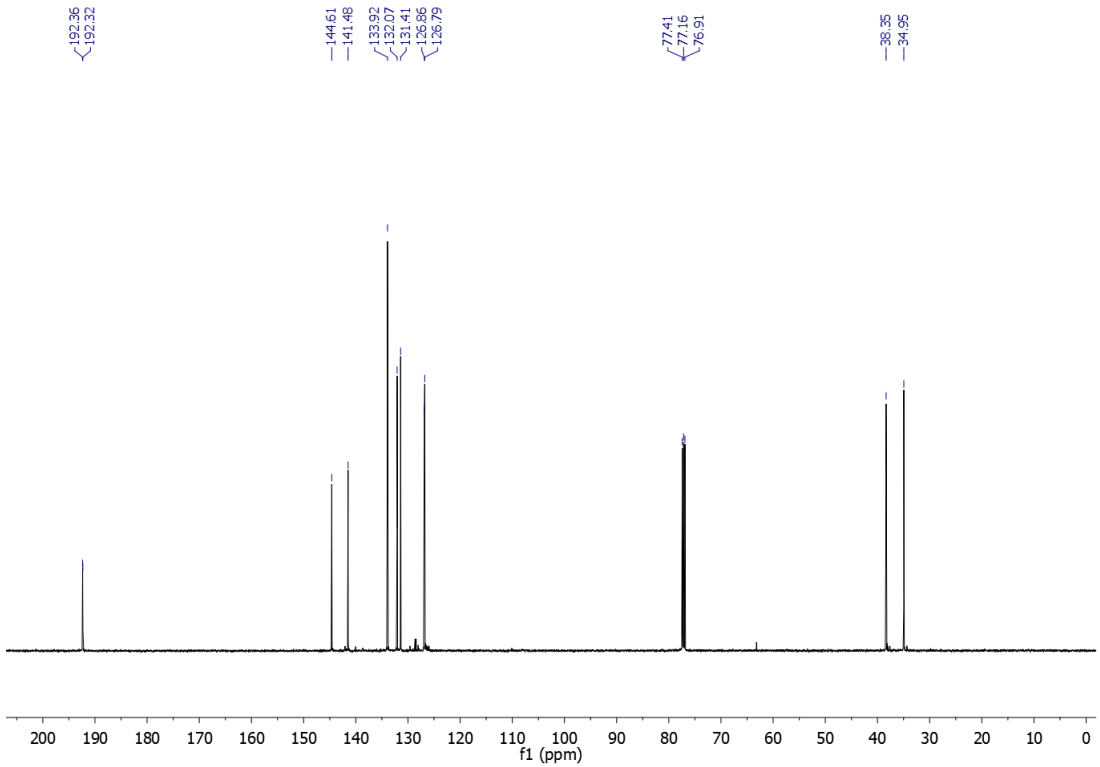

^{13}C NMR spectrum (126 MHz, $CDCl_3$) of monomer **7**

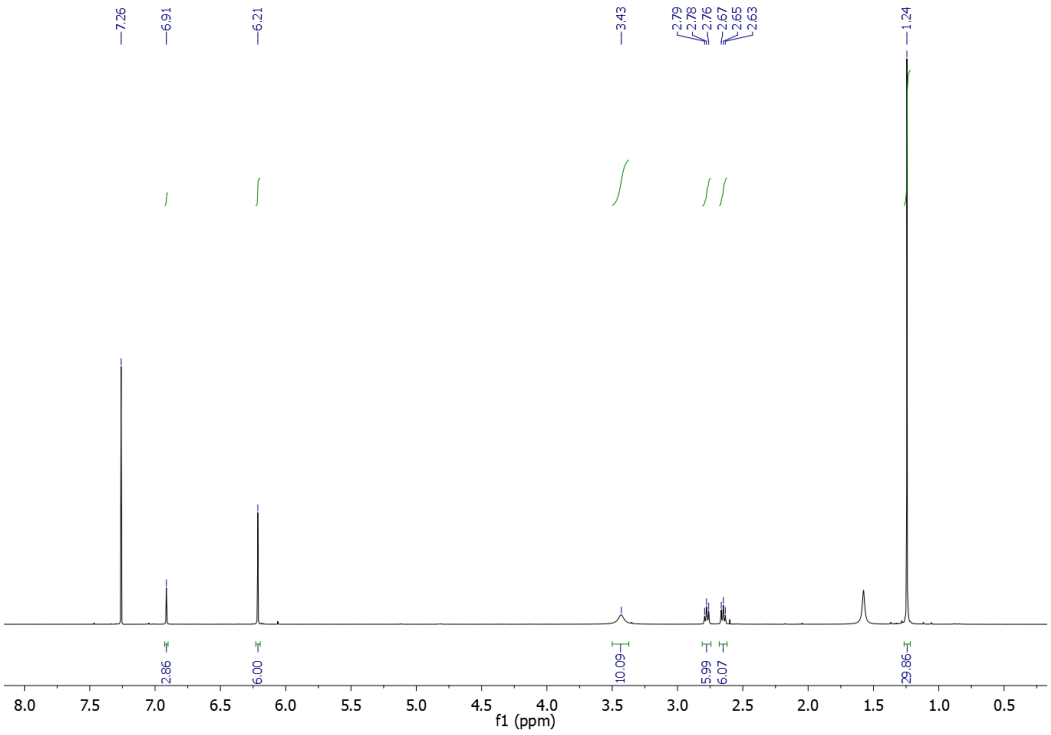

^{1}H NMR spectrum (500 MHz, $CDCl_3$) of monomer **9**

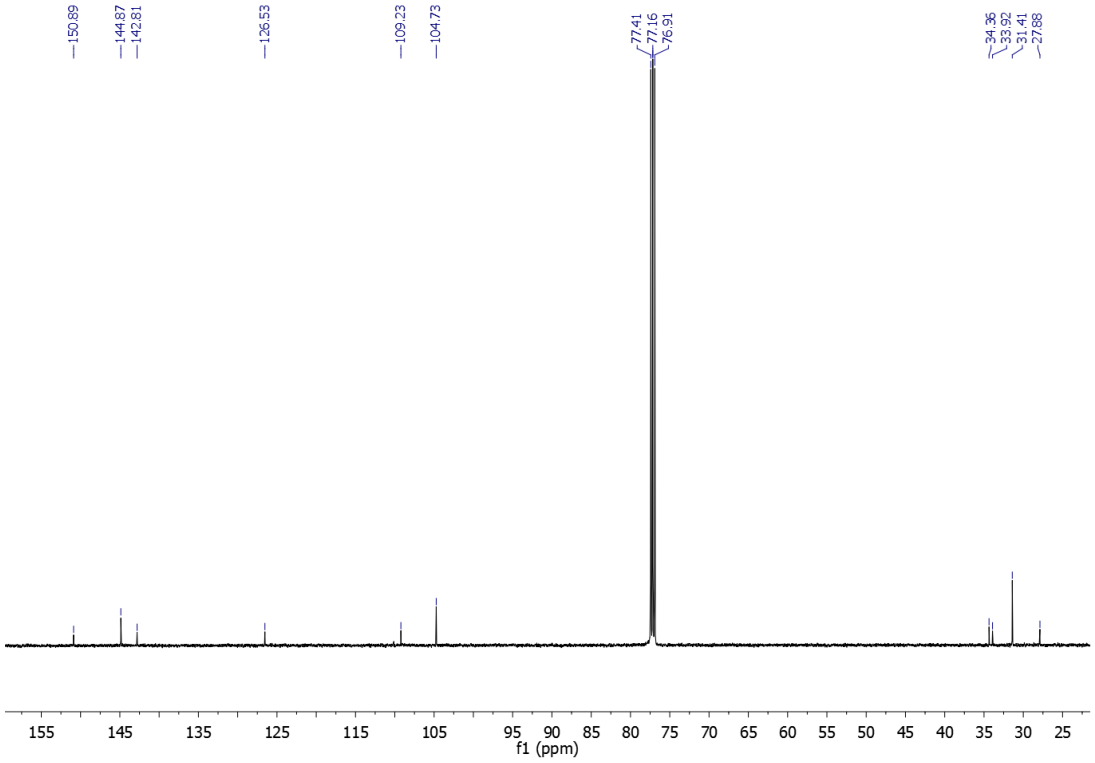

^{13}C NMR spectrum (126 MHz, $CDCl_3$) of monomer **9**

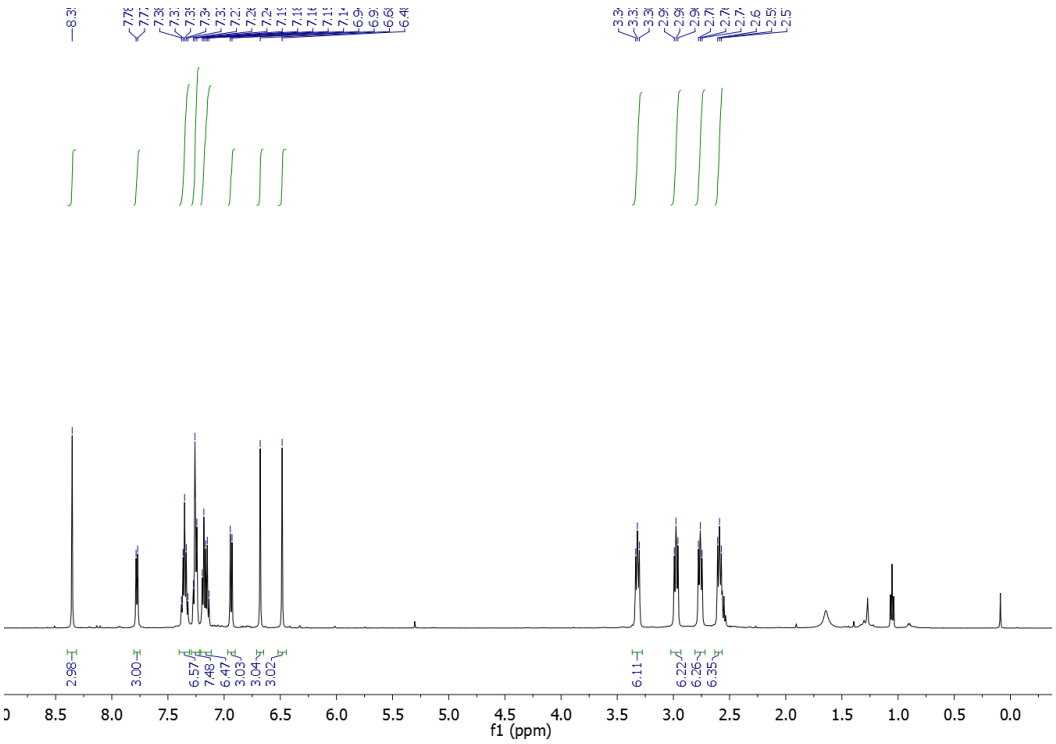

^{1}H NMR spectrum (500 MHz, $CDCl_3$) of **F-2TPh** stack

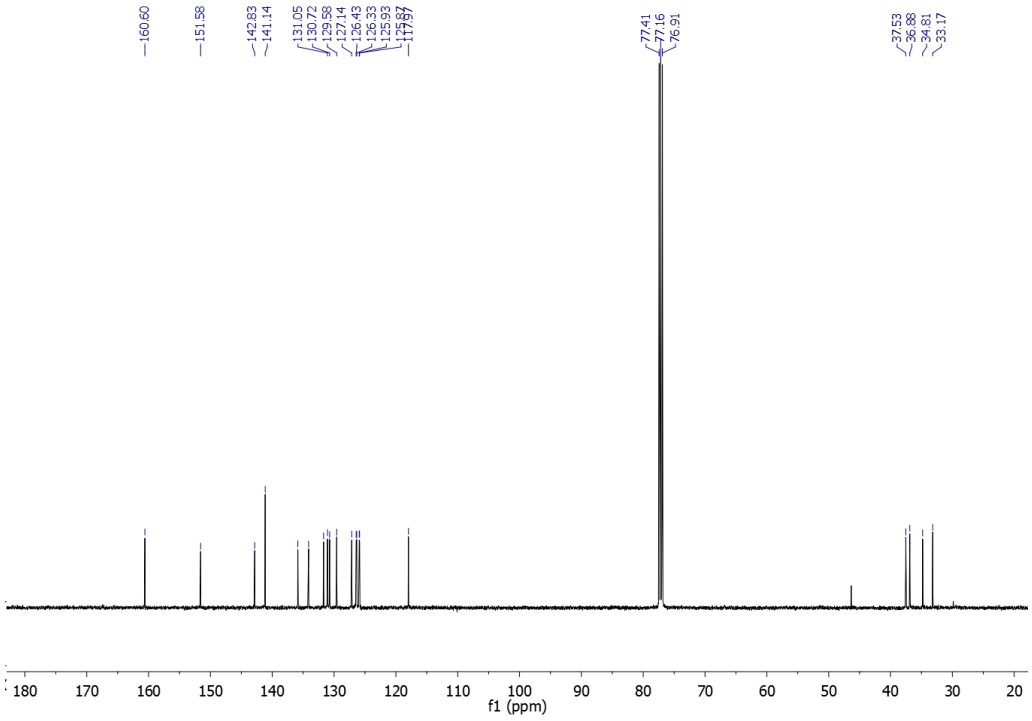

^{13}C NMR spectrum (126 MHz, $CDCl_3$) of **F-2TPh** stack

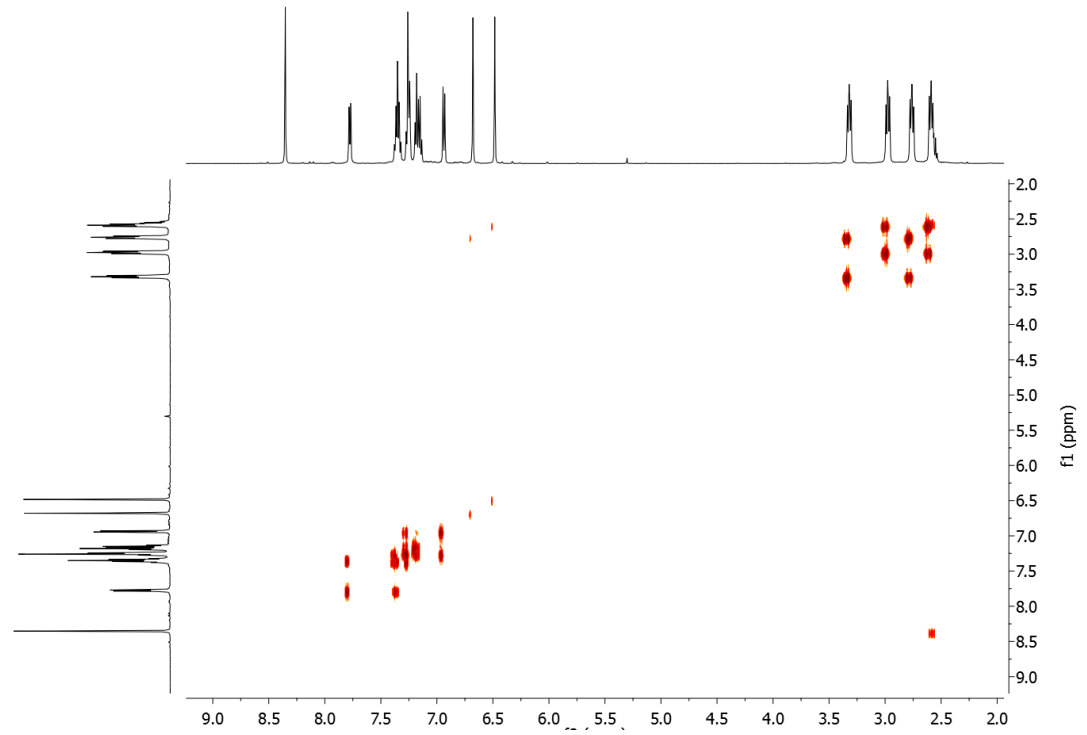

COZY NMR spectrum (500 MHz, $CDCl_3$) of **F-2TPh** stack

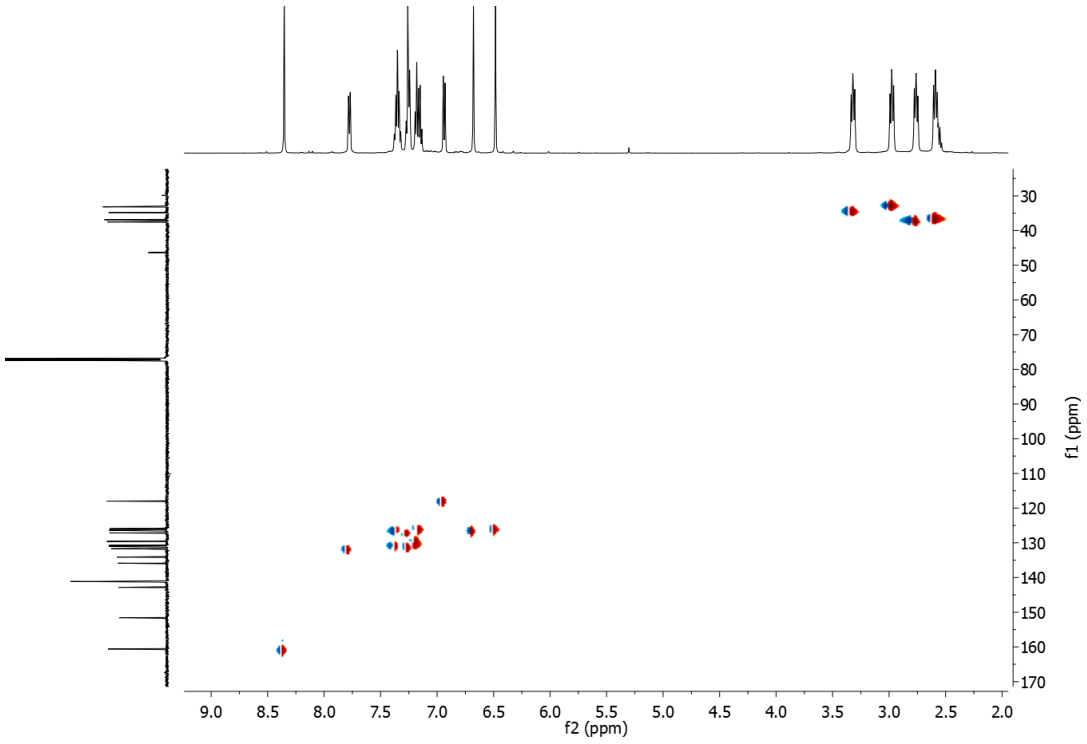

HSQC NMRspectrum (500 MHz, $CDCl_3$) of **F-2TPh** stack

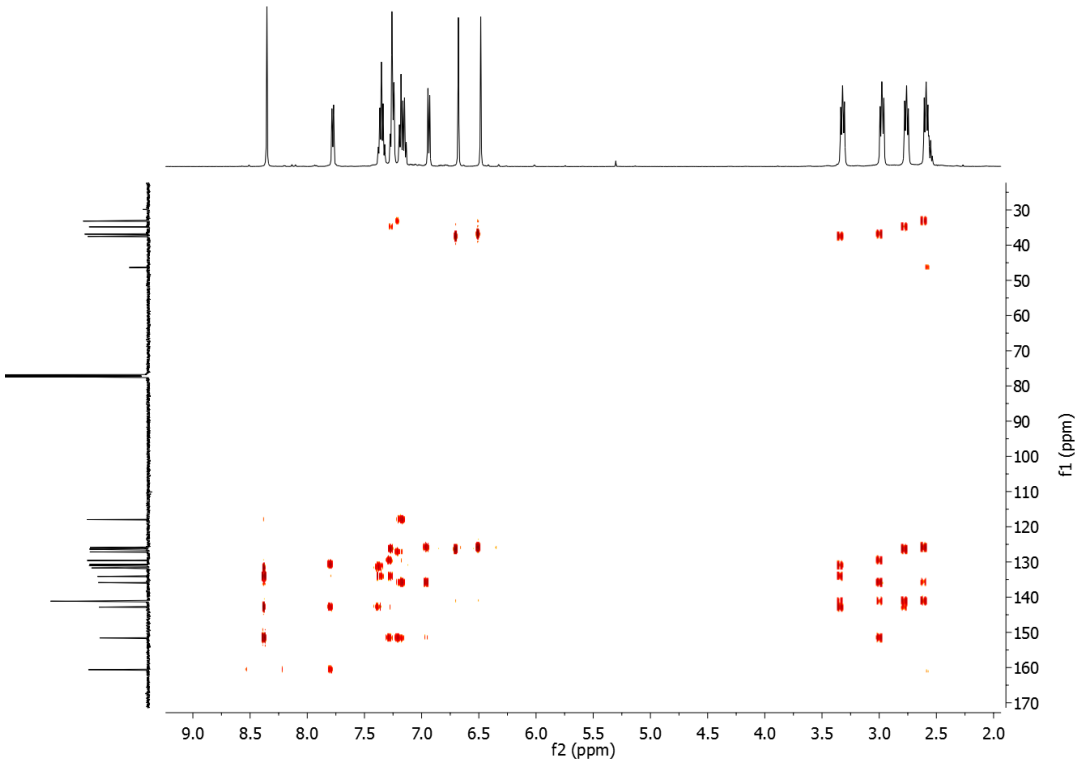

HMBC NMR spectrum (500 MHz, $CDCl_3$) of **F-2TPh** stack

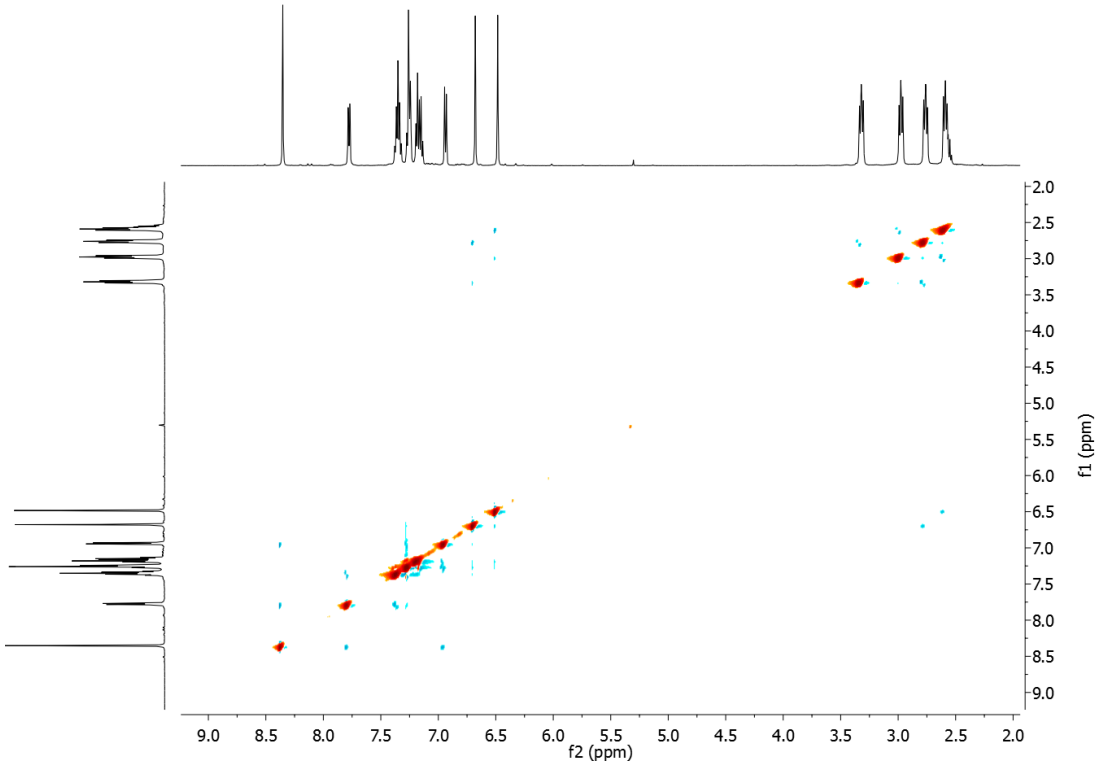

Roesy NMR spectrum (500 MHz, $CDCl_3$) of **F-2TPh** stack

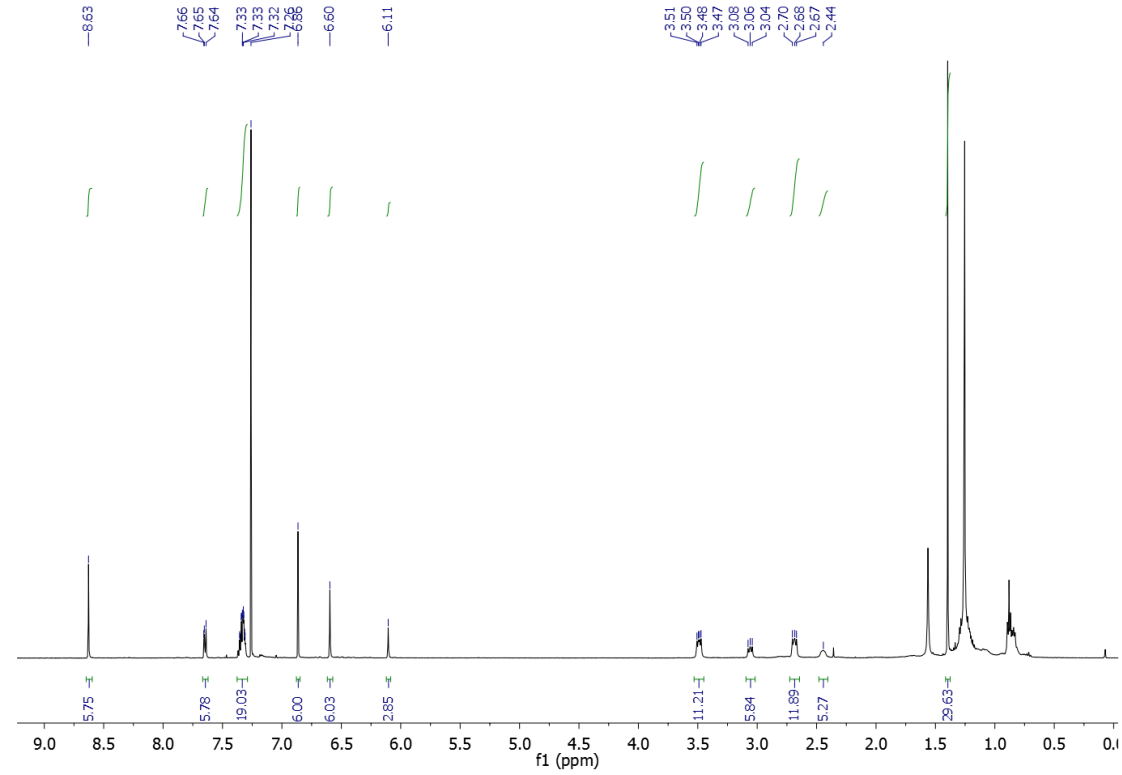

^{1}H NMR spectrum (500 MHz, $CDCl_3$) of **F-3TPh** stack

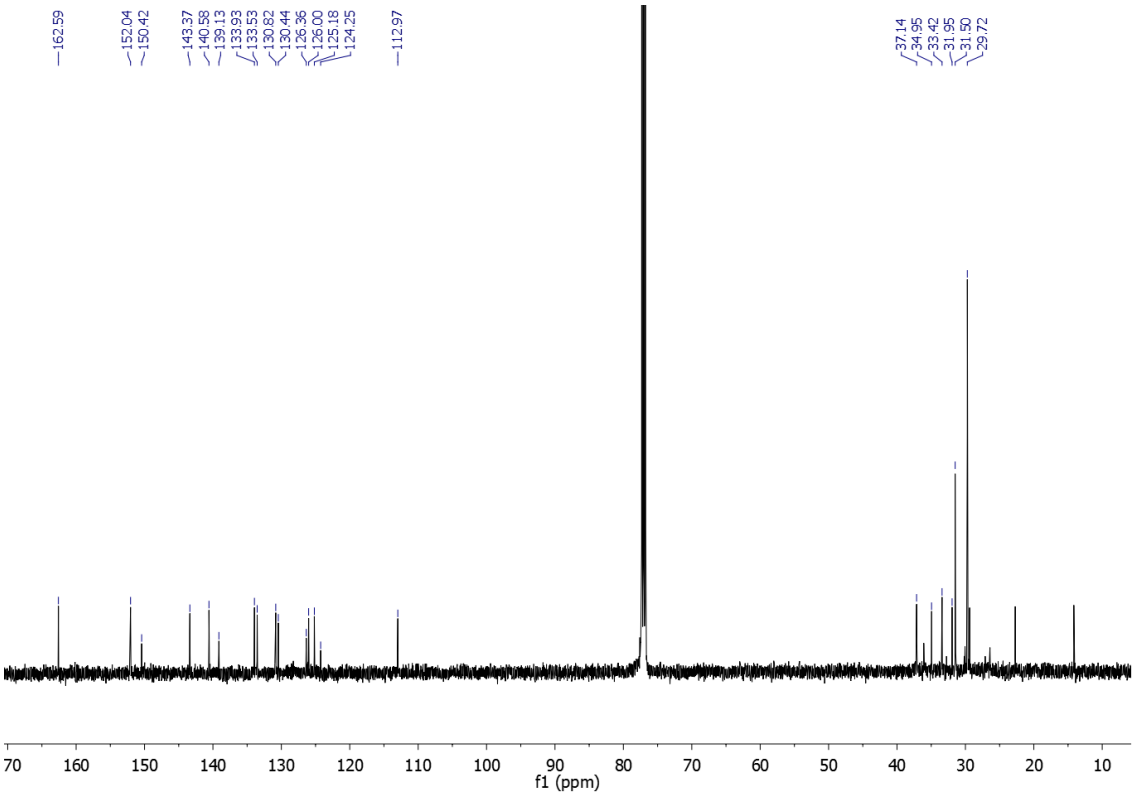

^{13}C NMR spectrum (126 MHz, $CDCl_3$) of **F-3TPh** stack

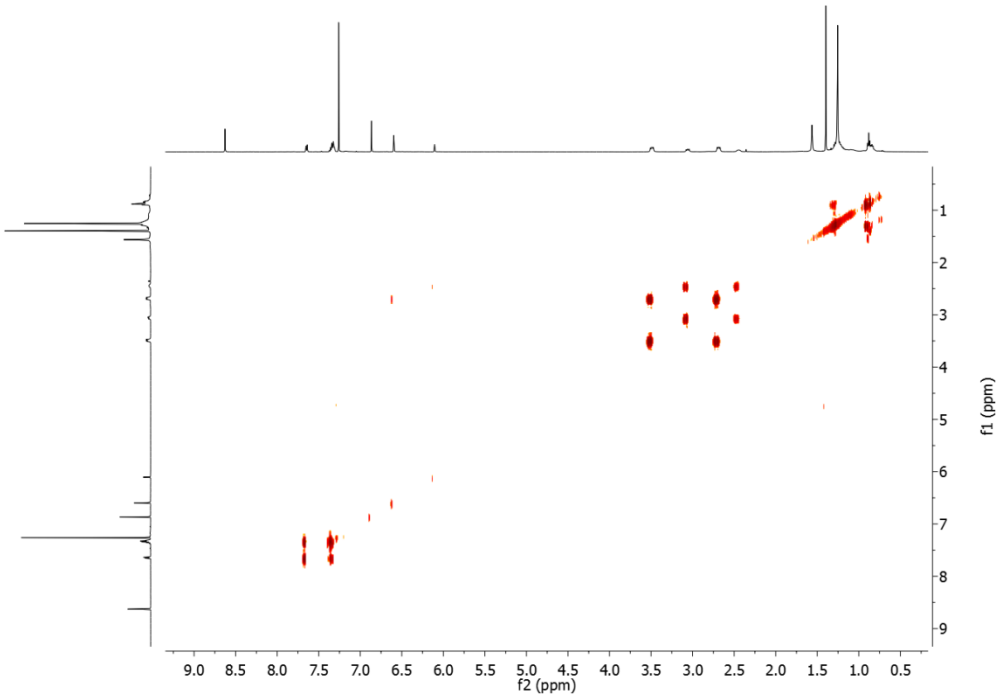

COSY NMR spectrum (500 MHz, $CDCl_3$) of **F-3TPh** stack

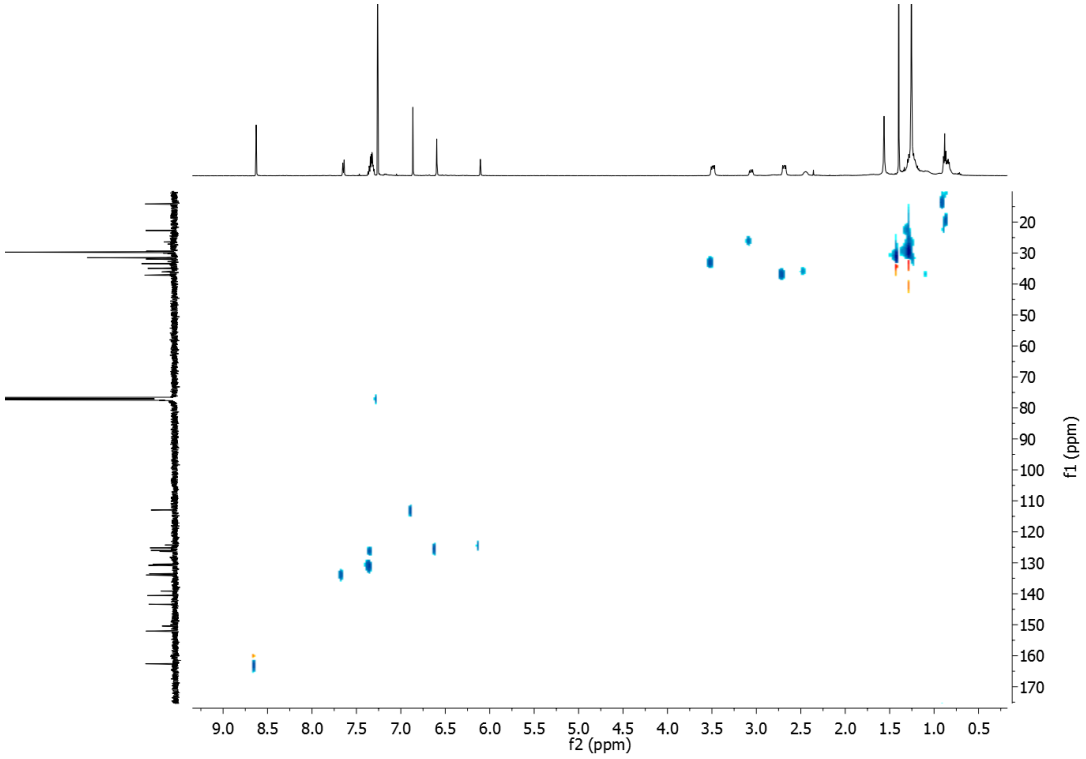

HSQC NMR spectrum (500 MHz, $CDCl_3$) of **F-3TPh** stack

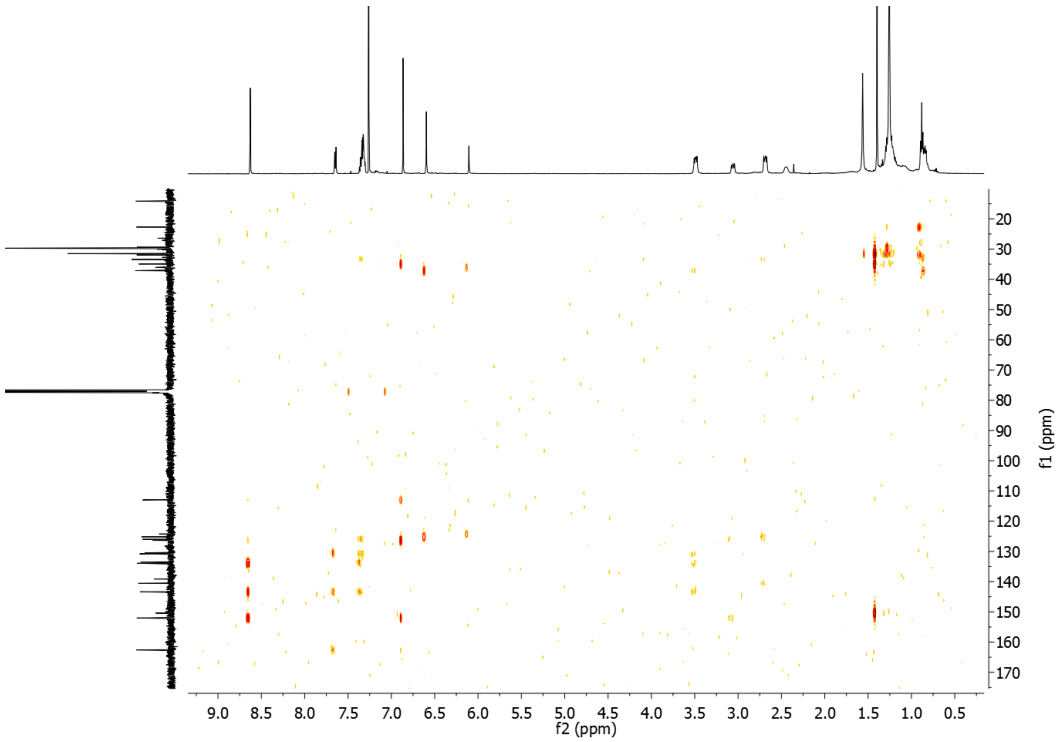

HMBC NMR spectrum (500 MHz, $CDCl_3$) of **F-3TPh** stack

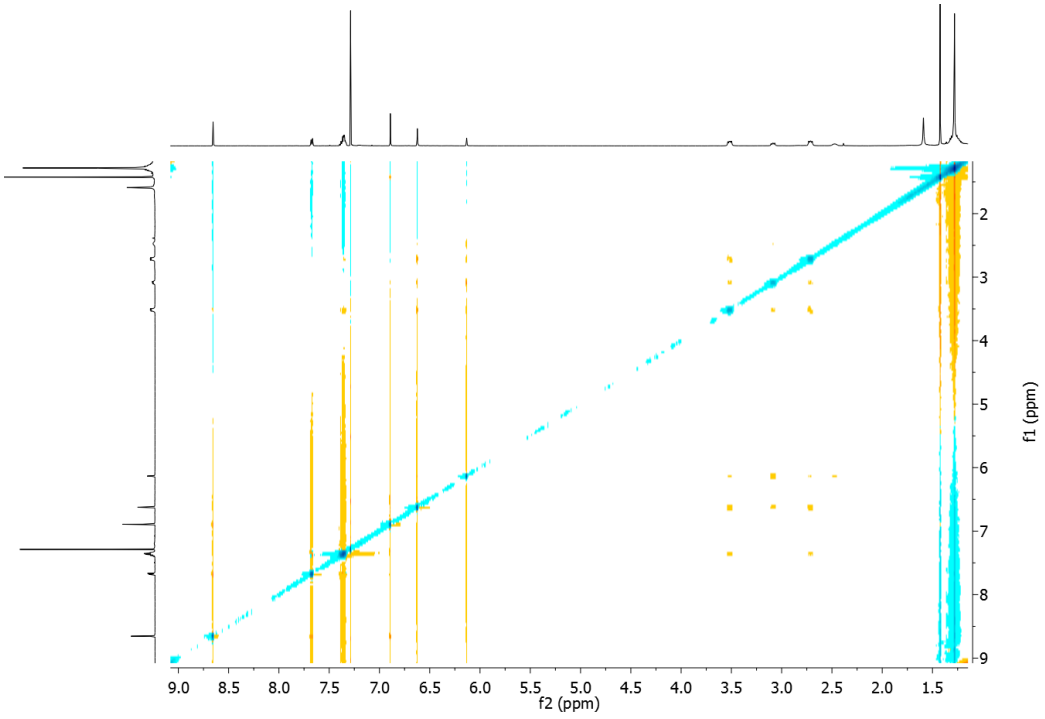

Roesy NMR spectrum (500 MHz, $CDCl_3$) of **F-3TPh** stack

Chapter 5 . Conclusion

We explored two- and three-tiered covalent stacks with a helical structure. The conformational racemization of these stacks was investigated with the help of NMR spectroscopy and computational modeling.

Rigid two- and three-tiered stacks (**2T′** and **3T′**) were successfully constructed. The misaligned stack $\mathbf{3T_{iso}}$ and incompletely assembled $\mathbf{2T_B}$ were formed along with the three-tiered stack, which highlighted the challenges of utilizing DCC in self-assembly. In DCC reactions, products that are significantly more stable than other possible products will be favored at equilibrium. However, the model calculations indicated that the energy of the most stable conformation of $\mathbf{3T_{iso}}$ was slightly lower than that of **3T**, explaining why $\mathbf{3T_{iso}}$ and **3T** were formed together. The formation of $\mathbf{3T_{iso}}$ indicated that small changes should be made to the monomers such that they can only assemble in one way. From the isolation of $\mathbf{2T_B}$, we conclude that the (unobserved) $\mathbf{3T_B}$ is strained relative to $\mathbf{2T_B}$. By introducing more flexible ethylenes as connections between the benzene core and the reactive arms in the monomers, the above problems were successfully solved. Flexible two- and three-tiered stacks (**F-2T′** and **F-3T′**) were isolated in good yields. There was no competing formation of byproducts along with the assembly of **F-3T′.** The introduced flexibility released the strain present in the rigid stacked structures. Therefore the DCC system targeted high symmetry structures at equilibrium.

The conformational behavior was studied for the two- and three-tiered stacks. The results of variable temperature NMR studies showed that **2T′** and **3T′** were quite different. **3T′** had much slower conformational racemization compared with **2T′**. From the computational results, we concluded that the additional tier deepens the energy well for the most-stable conformers and increases conformational coupling between the subunits. The ^{1}H NMR of **F-3T′** indicated that **F-3T′** had faster conformational racemization compared with **3T′**. The flexibility presented in the flexible three-tiered stack accelerated the speed of racemization.

In summary, we have developed an efficient strategy for the synthesis of two and three-tiered stacked architectures. The misaligned and incompletely assembled compounds demonstrated the intrinsic challenges of multicomponent self-assembly in three dimensions. Introduction of flexibility is an efficient solution to alleviate the strain in the rigid and compact

stacks. The high efficiency and the structural complexity of the products make the method attractive for construction of complex organic materials.

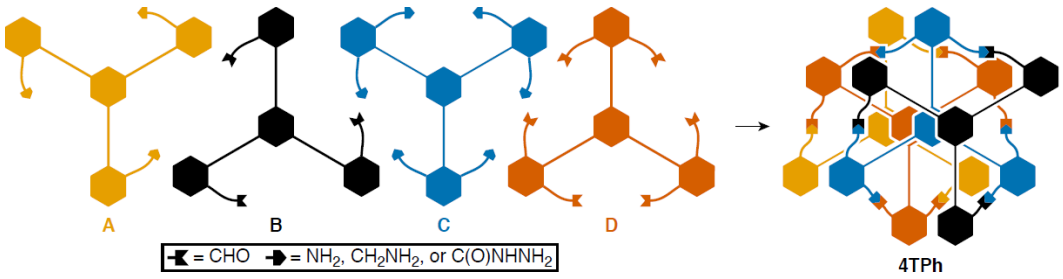

Scheme 5.1 Four components synthesis of four-tiered **4TPh**.

The strategy developed here could be applicable to the construction of heterosequenced four-tiered stacks in the future (**Scheme 5.1**). These stacks consist of four different monomers assembled using the directionality of imine bond. Control of sequence make the proposed four-tiered stacks good candidates for development of energy- and charge-transport materials. With one more tier than the three-tiered stacks, more interesting conformational behavior could be discovered with VT NMR and computational modeling analysis.

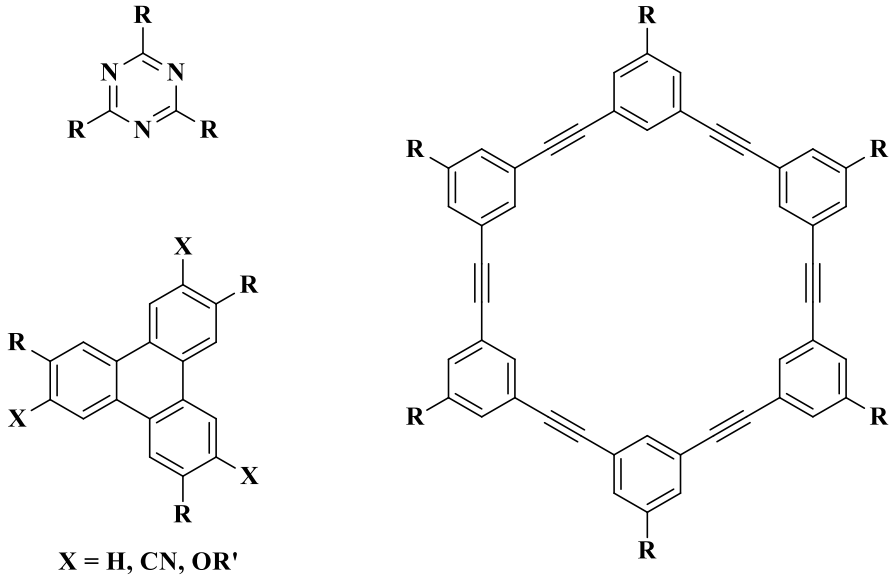

Scheme 5.2 Possible alternate core structures. (R = CC-Ar)

The synthetic techniques developed with benzene cores could be generally applicable to the synthesis of more complex covalent structures. Thus, the central cores could be replaced with other groups, such as triazines, triphenylenes and functional macrocycles. (**Scheme 5.2**)

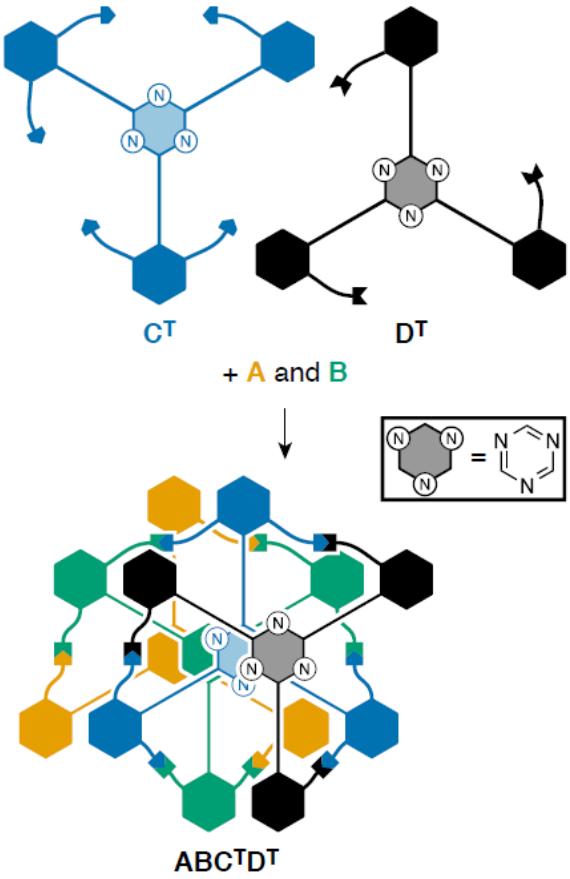

Scheme 5.3. Assembly of a stack mixing benzene and s-triazine cores.

Benzene cores and s-triazine cores could be mixed in the self-assembly of heterosequenced stacks. (**Scheme 5.3**) The mixed central cores could introduce complex electronic structure into the stacked structures. With the installment of functional macrocycles in the central cores, more interesting applications will be discovered with further investigation including gas storage and selectivity, catalysts, molecular recognition and chemical sensing.